

COSMIC SUPERSTRINGS:  
OBSERVABLE REMNANTS OF BRANE INFLATION

A Dissertation

Presented to the Faculty of the Graduate School

of Cornell University

in Partial Fulfillment of the Requirements for the Degree of

Doctor of Philosophy

by

Mark Charles Wyman

August 2006

© 2006 Mark Charles Wyman

ALL RIGHTS RESERVED

COSMIC SUPERSTRINGS:  
OBSERVABLE REMNANTS OF BRANE INFLATION

Mark Charles Wyman, Ph.D.

Cornell University

Brane inflation provides a natural dynamical model for the physics which underlie the inflationary paradigm. Besides their inflationary predictions, brane models imply another observable consequence: cosmic strings. In this dissertation I outline the background of how cosmic strings arise in brane inflationary models and how the properties of the strings and the models are mutually tied (Chapter 2). I then use cosmological observations to put limits on the properties of any actually-existing cosmic string network (Chapter 3). Next, I study the question of how cosmic superstrings, as the cosmic strings arising from string theory are known, could be distinct from classical gauge-theory cosmic strings. In particular, I propose an analytical model for the cosmological evolution of a network of binding cosmic strings (Chapter 4); I also describe the distinctive gravitational lensing phenomena that are caused by binding strings (Chapter 5). Finally, I lay out the background for the numerical study of a gauge theory model for the dynamics of cosmic superstring binding (Chapter 6).

## BIOGRAPHICAL SKETCH

Ortus a Bruce et Barabara Wyman, piis ac honestis parentibus, in Austinopole, civitatis Texiae capite, die octavo Augusti, anno salutis millesimo nongentesimo septuagesimo nono, tum paucis mensibus elapsis, baptizatur Marcus Carolus Wyman.

Domo facta Lacus Carolini, in oppido Ludoviciana, Gallicae quondam provinciae, olim Regi Solis deditae, haec humida habitatio facta est Marci patria.

Eodem loco praeter amorem parentum attentionemque habet plerosque, fortuna adjuvante, cognationum; imprimis avus et aviae, Nancy Wyman et Clinton ac Margaret Hart eum alunt.

Doctrina et prima eruditio spiritualis procedunt sub aegide ecclesiae Episcopalis quae nomine vocatur Boni Pastoris et Marco novem disciplinae satis sanae annos praebuit; oportet autem dicere magis libris peramatis et indefessis parentibus edocentibus in viam sanae doctrinae ingreditur.

Tum in Sancti Ludovici Catholica Schola tres annos operam studiis dat et ibidem quidam Carolus Zebley in Marci pectore physicorum amorem, magni futurum momenti, serit.

Tam pueriles praeter physica quam faciles illo loco studia sensit et ergo celeriter in alia altiores ad McNeese State Universitatem aggreditur.

Marco haec universitas favet: non solum panem quotidianum, parentibus eius magistris universitatis adlaborantibus, sed etiam disciplinam peritam in variis disciplinis praebet: artium res gestas, economicas, animarum iuvenum studium, linguam Gallicam recentem, et linguam Latinam et Graecam, sine faciendo mentionem nonnullorum annorum in piano instructionis - omnes haec res praeter eius cor studiorum: mathematicam, anglicas litteras, et physica.

Baccalaureis summa cum laude in iisdem disciplinis Marcum Universitatis Magistri ac Doctores adornant.

Perplacitam inter hanc diversitatem physica, fecunda imaginatione Marci capta studioque erecto, eum ducit in eandem disciplinam ad illam hederaceam turrim, Ithacae Novi Eboraci fundatam, Cornell Universitatem.

Apud Cornell quamquam studiorum altiorum duritia latam mentem Marci compescit, incipit tamen organo tiliarum studere, linguae operam dare Coreanae, nec minus ingentem eius intellegentiam exercere quam pro amore laborare, cuius causam videbitur; et praecipue communionem cum Romana Ecclesia, matre ac omnium ecclesiarum magistra, habere.

Quoniam anxietur sine dubio benevolus lector hunc iuvenem non vacare, inter tam multos labores quam arduos, conviviis ac amicis, audiendo ille lector consolabitur quod postquam oppidum Laertium advenit Marcus, convenit futuram sponsam, Minyoung Yi.

Quandoquidem ferventis amoris cursum non prosis perfunctoriis sed perpolitibus poesibus praedicare mos est, his paucis verbis necesse est lectori contento esse: laetabundam acturi sunt vitam et beatam, vel etiam videtur auctori hanc biographiam scribenti.

Societatis Fovendi Boni Temporis conditor in postremis apud Cornell Universitatem annis duobus Marcus factus est, in cuius societate multa voluta sunt bona tempora atque cuius consortium compensavit egressam, studiorum altiorum causa, Minyoung qui, fabula celebri inverso, tamquam nova Penelope, Marco in Ionii insula perstante et thesim texente, peragravit plagas.

Nunc tandem peregrinatione perfecta et solivagis diebus exhaustis, aestatis fine ineunte, Marcus et mulier futura, gentem nativam relinquentes, in regiones

meabunt septentrionales, quo ille adhibebit se ad scientiam physicorum provehendum sub patrocinio Perimetri Institutionis Contemplativorum Physicorum.

Born in the capital city of the great state of Texas, one of the United States of America, on the eighth day of August in A.D. 1979, the son of Bruce and Barbara Wyman, Mark Charles Wyman was christened in that name some months later. His family taking up habitation in Lake Charles, Louisiana soon thereafter, Mark came to call that Carolingian city his home. There he was fortunate enough to have, in addition to the love and attention of his parents, much of his extended family; he was particularly aided by the loving support of his grandparents, Nancy Wyman and Clinton and Margaret Hart. His education and early spiritual development took place under the aegis of Good Shepherd Episcopal Church, the day school of which provided Mark with 9 years of reasonably sound instruction; though it must be admitted that more of his education came by means of his beloved books and the tireless explanations of his patient parents. Next came three years at Saint Louis Catholic High School wherein his physics teacher, a certain Charles Zebley, engendered in Mark that love for physics which would prove to be decisively influential in his life. Otherwise bored with high school, however, Mark proceeded quickly into higher education at McNeese State University. That school was very good to Mark: not only did it provide him his daily bread – for his parents are there employed as professors of Environmental Science and Languages, respectively – but also with expert instruction in such divers subjects as art history, economics, child psychology, and the modern Gallic, classical Latin, and ancient Grecian tongues – not to mention several years' directed study of the piano – in addition to his core areas of study, *viz.*, mathematics, english literature, and physics. The faculty of the University awarded Baccalaureate degrees *summa cum laude*

to Mark in each of those three fields before he departed. Amidst this diversity of interests, it was physics that most captured young Mark's fertile imagination and eager study, leading him to enter graduate study in that field at Cornell University in Ithaca, New York. At Cornell, the rigors of graduate study somewhat narrowed the scope of Mark's activities; nonetheless, he found time there to commence study of the pipe organ, to make some attempts at mastering the language of the Hanguk peoples, and – most importantly – to make entry into communion with the Church of Rome. As the gentle reader at this point is no doubt harboring an understandable concern that this young man was left no time for society between his various pursuits, he should be comforted to learn that very soon after his arrival in the Odyssean city Mark met the girl who would become his wife, Minyoung Yi. As romance is best told in a form more poetical and less formal than the biographical sketch, the reader will have to content himself with a summary, *viz.*, that they lived happily ever after, or so it seemed that they would as this text was being written. Mark also found time in his last two years at Cornell to co-found a student group, the jovially-named Society for a Good Time, in the company of which many good times were allowed to roll, this being some limited compensation for the departure, for reasons of further education, of Minyoung who, like some new Penelope in a reversal of the famous tale, wandered whilst Mark wove his thesis ensconced in those Ionian hills.

But now has come the end of that long and arduous Ithacan sojourn. At the close of the summer, the purpose held by Mark and his bride-to-be is to stir from the country of their birth to abide, for a time, in its northern neighbor, where Mark has been offered fixed-term employment in research at the Perimeter Institute for Theoretical Physics.

Mariae semper Virgini  
Dei Matri Ecclesiaeque  
Caelesti Nutrici meae et almae  
Terrestribus et parentibus  
abundanter amorem ac vitam donantibus  
hoc opus  
offeret et dedicat  
Marcus Carolus Ambrosius Wyman

## ACKNOWLEDGEMENTS

First of all, I would like to acknowledge Ira Wasserman, my thesis advisor, who took me on five years ago unformed and protean and taught me to be a scientist. I hope that a lot of his good sense, intuition, and attitude towards theoretical physics and astronomical observation, as well as his practical diligence in solving research problems, have rubbed off on me! I also thank Henry Tye for letting me be a part time member of his research group and thus introducing me to the wild and wooly world of string theory from whence this thesis has sprung. Thanks are furthermore due to David Chernoff, with whose help I conducted my first research project and whose steady, patient explanations of various physical systems, programming algorithms, and academic prose style made my transition from ignorant student to genuine researcher far less painful than it would otherwise have been. Particular thanks are also due to Levon Pogosian, my collaborator on several papers, who provided a great deal of advice and friendly help from the perspective of one closer to my age and experience. Finally, I thank Riccardo Giovanelli for serving on my special Committee and patiently putting up with all this far-out theoretical research.

Outside of the professional realm, my chief thanks go to my fiancée Minyoung and my parents Bruce and Barbara for their encouragement of my pursuit of this degree. I thank Minyoung in particular for her unswerving love, attention, and companionship; also for helping me to develop a self-disciplined work ethic which has allowed this project to come to a finite termination and for patiently listening to me practice my research talks with ready advice and admonishment by means of which my speaking skills have so much improved. My parents, of course, established the very foundations on which all my academic endeavors have been

built through their years-long fostering of my educational pursuits, being ever supportive and, while always ready to provide advice and parental perspective, never attempting to force me along any particular career path. Their constant love, unconditional support, and irrepressible confidence in me were and will always be indispensable. I should also here mention my sister Kate whose friendship and love were always available to buoy me up and whose marked talent for teasing made it impossible for me to become a puffed-up prig; I thank her for the former, while the world, particularly my future students and colleagues, should thank her for the latter!

It is true of nearly everyone, and particularly true of me, that without friends for daily camaraderie and support it would be impossible to reach the end of so long a degree program while remaining sane. While Minyoung, my favored companion, was absent from Cornell for half of my tenure here, I have been extremely fortunate in having a bevy of friends who filled the gap. First my friends in the department of Physics, people who proved that not all physicists were boring and one-sided; though indeed most of them have either already left Physics or are bound for careers outside of the field, which may tell you something: Rich Helms, lawyer-to-be and indefatigable political conversationalist, the only other former Limbaugh “dittohead” in the department of Physics; Ethan Bernard, tinkerer extraordinaire and a deeply thoughtful man, who though persistently in error about many important things is nonetheless always a joy to speak (and drink) with; Marko Nantias, locus of leaven and liveliness in the department, the only person ever to ask whether he might come to Mass with me to meet women; Jeandrew Brink, longtime office mate and dear friend, whose love of the simplicity of life and the great outdoors made her a valuable refuge in a self-consciously sophisticated secular school; Stephan Braig,

who reminded me of myself, albeit with less religion and more german practicality; Deniz Sezer, who reminded me that physics and math were a fun thing to study when I had nearly forgotten; Oliver Dickie, constant companion of my first year, an amiable New Zealander who never thought it too early for a pint; also Matt Shepherd, Karen Masters, Kristine Spekkens, John Karcz, Dan Johnson, Bjoern Schmekel, as well as Henry Tye's group: Nick Jones, Saswat Sarangi, Ben Shlaer, Louis Leblond, and Sarah Shandera. My second batch of friends were those with whom I shared a communion even deeper than a shared scientific field of study, namely that of the Catholic Church: Joseph Yarbrough, translator of my biography, a deceptively relaxed latinist and philosopher for whom a lengthy jog followed by a garrulous symposium is the daily ideal; Mathew Lu, sharp-witted tech geek and true analytic philosopher, who taught me everything from why Kant is important to how to drink scotch whisky; Jeffrey Corbeil, a gentle giant of an engineer and a considered contrarian, one of few people who may read more quickly and constantly than I do; also Rachel Smith, Adam Sasiadek, John DeBarbieri, Robert Gahl, and Michelle Raczka.

Lastly, I want to thank those physicists and other academics whose example and counsel helped make my entry into the academy possible and relatively painless: Scott Goins, a classicist and great friend of mine – my confirmation sponsor and the first real academic scholar whom I met outside of my family; Charles Zebley, who first taught me physics; John Knox, whose realism about graduate school life saved me untold trouble; also Tommy Bogle, James Edmonds, Robert Doucette, John and Carol Wood, Lane and Julie Miller, and Robert Cooper.

I also wish to acknowledge the National Science Foundation Graduate Research Fellowship Program, the Cornell Physics Department Boochever Fellowship, and

the National Aeronautics and Space Administration Graduate Student Researchers Program for financial support.

## TABLE OF CONTENTS

<b>1</b>	<b>Introduction</b>	<b>1</b>
<b>2</b>	<b>From Brane Inflation to Cosmic Strings: Theoretical Background</b>	<b>9</b>
2.1	Introduction . . . . .	9
2.2	Brane Inflation and Cosmic String Properties . . . . .	11
2.2.1	Coulombic Inflation . . . . .	14
2.2.2	Power Law Inflation . . . . .	17
2.2.3	Cosmic String Properties . . . . .	19
2.2.4	Tensor modes . . . . .	22
<b>3</b>	<b>Cosmological Constraints on a Network of Cosmic Strings</b>	<b>24</b>
3.1	Introduction . . . . .	24
3.2	The Model and Analysis . . . . .	25
3.2.1	The Cosmic String Model . . . . .	29
3.2.2	Markov Chain Monte Carlo . . . . .	34
3.3	Results . . . . .	35
3.3.1	The fraction in strings and $G\mu$ . . . . .	35
3.3.2	The B-polarization spectrum . . . . .	41
3.4	Summary . . . . .	42
<b>4</b>	<b>Networks of Cosmic Superstrings</b>	<b>48</b>
4.1	Introduction . . . . .	48
4.2	A Multi-Tension Velocity-Dependent One Scale Model . . . . .	55
4.3	F- and D-String Network . . . . .	64
4.4	Network Results . . . . .	69
4.4.1	Scaling . . . . .	71
4.4.2	Low-F Catastrophe . . . . .	73
4.4.3	Final Spectra . . . . .	73
4.5	Observational Consequences . . . . .	74
<b>5</b>	<b>Cosmic Superstring Lensing</b>	<b>85</b>
5.1	Introduction . . . . .	85
5.2	Review of straight string lensing . . . . .	87
5.3	Lensing by $Y$ -Junctions . . . . .	90
5.4	Conclusion . . . . .	95
5.5	Appendix: Fly's Eye Effect . . . . .	96
<b>6</b>	<b>A Model for Cosmic Superstring Binding</b>	<b>97</b>
6.1	Introduction . . . . .	97
6.2	Current Status . . . . .	101
	<b>Bibliography</b>	<b>103</b>

## LIST OF TABLES

3.1	Prior constraints on the parameters . . . . .	35
3.2	The best fit results . . . . .	37
4.1	The relative populations of the three lowest-lying tension states, which in all cases dominate the networks' energy density. . . . .	75

## LIST OF FIGURES

3.1	The CMB TT and TE spectra (solid lines) sourced by cosmic strings with wiggleness parameter $\alpha_r = 1.9$ , as well as the adiabatic spectra for the same cosmological parameters (dashed lines) and WMAP's first year data. The string spectra are normalized so that the <i>total</i> TT power is the same for the two lines, which corresponds to $B = 1$ .	27
3.2	The string-generated matter power spectrum (solid line) for the same parameters as in Fig. 3.1, i.e., for $B = 1$ . The dashed line represents the linear spectrum from adiabatic perturbations at $z = 0$ .	28
3.3	The one-dimensional projected PDFs for the 8 parameters varied by our Markov Chain Monte Carlo code; note that $\omega_B = \Omega_B h^2$ , $\omega_M = \Omega_M h^2$ . The solid line represents the PDFs for models where cosmic strings are included; the dashed line represents the PDFs for models with $B = 0$ , i.e. without cosmic strings. Each curve has been rescaled such that its area is unity. For each PDF the lightly shaded regions are excluded at the 68% confidence region; the dark regions are excluded at the 95% confidence region. . . . .	36
3.4	The PDF for the cosmic string weighting parameter, $B \equiv (G\mu/1.1 \times 10^{-6})^2$ . . . . .	38
3.5	The PDF for the combination parameter $f$ , which quantifies the fractional contribution of cosmic strings to the total $C_l^{TT}$ spectrum. The solid line shows $f$ from our full analysis, with the 68 % (light) and 95 % (dark) confidence regions shaded. The dotted line is the result for $f$ from our previous three parameter analysis. . . . .	41
3.6	The B-type polarization spectra for $\alpha_r = 1.9$ (dashed lined) and $\alpha_r = 1$ (solid line) both corresponding $f = 0.1$ . The light dotted line is the B-mode expected from gravitational lensing of adiabatic E-mode polarization; the light dash-dotted line is the B-mode expected from gravity wave-sourced polarization, for tensor-to-scalar ratio $r = 0.1$ . . . . .	43
4.1	A schematic view of a string intersection. The intersection angle, $\theta$ , determines whether the additive $-(p + p', q + q')$ – or subtractive $-(p - p', q - q')$ – binding occurs. . . . .	66

4.2	Comparison among three different sets of network initial conditions, all taking $F = 1, P = 0$ . The higher three lines represent the evolution of the overall density in cosmic strings (summed over all string states), $\tilde{\Omega}_{cs} \equiv \Omega_{cs}/((8/3)\pi G\mu_{(0,1)})$ , with scale factor, $a$ . The lower three lines represent the evolution of the density in $(0, 1)$ , or $D$ -strings, $\tilde{\Omega}_{cs}^{(0,1)} \equiv \Omega_{cs}^{(0,1)}/((8/3)\pi G\mu_{(0,1)})$ , with $a$ . Our standard initial conditions, equal initial populations of $(1, 0)$ and $(0, 1)$ strings and $HL = 1$ , are shown by the dashed lines. The solid line represents the results from a network run with a short initial length scale ( $10^{-2}$ of our usual choice) and with over half of the initial string $(p, q)$ states in our network equally populated. Finally, the dotted line shows the results for a very large initial population of strings – $\tilde{\Omega}_{cs} \sim 1000$ – equally spread over half of the tension states included in our network, with our usual choice for the initial network length scale. For all the runs shown here we have set the superstring coupling, $g_s = 1.0$ . . . . .	80
4.3	The bottom panel shows the evolution of $\tilde{\Omega}_{cs} = \Omega_{cs}/((8/3)\pi G\mu_{(0,1)})$ for various parameter values, taking the string coupling $g_s = 1.0$ . The top panel shows the rate of change in the comoving number density $N\eta^2$ ; in the scaling regime, $d \log N\eta^2/d \log \eta = 0$ . . . . .	81
4.4	The final scaling-era spectra for a variety of parameter combinations, taking the string coupling $g_s = 1.0$ , with $N_{(0,1)}$ normalized to unity and the other number densities altered accordingly. . . . .	82
4.5	The bottom panel shows the evolution of $\tilde{\Omega}_{cs} = \Omega_{cs}/((8/3)\pi G\mu_{(0,1)})$ for various parameter values, taking the string coupling $g_s = 0.5$ . The top panel shows the rate of change in the comoving number density $N\eta^2$ ; in the scaling regime, $d \log N\eta^2/d \log \eta = 0$ . . . . .	83
4.6	The final scaling-era spectra for a variety of parameter combinations, taking the string coupling $g_s = 0.5$ , with $N_{(0,1)}$ normalized to unity and the other number densities altered accordingly. . . . .	84
5.1	Illustration of lensing of a single galaxy by a $(p, q)$ network junction. Note that each image is partially obscured, which is a generic feature of cosmic string lensing events [105]. This image is an imaginative construction, not an actual observation. . . . .	87
5.2	A schematic view of the lensing due to a single string in the most general case; when the string's velocity is non-zero, the angular separation vector is perpendicular to the apparent string, rather than to the actual string. . . . .	90

5.3	The imaging pattern of a three-way junction. The dark lines represent the force-balanced string junction; in reality, strings themselves are invisible. The dotted and dot-dashed lines represent, schematically, the angular separation vectors associated with the strings. We suppress the heads of the vectors, since their orientation is arbitrary. For string tensions in the upper range allowed by observations – that is, $G\mu \sim 10^{-7}$ [21] – the size of the angular separation vectors would be of order 1 arc-second. The stars represent the lensed images, with the angular separation vectors drawn in for illustrative purposes. . . . .	91
5.4	The imaging pattern for two overlapping cosmic strings. The dotted and dot-dashed lines represent, schematically, the angular separation vector associated with the strings. Notice that only the object and two of the three images are visible. . . . .	92
5.5	The imaging pattern for three overlapping cosmic strings. Only the object and two of the seven images are visible. . . . .	94
5.6	This set-up of strings and associated images is unlikely ever to occur in nature. It is included for illustrative purposes. . . . .	96

# CHAPTER 1

## INTRODUCTION

Through a remarkable series of observational successes the adiabatic, cold dark matter-cosmological constant model of the cosmos has come to be accepted as a cosmological “standard model” [1, 2, 3, 4, 5]. In this model, the hot big bang was preceded by an epoch of drastic, accelerated expansion known as inflation. This period of expansion homogenized and flattened the universe. It also caused a nearly length-scale-invariant primeval spectrum of quantum mechanical field fluctuations to be expanded to cosmologically sized density perturbations, thus providing the initial, tiny inhomogeneities in density that eventually grew into the clumpiness, or structure – clusters, galaxies, stars, and planets – that we observe today. What we call the big bang was, in this view, a rapid reheating of the universe that occurred as the inflationary epoch ended. Despite its remarkable observational success, this paradigm is still essentially an *ad hoc* product. No currently-established physics can fully account for the existence of an inflationary epoch. Nor can we explain the sudden reheating of a cold, post-inflationary universe into a hot big bang. We have guessed the necessary ingredients for successfully modeling the early universe; we do not know where they come from or how they fit together.

In light of these demands, the current best hope for making compelling, comprehensive models of the early universe comes from string theory, within a recently-proposed heuristic structure known as the “brane world.” In the “brane world” picture, our observable universe is confined to a multi-dimensional Dirichlet-brane, or D-brane (a kind of membrane or domain wall) with three large spatial dimensions that is embedded in a higher dimensional world. The matter fields and forces with which we are familiar are, in this picture, seen as string-theory excitations

living on this membrane. Though there are more than three spatial dimensions present, they are invisible to us because the extra dimensions are too tiny to be noticed: we say they are compactified. In this model, the ingredients necessary for the inflationary paradigm are provided by the interaction of branes, thought of as truly fundamental objects, in the early universe: inflation is caused by the mutual attraction and falling together of two or more primordial branes; the reheating of the universe or hot big bang is brought about by the violently energetic collision of the branes when they meet [6, 7, 8]. In a recent theoretical advance, one fully realized, observationally viable model of “brane inflation” has been proposed [9], addressing concerns that such brane models were contrived or incomplete. Now that they can be considered to be complete models, the next question is whether these so-called “brane inflation” models can make any testable predictions beyond meeting the requirements of the inflationary paradigm.

Soon after brane inflation was proposed, such a tell-tale prediction was discovered: brane inflationary models nearly always predict the production of a network of cosmic strings at the end of the inflationary epoch [10]. Cosmic strings are linear topological defects of cosmological size. They are thought to arise following primordial phase transitions. In 1980, Zeldovich suggested that cosmic strings could be a natural source of primordial anisotropy for the seeding of large scale structure [13], and throughout the 1980s they were considered a competitor to inflation for explaining the origin of structure formation. They were first studied in the context of the Grand Unified Theory (GUT) phase transition in the very early universe. Estimates of the GUT phase transition scale predicted cosmic strings with a dimensionless tension of  $G\mu \sim 10^{-6}$ . Strings at this tension predicted CMB fluctuations [11, 12] at the same scale as those observed by the COBE experiment

[14], making it plausible to identify strings as the source of the primordial density fluctuations. However, observations of galactic clustering power spectra were inconsistent with the power spectra predicted by cosmic string networks that were normalized to the COBE-scale anisotropies in realistic cosmologies [15]. Finally, as observations of the CMB improved, the observed anisotropy spectra were found to disagree with the spectra predicted by string networks, definitively ruling out strings as the primary source for the primordial perturbations, though they were not ruled out as a subdominant contributor to the primordial perturbation spectra [16]. These observations chilled interest in strings for some time. The recent discovery that many brane inflationary models produce cosmic strings with tensions in the range [10]

$$10^{-6} > G\mu > 10^{-11}$$

– that is, below the observational bound – has led to a renaissance in the study of cosmic strings [17]. Theorists, eager to find distinctive signatures for string theory models of the early universe, have come to view cosmic strings as a desirable phenomenological aspect of these models since even a subdominant network of cosmic strings may be independently observable.

If they are characterized by energy and density of sufficient magnitude, cosmic strings possess a wide array of distinctive observable signatures, from gravitational lensing and gravitational radiation to large scale cosmological effects like vector-mode polarization of the cosmic microwave background (CMB) radiation (see ref. [18] for a review). It is furthermore quite natural in brane inflationary models for the properties of cosmic strings to be intimately related to the particular inflationary parameters realized within those models. Chapter 2 of this thesis and references therein describe how cosmic string and brane inflationary properties are

tied together in several simple cases. This sort of interdependence makes such brane inflation models more readily testable: one can imagine comparing various cosmological and cosmic string observations to see which particular models can provide a consistent account for them all. Indeed, even the continued non-detection of cosmic strings can be useful in discriminating among such theories by eliminating those theories that necessarily predict prominent cosmic string signatures.

After this background is established in Chapter 2, we explore what limits on cosmic string properties are already in place. We do this to determine whether cosmic strings are still viable as observable phenomena. Cosmic strings are active sources of density perturbations and can exist to the present day. The cosmological density and energy scale of any extant cosmic string network are thus limited by the remarkable agreement between the predictions of adiabatic inflationary models and current, high-precision cosmological observations. An investigation into the limits already imposed by current cosmological observations is the subject of Chapter 3. The results of this analysis are encouraging: cosmic string properties are indeed restricted by modern observations, but not to the point that they are already ruled out for observation through other avenues.

The remainder of this thesis examines how cosmic strings produced in brane inflation could be phenomenologically distinct from old style cosmic strings. If cosmic strings are eventually observed, we will need distinctive predictions to discriminate among different models for their formation. Chapter 4 describes an analytical model for the cosmological evolution of networks of such strings, taking their distinctive qualities into account. In this chapter we also use the findings of our model to make a series of predictions for distinctive observational signatures of these new-style cosmic strings. Chapter 5 fleshes out one of these predictions,

concerning the distinctive gravitational lensing phenomena associated with these cosmic strings. Finally, in Chapter 6 we discuss ongoing work aimed at improving our understanding of the cosmic string dynamics that govern network evolution.

The determination of current observational bounds on cosmic string network properties that appears in Chapter 3 is a continuation and updating of the work of a variety of groups [16, 19, 20, 21]. Our approach, in brief, is to assume that cosmic string-sourced perturbations exist alongside the observationally-favored adiabatic perturbations from inflation, but at a subdominant level. We then take the relative amplitude of the cosmic string-sourced perturbation spectrum as an extra cosmological parameter and use a standard Markov Chain Monte Carlo method to explore the multi-dimensional cosmological parameter space – that is to say, we determine how much of a cosmic string network contribution can be added to the adiabatic / inflationary CMB  $C_{\ell S}$  and Large Scale Structure / Galaxy redshift power spectrum without damaging the good fit of the composite spectrum to the observational data. Doing this in a statistically rigorous way, we find that any cosmic string network is limited to producing less than 7 (14)% of the primordial density perturbations at 68 (95)% confidence.

In our analysis of the CMB and galaxy power spectra, we made the assumption that the network of cosmic strings we were studying was characterized by a single tension scale, the kind of network that would be produced by a primordial phase transition in a single field – in other words, a single species of cosmic strings. This assumption follows the cosmic string work done in the past. New results from string theory, however, suggest that the cosmic string networks arising from brane inflation could be much richer. The principal novel property of cosmic “superstrings” – as cosmic strings from string theory are sometimes called, to distinguish

them from old-style cosmic strings – is that they can come in a variety of species [22, 23]. The simplest scenario involves two basic kinds of strings: fundamental F-strings (with tension  $\mu_F$ ) and one-dimensional Dirichlet branes, or D-strings (with tension  $\mu_D = \mu_F/g_s$ , where  $g_s$ , possibly  $\sim \alpha_{GUT} \sim 0.05$ , is the string coupling constant). These two fundamental species can also appear as bound states, dubbed “ $(p, q)$ ” strings, which are formed by combining  $p$  F-strings with  $q$  D-strings; these bound states have tension

$$\mu_{(p,q)} = \mu_F \sqrt{(p - Cq)^2 + q^2/g_s^2},$$

where  $C$  is a dimensionless number, the expectation value of the RR scalar [23]. The new richness in cosmic superstring phenomenology arises from this variety of possible states: in place of a single-tension network it is now possible to imagine interacting networks with a widely ranging spectrum of tensions. The nature of each observational phenomenon associated with strings is determined by the string tension. Thus, multi-tension networks are able to exhibit far more variety in their phenomenology than networks characterized by only a single tension ever could.

When a pair of superstrings,  $\alpha = (p, q)$  and  $\beta = (p', q')$ , meet, a variety of interactions are possible. The simplest, which occurs when  $\alpha = \beta$ , is reconnection, also known as intercommutation – the vortices interact and “trade partners.” This was the only kind of interaction possible for old style cosmic strings. Even this simplest interaction is changed by string theory dynamics, however. Whereas gauge strings interact virtually every time they cross [18], the higher-dimensional nature of superstrings may cause their effective interaction probability,  $p$ , to be quite small. This is because superstrings sometimes “miss” each other in the higher dimensions [23, 24] and thus fail to interact at all. This lowered reconnection probability, by itself, changes the way that cosmic strings networks evolve. The interdependence of

reconnection rate and network evolution is quite subtle, however, and is still being studied [25]. New interaction physics come into play when  $\alpha \neq \beta$ . In this case, depending on the angle of intersection in their collision, the interaction between  $\alpha$  and  $\beta$  can produce two different kinds of bound-state links:  $\gamma^\pm = (p \pm p', q \pm q')$ . Because the link is a bound state (i.e.  $\mu_\gamma \leq \mu_\alpha + \mu_\beta$ ) it will grow – presumably near the speed of light – so that two strings,  $\alpha$  and  $\beta$ , combine to form a single  $\gamma$  string. A network can thus evolve by forming bound states even if the  $\alpha = \beta$  reconnection probability is negligible. See Chapter 4 or refs. [23] for much more detail on the physics of these interactions.

In Chapter 4 [26], we propose an analytical model for the cosmological evolution of these binding-and-intercommuting, multi-species networks. To achieve this we were forced to make a simplifying assumption. This assumption is that all strings in a network, regardless of their tension, can be characterized by a single length scale,  $L$  (this assumption holds if the time for the binding reaction that creates higher tension states to spread to sizes of order  $L$  is short compared with cosmological time scales). The central finding of our network model is that the lowest lying three tension states – the  $(1, 0)$ ,  $(0, 1)$ , and  $(1, 1)$  states – dominate the cosmic string energy density. We also find that these “reactive” networks of multiple tension strings do reach a scaling solution – that is, they neither come to dominate the energy density of the universe nor effectively vanish from the cosmos at any epoch, but instead contribute a nearly fixed, low fraction of the universe’s energy density during each epoch.

Having a model for the evolution of a multi-tension string network is just a beginning. To exploit the possible phenomenology of cosmic “superstrings” we must also deepen our understanding of what makes these “superstrings” unique.

As a start, we identify an array of possible, unique observational properties of such string networks in §4.5 (see also ref. [27] for a review). In Chapter 5 [28], we work out one such possibility in greater detail: the distinctive gravitational lensing property of networks of  $(p, q)$ -strings, particularly their ability to produce nearly-identical triple images in the vicinity of binding junctions.

Finally, in Chapter 6 we lay out the background for some ongoing research. We hope to test the assumption that underlies the analytic multi-tension string network described above. Our assumption that strings immediately “zip up,” or bind following inter-string collision events may not accurately characterize the physics of string binding. To investigate this assumption, we are modifying a lattice gauge theory computer code [29] to manifest one, or several, gauge theory models for binding vortices [30, 31]. In doing this, we hope to mimic the success of Shellard and Matzner, who in the 1980s definitively characterized the intercommutation of gauge strings [32]. Their results could then be assumed in subsequent models. We hope to provide the same kind of definitive result for cosmic string binding dynamics.

CHAPTER 2  
FROM BRANE INFLATION TO COSMIC STRINGS:  
THEORETICAL BACKGROUND

First appeared as *Observational Constraints on Cosmic String Production During Brane Inflation* in *Phys Rev D* **D68** (2003) 023506.

## 2.1 Introduction

Observations of the cosmic microwave background (CMB) [14, 33] support the idea that the standard big bang phase of the expansion of the universe was preceded by inflation [34]. Recent results from the Wilkinson Microwave Anisotropy Probe (WMAP) [1, 2, 3, 35, 36] constrain the properties of proposed inflationary models tightly, but although some models are now excluded, numerous possibilities remain. A further challenge to observational cosmology is to try to hone in on a small class of viable models, even if identifying a single, correct theory of inflation may prove impracticable.

All of the data collected up until now are consistent with a relatively pristine Universe in which the perturbations observed today result from the amplification and distortion of a relatively featureless, Gaussian spectrum of fluctuations produced by quantum effects during inflation. However, it is likely that inflation itself could have left behind other remnants – such as cosmic strings – which could actively perturb both the CMB and dark matter of the Universe up to the present day.

It is well-known that cosmic strings cannot be wholly responsible for either the CMB temperature fluctuations or the observed clustering of galaxies [16]; roughly

speaking, the implied limits on the cosmic string tension  $\mu$  allowed by observations is  $G\mu \lesssim 10^{-6}$ . However, now that cosmology has entered an era in which the properties of the Universe are being revealed to unprecedented precision, a natural question is to what extent the observations can allow previously unwanted ingredients, such as cosmic strings (e.g. [19]). Indeed, as the precision of cosmological observations increases, we might hope to be able to distinguish among numerous presently viable models for inflation by the properties of the cosmic strings they predict.

Although the idea that inflationary cosmology might lead to cosmic string formation is not new [37, 38], it has received new impetus from the brane world scenario suggested by superstring theory. In brane world cosmology, standard model particles and interactions correspond to open string (brane) modes, while the graviton, the dilaton and the radions are closed string (bulk) modes. Thus, our 3D Universe can be thought of as residing on a brane or stack of branes with three dimensions of cosmological size. These branes in turn reside in extra dimensions that are compactified. In such a model, inflation can result during the collisions of branes coalescing to form, ultimately, the brane on which we live [6].

In these brane inflation models, the separations between branes in the compactified dimensions are scalar fields (open string modes) that can act as inflatons, with the interaction potential between spatially separated branes providing the inflaton potential. Details of the brane inflation scenario depend on both qualitative and quantitative features, such as whether collisions involve a brane-antibrane pair [39] or two branes coalescing at an angle [40], as well as parameters such as the sizes of the compactified dimensions [10, 39, 41]. Qualitatively, though, it appears easy to find models that predict adiabatic temperature and dark matter fluctuations

capable of reproducing all currently available observations. A seemingly unavoidable outcome of brane inflation, though, is the production of a network of cosmic strings [10], whose effects on cosmological observables ranges from negligible to substantial, depending on the specific brane inflationary scenario [22].

## 2.2 Brane Inflation and Cosmic String Properties

Recently, the brane world scenario suggested by superstring theory was proposed, where the standard model of the strong and electroweak interactions are open string (brane) modes while the graviton and the radions are closed string (bulk) modes. The relative brane positions (i.e., brane separation) in the compactified dimensions are scalar fields that have just the right properties to act as inflatons. Thus, the brane inflation scenario emerges naturally in the brane world [6]. In this picture, the inflaton potential is due to the exchange of closed string modes between branes; this is the dual of the one-loop partition function of the open string spectrum, a property well-studied in string theory [42]. This interaction is of gravitational strength, resulting in a very weak (flat) potential, ideally tailored for inflation.

The potential is essentially dictated by the attractive gravitational (and the Ramond-Ramond) interaction between branes. As the branes move towards each other, slow-roll exponential inflation takes place. This yields an almost scale-invariant power spectrum for density perturbation, except there is a slight red-tilt (at a few percent level). As they reach a distance around the string scale, the inflaton potential becomes quite steep so that the slow-roll condition breaks down. At around the same time, a complex tachyon appears, so inflation ends rapidly as the tachyon rolls down its potential. In effect, inflation ends when the branes

collide, heating the universe to start the standard big bang phase of cosmological expansion. This brane inflationary scenario may be realized in a number of ways [10, 39, 41]. The scenario is simplest when the radion and the dilaton (bulk) modes are assumed to be stabilized by some unknown non-perturbative bulk dynamics at the onset of inflation. Since the inflaton is a brane mode, and the inflaton potential is dictated by the brane mode spectrum, it is reasonable to assume that the inflaton potential is insensitive to the details of the bulk dynamics.

Coupling of the tachyon to inflaton and standard model fields can allow efficient heating of the universe if certain conditions on the coupling of the tachyon to standard model particles are met [43]. As the tachyon rolls down its potential, besides heating the universe, the vacuum energy also goes to the production of defects, in particular, cosmic strings. The effect of the resulting cosmic string network may be negligible or rather substantial, depending on the particular brane inflationary scenario [10, 22]. However, in all cases, we expect the density perturbation power spectrum in CMB to be dominated by the adiabatic fluctuations arising from quantum fluctuations of the inflaton during brane inflation, not by the nonadiabatic contributions from cosmic strings. However, the contribution to the density perturbation power spectrum in CMB coming from the cosmic string network may be large enough to be observable.

We devote this section to a review of the implications of brane inflation. The review given here is basic and, we hope, suggestive of the field. More up-to-date calculations along these lines can be found in refs. [44, 45]. For a broad set of models, we present results for the slow roll evolution, fluctuation spectra, string mass scale, and associated cosmic string tension. (These results follow directly from the treatments in refs. [10, 39, 41].) We consider the collision of a  $Dp$

brane with a  $Dp$  brane at an angle  $\theta$ ; collision with a  $Dp$  antibrane corresponds to  $\theta = \pi$ . (Here and throughout this section, we follow [10], which contains more details and discussion). Of the ten spacetime dimensions, one is the time, three are the large spatial dimensions we live in, and the rest are compactified. Of the compact dimensions,  $p - 3$  are parallel to the brane, and we take their compactification lengths to be  $\ell_{\parallel} = 2\pi r_{\parallel}$ , implying a volume  $V_{\parallel} = \ell_{\parallel}^{p-3}$ . Of the remaining  $d = 9 - p$  dimensions, we take  $d - d_{\perp}$  to be compactified with a size  $2\pi/M_s$ , where  $M_s$  is the string scale, while the remaining  $d_{\perp}$  are compactified with a size  $\ell_{\perp} = 2\pi r_{\perp} > 2\pi/M_s$ . The 10-dimensional gravitational coupling constant is

$$\kappa^2 = 8\pi G_{10} = \frac{g_s^2 (2\pi)^7}{2M_s^8} \quad (2.1)$$

where  $g_s$  is the expectation value of the dilatonic string coupling, which is related to the standard model gauge coupling  $\alpha(r_{\parallel})$  on a scale  $1/r_{\parallel}$  by

$$g_s = 2(M_s r_{\parallel})^{p-3} \alpha(r_{\parallel}) ; \quad (2.2)$$

the 4-dimensional Planck scale  $M_P = (8\pi G)^{-1/2}$  is then

$$g_s^2 M_P^2 = \frac{M_s^2 (M_s r_{\perp})^{d_{\perp}} (M_s r_{\parallel})^{p-3}}{\pi} . \quad (2.3)$$

The outcome of brane inflation will therefore depend on several parameters,  $p$ ,  $d_{\perp}$ ,  $r_{\perp}$ ,  $r_{\parallel}$  and  $\alpha(r_{\parallel})$ .

We will distinguish between two different potentials for the interaction between branes, depending on their separations. (See [39, 40, 41].) For some scenarios, a fixed lattice of branes is considered to be spread throughout the compactified dimensions, with a moving brane placed inside one lattice square. At separations small compared to the lattice size of the compactification topology, the interaction is ‘‘Coulombic’’, with a potential of the form  $V(y) = V_0 - U/y^{d_{\perp}-2}$  for a separation

$y$  in the large compact dimensions. This potential is suitable for inflation resulting from the collision of a pair of relatively nearby branes at a small angle [40]. When the separation is nearly equal to the lattice size, an expansion about zero displacement from the anti-podal point gives  $V(y) = V_0 - U'y^\sigma$ , where  $\sigma$  depends on the compactification topology. This potential is suitable for the brane-anti-brane scenario (which corresponds to branes at angle  $\pi$ ). In the next two subsections, we summarize the inflation scenario for interbrane potentials of these two general forms.

### 2.2.1 Coulombic Inflation

Consider a potential of the form

$$V(\psi) = V_0 \left( 1 - \frac{\eta}{(d_\perp - 2)\psi^{d_\perp - 2}} \right), \quad (2.4)$$

with  $\psi \propto y$ , the interbrane spacing; for the special case  $d_\perp = 2$  this becomes a logarithmic potential, but the results we derive below may be applied to this special case. (We only consider  $d_\perp - 2 \geq 0$  here to simplify our analysis, since the results generalize easily to the logarithmic case.) In the slow roll approximation, the equation of motion for  $\psi$  becomes

$$\frac{d\psi}{dL} = -\frac{\eta M_P^2}{\psi^{d_\perp - 1}}, \quad (2.5)$$

where  $L = \ln a$  is the logarithm of the scale factor  $a(t)$ , which we take to be zero at the start of inflation. The slow roll solution is then

$$\psi = \left[ \psi_i^{d_\perp} - d_\perp \eta M_P^2 L \right]^{\frac{1}{d_\perp}} = \left[ d_\perp \eta M_P^2 (L_{\text{inf}} - L) \right]^{\frac{1}{d_\perp}} \equiv (d_\perp \eta M_P^2 L_r)^{\frac{1}{d_\perp}}, \quad (2.6)$$

where the starting value of the field is  $\psi_i$ , the total number of e-folds in inflation, is

$$L_{\text{inf}} = \frac{\psi_i^{d_\perp}}{d_\perp \eta M_P^2}, \quad (2.7)$$

and  $L_r = L_{\text{inf}} - L$  is the total number of e-folds *remaining* in inflation. The curvature fluctuation spectrum is then

$$\Delta_{\mathcal{R}}^2(k) = \frac{H^4}{4\pi^2\dot{\psi}^2} = \frac{V_0(d_{\perp}L_r)^{2\left(1-\frac{1}{d_{\perp}}\right)}}{12\pi^2\eta^{\frac{2}{d_{\perp}}}M_P^{2+\frac{4}{d_{\perp}}}} \quad (2.8)$$

where  $L_r$  is evaluated when  $k/a = H$ , or  $\ln(k/k_0) = L_{r,0} - L_r$ , where  $k_0$  is a reference scale, which crosses with  $L_{r,0}$  e-folds remaining in inflation. The fluctuation spectrum is very flat, with only slowly varying scalar index,  $n_s(k)$ :

$$\begin{aligned} n_s(k) - 1 &= \frac{d \ln \Delta_{\mathcal{R}}^2(k)}{d \ln k} = -\frac{2}{L_r(k)} \left(1 - \frac{1}{d_{\perp}}\right) \simeq -0.03 \left[\frac{60}{L_r(k)}\right] \left(1 - \frac{1}{d_{\perp}}\right) \\ \frac{dn_s(k)}{d \ln k} &= -\frac{2}{L_r^2(k)} \left(1 - \frac{1}{d_{\perp}}\right) \simeq -6 \times 10^{-4} \left[\frac{60}{L_r(k)}\right]^2 \left(1 - \frac{1}{d_{\perp}}\right), \end{aligned} \quad (2.9)$$

both of which are in the range of uncertainty of the determinations in [2].

The challenge to this, or any other, inflation model is to have sufficient inflation as well as small curvature fluctuation. Since the precise value of  $L_{\text{inf}}$  depends on initial conditions as well as parameters of the model, let us first consider the constraints on the latter implied by comparing Eq. (2.8) to the WMAP result  $\Delta_{\mathcal{R}}^2(k_0) = 2.95 \times 10^{-9} A(k_0)$  with  $A(k_0) = 0.9 \pm 0.1$ . To do this, let us consider a particular model with  $p = 4$  and a small collision angle,  $\theta$ ; then we have

$$\begin{aligned} \psi &= y \sqrt{\frac{\tau_4 \ell_{\parallel}}{2}} \\ V_0 &= \frac{\tau_4 \ell_{\parallel} \theta^2}{4} \\ \frac{\tau_4 \ell_{\parallel}}{2} &= \frac{M_s^4}{32\pi^3 \alpha(r_{\parallel})} \\ \eta &= \frac{\beta(d_{\perp})}{16\pi} \theta M_s^{6-d_{\perp}} \left(\frac{\tau_4 \ell_{\parallel}}{2}\right)^{\frac{d_{\perp}-4}{2}} \\ \Delta_{\mathcal{R}}^2(k) &= \frac{(\theta d_{\perp} L_r)^{2\left(1-\frac{1}{d_{\perp}}\right)}}{24 [64\beta(d_{\perp})]^{\frac{2}{d_{\perp}}} \pi^{2+\frac{10}{d_{\perp}}} [\alpha(r_{\parallel})]^{\frac{4}{d_{\perp}}}} \left(\frac{M_s}{M_P}\right)^{2+\frac{4}{d_{\perp}}}, \end{aligned} \quad (2.10)$$

where

$$\tau_p = \frac{M_s^{p+1}}{(2\pi)^p g_s} \quad (2.11)$$

$$\beta = \begin{cases} \frac{1}{2\pi^{d_\perp/2}} \Gamma\left(\frac{d_\perp-2}{2}\right) & d_\perp > 2 \\ \frac{1}{\pi} & d_\perp = 2. \end{cases} \quad (2.12)$$

Let us consider the specific example  $d_\perp = 2$ ; for this case we find

$$\Delta_{\mathcal{R}}^2(k) = \frac{\theta L_r}{768\pi^6 [\alpha(r_\parallel)]^2} \left(\frac{M_s}{M_P}\right)^4 \quad [d_\perp = 2], \quad (2.13)$$

and therefore the string scale is determined to be

$$\frac{M_s}{M_P} \simeq 2.5 \times 10^{-2} [25\alpha(r_\parallel)]^{1/2} [A(k_0)]^{1/4} \left(\frac{10}{\theta L_r}\right)^{1/4} \quad [d_\perp = 2] \quad (2.14)$$

that is, on the same order of energy as the GUT scale,  $10^{15}$  GeV. Larger  $d_\perp$  leads to smaller  $M_s/M_P$ ; thus if  $d_\perp = 4$  we find

$$\Delta_{\mathcal{R}}^2(k) = \frac{(\theta L_r)^{3/2}}{12\sqrt{2}\pi^{7/2}\alpha(r_\parallel)} \left(\frac{M_s}{M_P}\right)^3 \quad [d_\perp = 4], \quad (2.15)$$

which in turn requires

$$\frac{M_s}{M_P} \simeq 1.6 \times 10^{-3} [25\alpha(r_\parallel)]^{1/3} [A(k_0)]^{1/3} \left(\frac{10}{\theta L_r}\right)^{1/2} \quad [d_\perp = 4]. \quad (2.16)$$

The total number of e-folds in inflation is

$$\begin{aligned} L_{\text{inf}} &= \frac{(M_s y_i)^{d_\perp} M_s^2}{64\pi^5 \beta(d_\perp) \theta [\alpha(r_\parallel)]^2 M_P^2} = \frac{\pi^{\frac{d_\perp(d_\perp-1)}{d_\perp+2}} (2\zeta_i M_s r_\perp)^{d_\perp}}{\theta^{\frac{3d_\perp}{d_\perp+2}} (d_\perp L_r)^{\frac{2(d_\perp-1)}{d_\perp+2}}} \left[ \frac{3\Delta_{\mathcal{R}}^2(k)}{8\beta(d_\perp)\alpha^2(r_\parallel)} \right]^{\frac{d_\perp}{d_\perp+2}} \\ &\simeq \frac{0.025[A(k_0)]^{1/2}}{[25\alpha(r_\parallel)](10\theta)} \left(\frac{10}{\theta L_r}\right)^{1/2} (\zeta_i M_s r_\perp)^2 \quad [d_\perp = 2] \\ &\simeq \frac{0.025[A(k_0)]^{2/3}}{[25\alpha(r_\parallel)]^{4/3}(10\theta)} \left(\frac{10}{\theta L_r}\right) (\zeta_i M_s r_\perp)^4 \quad [d_\perp = 4], \end{aligned} \quad (2.17)$$

where we have let  $y_i = 2\pi r_\perp \zeta_i$  with  $\zeta_i \lesssim 1$ . To get  $L_{\text{inf}} \gtrsim 60$ , we must require  $\zeta_i M_s r_\perp \gtrsim 50$  for  $d_\perp = 2$  or  $\zeta_i M_s r_\perp \gtrsim 10$  for  $d_\perp = 4$ . Note, though, that for large  $\theta$ , it is not possible to have enough expansion during inflation. In this case, the images of one brane exert non-trivial forces on the other brane, resulting in a power-law type potential.

## 2.2.2 Power Law Inflation

Next, we consider potentials of the form

$$V(\psi) = V_0 (1 - \eta\psi^\sigma) ; \quad (2.18)$$

such potentials arise for a brane situated near the origin. The value of  $\sigma$  depends on the compactification topology. For hypercubic compactification,  $\sigma = 4$ , whereas in other cases,  $\sigma = 2$ . Note that in actuality the potential need not depend just on interbrane separation in such a picture, and the trajectory of the brane can be complicated. Here, though, we confine ourselves to simple one dimensional (diagonal) brane motion.

Following Eq. (2.18), we see that the origin –  $\psi = 0$  – is an unstable equilibrium point, and any perturbation away from it will result in slow motion of the brane. For  $\sigma > 2$ , the slow roll solution is

$$\psi = [\psi_i^{\sigma-2} - \sigma(\sigma-2)\eta M_P^2 L]^{\frac{1}{\sigma-2}} = [\sigma(\sigma-2)\eta M_P^2 L_r]^{\frac{1}{\sigma-2}} , \quad (2.19)$$

and the total number of e-folds in inflation is

$$L_{\text{inf}} = \frac{\psi_i^{\sigma-2}}{\sigma(\sigma-2)\eta M_P^2} , \quad (2.20)$$

where  $\psi_i$  is the starting value for the inflaton. Quantum fluctuations will imply  $\psi_i = \zeta_i H/2\pi$ , where  $\zeta_1 \sim 1$ . The curvature fluctuation spectrum is

$$\Delta_{\mathcal{R}}^2(k) = \frac{V_0(\sigma-2)^2[\sigma(\sigma-2)\eta]^{\frac{2}{\sigma-2}} M_P^{\frac{2(4-\sigma)}{\sigma-2}} L_r^{\frac{2(\sigma-1)}{\sigma-2}}}{12\pi^2} . \quad (2.21)$$

The implied fluctuation spectrum is acceptably flat:

$$\begin{aligned} n_s(k) - 1 &= \frac{d \ln \Delta_{\mathcal{R}}^2(k)}{d \ln k} = -\frac{2(\sigma-1)}{(\sigma-2)L_r(k)} \simeq -\frac{0.03(\sigma-1)}{\sigma-2} \left[ \frac{60}{L_r(k)} \right] \\ \frac{dn_s(k)}{d \ln k} &= -\frac{2(\sigma-1)}{L_r^2(k)(\sigma-2)} \simeq -6 \times 10^{-4} \left( \frac{\sigma-1}{\sigma-2} \right) \left[ \frac{60}{L_r(k)} \right]^2 \end{aligned} \quad (2.22)$$

For  $\sigma = 4$ , Eqs. (2.21) and (2.20) become

$$\begin{aligned}\Delta_{\mathcal{R}}^2(k) &= \frac{8\eta V_0 L_r^{3/2}}{3\pi^2} \\ L_{\text{inf}} &= \frac{\zeta_i^2 V_0}{96\pi^2 M_P^4 (\eta V_0)} ;\end{aligned}\tag{2.23}$$

the observational constraints on the curvature fluctuation spectrum therefore require

$$\eta V_0 = \frac{3\pi^2 \Delta_{\mathcal{R}}^2(k)}{8L_r^{3/2}} \simeq 2.5 \times 10^{-11} A(k_0) \left(\frac{60}{L_r}\right)^{3/2},\tag{2.24}$$

i.e. the potential must be extremely flat. This requirement is well-known from studies of new inflation, which sometimes idealize the potential to Eq. (2.18) with a small dimensionless parameter  $\lambda$  equivalent to  $\eta V_0$ . In ref. [10], a particular toroidal compactification is proposed where this small parameter is ( $F$  is a geometrical factor related to the compactification geometry)

$$\eta V_0 \simeq \frac{g_s \theta^4 F \beta}{16\pi \alpha^3} \left(\frac{M_s}{M_P}\right)^4,\tag{2.25}$$

which can be small enough for  $\theta \sim 0.1$  provided that

$$\frac{M_s}{M_P} \simeq 10^{-3}.\tag{2.26}$$

In this picture, the flatness of the effective potential is attributed to a relatively small value of the string scale compared with the Planck mass.

Special treatment is needed for  $\sigma = 2$ , which is expected for any non-hypercubic compactification topology. For this case, the scale factor grows like a powerlaw in time during slow roll:

$$\psi = \psi_i \left(\frac{a}{a_i}\right)^{2\eta M_P^2} = \psi_f \left(\frac{a}{a_f}\right)^{2\eta M_P^2},\tag{2.27}$$

where  $\psi_f$  and  $a_f$  are the values of the field and scale factor at the end of slow rolling. Since  $d \ln \psi / d \ln a = 2\eta M_P^2$ , we require  $\eta M_P^2 \ll 1$  for slow rolling. It is

easy to see that for this potential,  $\ddot{\psi}/3H\dot{\psi} = 2\eta M_P^2/3 \ll 1$ . Slow roll ends, for this potential, only when  $\dot{\psi}^2/2V_0 = 2\eta^2 M_P^2 \psi^2/3 \simeq 1$ , or  $\psi_f \simeq (\eta M_P)^{-1} \gg M_P$ , or when the polynomial approximation to the potential fails, which happens when the brane moves a substantial fraction of a lattice spacings. The total number of e-folds in inflation is

$$L_{\text{inf}} = \frac{\ln(\psi_f/\psi_i)}{2\eta M_P^2} = \frac{\ln(y_f/y_i)}{2\eta M_P^2} . \quad (2.28)$$

The curvature fluctuation spectrum for this case is

$$\Delta_{\mathcal{R}}^2(k) = \frac{(H/2\pi\psi_f)^2 e^{4\eta M_P^2 L_r}}{4(\eta M_P^2)^2} = \frac{(H/2\pi\psi_i)^2 (a_i/a)^{4\eta M_P^2}}{4(\eta M_P^2)^2} = \frac{(H/2\pi\psi_i)^2 (a_i H/k)^{4\eta M_P^2}}{4(\eta M_P^2)^2} , \quad (2.29)$$

where evaluating at horizon crossing implies that  $k = Ha$ , which has been used to get the final form of the spectrum. In this case,

$$n_s - 1 = \frac{d \ln \Delta_{\mathcal{R}}^2(k)}{d \ln k} = -4\eta M_P^2 , \quad (2.30)$$

which is independent of  $k$ . The WMAP analysis implies that  $\eta M_P^2 \lesssim 0.01$ . From the first form of Eq. (2.29), and  $\eta M_P^2 \simeq 0.01$ , it follows that the observed temperature fluctuations can be accounted for if ( $V_0 = 2\tau_4 \ell_{\parallel}$ )

$$\frac{H}{2\pi\psi_f} \sim (2\pi M_P y_f)^{-1} \sim 10^{-7} \left( \frac{\eta M_P^2}{0.01} \right) , \quad (2.31)$$

in which case  $L_{\text{inf}} \sim 10^3$ . For  $y_f \simeq 2\pi r_{\perp}$ , this relation implies

$$\frac{M_s}{M_P} \sim 10^{-6} \left( \frac{\eta M_P^2}{0.01} \right) M_s r_{\perp} , \quad (2.32)$$

which is generally smaller than our previous estimates unless  $M_s r_{\perp} \sim 10^3$ .

### 2.2.3 Cosmic String Properties

Because the inflaton and the ground state open string modes responsible for defect formation are different, and the ground state open string modes become tachyonic

and develop vacuum expectation values only towards the end of the inflationary epoch, various types of defects (lower-dimensional branes) may be formed. *A priori*, defect production after inflation may be a serious problem. Fortunately, the properties of superstring / brane theory tell us defect production is not a problem in these models. When considered in the context of cosmological evolution, brane models for inflation can only produce copious numbers of one kind of defect: cosmic strings [10]. In superstring theory,  $Dp$ -branes come with either odd  $p$  (in IIB theory) or even  $p$  (in IIA theory). The collision of a  $Dp$ -brane with another  $Dp$ -brane at an angle (or with an anti- $Dp$ -brane) yields  $D(p-2)$ -solitons (i.e., codimension 2). Topologically, a variety of defects may be produced. Because they have even codimensions with respect to the branes that collide, they have specific properties [46]. Cosmologically, since the compactified dimensions tangent to the brane are smaller than the Hubble size, the Kibble mechanism works only if all the codimensions are tangent to the uncompactified dimensions. As a consequence, only cosmic strings may be copiously produced [10].

The observational imprint of cosmic strings is determined primarily by the product of Newton's constant and the cosmic string tension,  $G\mu$ , assuming the evolution of the string network can reach the scaling regime. The value of  $\mu$  implied by superstring cosmology depends on several parameters, but is most sensitive to the string scale,  $M_s$ . To get an order of magnitude estimate, we may use the small  $\theta$  case, which is arguably the most likely inflationary scenario.

The cosmic strings may be D1-branes, but most likely, they are  $D(p-2)$ -branes wrapping around  $(p-3)$ -cycles in the compactified dimensions. If the D1-brane is the cosmic string (i.e.,  $p=3$ ), its tension is simply the cosmic string tension:

$$\mu = \tau_1 = \frac{M_s^2}{2\pi g_s} . \quad (2.33)$$

However, we expect the string coupling generically to be  $g_s \gtrsim 1$ . (It is well-known that radion and dilaton moduli are not stabilized by perturbative dynamics in string theory. Presumably, any superstrongly coupled string model is dual to a weakly coupled one, and thus cannot stabilize the moduli either. We therefore expect a moderately strong string coupling, since only in this case will we find non-trivial dynamics.) To obtain a theory with a weakly coupled sector in the low energy effective field theory (i.e., the standard model of strong and electroweak interactions with weak gauge coupling constant  $\alpha$ ), it then seems necessary to have the brane world picture, in which we have the  $Dp$ -branes for  $p > 3$ , where the  $(p - 3)$  dimensions are compactified to volume  $V_{\parallel}$ . Now the cosmic strings are  $D(p - 2)$ -branes, with the  $(p - 3)$  dimensions compactified to the same volume  $V_{\parallel}$ . Noting that a  $Dp$ -brane has tension  $\tau_p = M_s^{p+1}/(2\pi)^p g_s$ , the tension of such cosmic strings is

$$\mu = \frac{M_s^{p-1} V_{\parallel}}{(2\pi)^{p-2} g_s} = \frac{M_s^2 v_{\parallel}}{2\pi g_s} = \frac{M_s^2}{4\alpha\pi} \simeq 2M_s^2 \quad (2.34)$$

for  $\alpha \simeq \alpha_{GUT} \simeq 1/25$ . For one pair of branes at angle  $\theta$ , only this type of cosmic strings is produced topologically. For a large enough stack of branes colliding, the  $D1$ -branes may also be allowed topologically, but they are not produced cosmologically. Thus,  $\mu \simeq 2M_s^2$  is a reasonably general estimate. We considered estimates of  $M_s$  implied in various scenarios for brane inflation in § 2.2.1 and 2.2.2. These estimates are broadly consistent with

$$10^{-6} \gtrsim G\mu \gtrsim 10^{-11} , \quad (2.35)$$

although a smaller range is obtained in any specific model or class of setups. For example, for branes colliding at a small angle, a likely range is

$$5 \times 10^{-7} \gtrsim G\mu \gtrsim 7 \times 10^{-8} . \quad (2.36)$$

Thus, brane inflation can lead to cosmic string tensions below, but not far below, current observational bounds.

## 2.2.4 Tensor modes

During slow roll, the tensor power is

$$\Delta_h^2(k) = \frac{128G^2V_0}{3} = \frac{2V_0}{3\pi^2M_P^4} \quad (2.37)$$

and is smaller than the scalar power by the factor

$$r(k) = 8M_P^2 \left( \frac{V'}{V} \right)^2 = \frac{8}{M_P^2} \left( \frac{d\phi}{d \ln a} \right)^2. \quad (2.38)$$

How small  $r(k)$  is depends on the specific brane inflation model. For branes intersecting at an angle  $\theta$  we find that

$$\begin{aligned} \Delta_h^2(k) &= \frac{2V_0}{3\pi^2M_P^4} = \frac{\theta^2 M_s^4}{96\pi^5\alpha(r_{\parallel})M_P^4} \\ &= 3.3 \times 10^{-12} (10\theta)^2 [25\alpha(r_{\parallel})] \left[ \frac{10A(k_0)}{\theta L_r} \right] \quad [d_{\perp} = 2] \\ &= 5.4 \times 10^{-17} (10\theta)^2 [25\alpha(r_{\parallel})]^{1/3} [A(k_0)]^{4/3} \left( \frac{10}{\theta L_r} \right)^2 \quad [d_{\perp} = 4] \end{aligned} \quad (2.39)$$

In this case, the amplitude of the scalar mode is smaller than the amplitude of the perturbations due to cosmic strings by a small numerical factor times  $\theta^2$ . For powerlaw brane-antibrane inflation,  $\theta \rightarrow \pi$ , and  $V_0 = M_s^4/(2\pi)^3\alpha$  [39, 10], so for this case we find

$$\Delta_h^2(k) = \frac{M_s^4}{12\pi^5\alpha M_P^4}. \quad (2.40)$$

Nominally, these perturbations can be comparable to those induced by cosmic strings, although they may be relatively suppressed by the small numerical factor  $(12\pi^5\alpha)^{-1} \simeq 0.007/(25\alpha)$ . However, the spectrum of fluctuations produced by cosmic strings will still distinguish them from those due to primordial tensor modes.

Both strings and the primordial tensor modes result in the B-type polarization of the CMBR. The predicted angular power spectrum,  $C_l^{BB}$ , has been calculated for tensor modes from inflation (see *e.g.* ref. [47]). It has a generic feature that most of the power is on larger angular scales, in the region  $l \lesssim 100$ . This is very different from the shape of the  $C_l^{BB}$  spectrum predicted by cosmic strings. There the dominant contribution comes from the vector modes and, as will be explained in Chapter 3 and illustrated in Fig. 3.6, most of the power is on smaller scales:  $700 \lesssim l \lesssim 1000$ .

As of today, the B-type polarization has not been detected [48] and the experimental constraint on  $r(k)$  is rather mild:  $r(k_0 = 0.002\text{Mpc}^{-1}) \lesssim 0.71$  [35].

CHAPTER 3  
COSMOLOGICAL CONSTRAINTS ON A NETWORK OF COSMIC  
STRINGS

First appeared as *Bounds on Cosmic Strings from WMAP and SDSS* in Phys. Rev. **D72** (2005) 023513; modified in light of ref. [49].

We find the constraints from WMAP and SDSS data on the fraction of cosmological fluctuations sourced by local cosmic strings using a Markov Chain Monte Carlo (MCMC) analysis. In addition to varying the usual 6 cosmological parameters and the string tension ( $\mu$ ), we also varied the amount of small-scale structure on the strings. Our results indicate that cosmic strings can account for up to 7 (14)% of the total power of the microwave anisotropy at 68 (95)% confidence level. The corresponding bound on the string mass per unit length, within our string model, is  $G\mu < 1.8(2.7) \times 10^{-7}$  at 68 (95)% c.l. We also calculate the B-type polarization spectra sourced by cosmic strings and discuss the prospects of their detection.

### 3.1 Introduction

While cosmic strings could not have seeded all of the structure in the Universe, they could have created a subdominant yet non-negligible fraction of the primordial cosmological fluctuations [37, 38, 50]. This idea has recently received renewed attention with the realization that cosmic strings are produced in a wide class of string theory models of the inflationary epoch [10, 22, 45, 51, 52]. In these models, inflation can arise during the collisions of branes that coalesce to form,

ultimately, the brane on which we live [6, 39, 40, 41]. Brane inflation predicts adiabatic temperature and dark matter fluctuations capable of reproducing all currently available observations. In addition, the collision at the conclusion of brane inflation can produce a network of local cosmic strings [10], whose effects on cosmological observables range from negligible to substantial, depending on the specific scenario [22]. It has also been shown that strings could form at an observationally acceptable level at the end of the D-term inflation in SUSY GUT models [38]. As the precision of cosmological observations increases, one might hope to distinguish among the numerous presently-viable models of inflation by studying and constraining the properties of the cosmic strings they predict.

The aim of this chapter's analysis is to constrain the properties of cosmic strings by using the power spectrum data from the WMAP and SDSS experiments. There are other ways to constrain cosmic strings – some of them promising to produce much tighter bounds than those that will ever be possible with power spectrum data. We give a brief review of other methods in the summary section, Sec. 3.4.

The rest of this paper is organized as follows. In Sec. 3.2 we give a detailed account of the model and the methods used. We show the results in Sec. 3.3 and conclude with a discussion in Sec. 3.4.

## 3.2 The Model and Analysis

The fluctuations resulting from brane inflation are expected to be an incoherent superposition of contributions from adiabatic perturbations initiated by curvature fluctuations and active perturbations induced by the decaying cosmic string network. The resulting CMB angular spectra can be written as a sum of the adiabatic

and string contributions:

$$C_l = C_l^{\text{ad}} + C_l^{\text{cs}}. \quad (3.1)$$

Analogous expressions hold for matter density spectra. We restrict our study to a flat FRW universe and vary the following cosmological parameters: the Hubble constant  $h$ , the matter density  $\Omega_M h^2$ , the baryon density  $\Omega_b h^2$ , and the reionization optical depth  $\tau$ . In addition, we vary the galaxy bias factor  $F_b$ , the amplitude  $A_s$  and the spectral index  $n_s$  of the primordial scalar power spectrum, as well as the string mass per unit length,  $G\mu$ , and the string wiggleness parameter  $\alpha_r$  (to be defined in Sec. 3.2.1).

We used a suite of different codes to produce and analyze the spectra. The model we employed for the cosmic string-generated perturbations is described in the subsection below. The string CMB and matter spectra were calculated using a modification [53] of CMBFAST [54] (see Figs. 3.1 and 3.2 for representative string induced spectra). We first evaluated and stored the string spectra on a grid of parameters. During our calculations, the spectra were obtained by interpolation on the grid. The adiabatic matter spectra were also stored on a grid after having been evaluated using a publicly available version of CMBFAST. For the adiabatic CMB spectra, we used the package CMBWarp [55].

To compare the theoretical linear matter power spectrum  $P^L(k)$  generated by our code with the SDSS results, we first applied the halo-fitting procedure of Smith et al. [56] to obtain the non-linear spectra,  $P^{\text{NL}}(k)$ . This procedure is only valid for the adiabatic contribution to the  $P(k)$  spectrum, so using it for the cosmic string contribution introduces some inaccuracy into our model. However, as we can see in Fig. 3.2, the string power spectrum is considerably weaker than the adiabatic power spectrum on all but the smallest length scales even in models

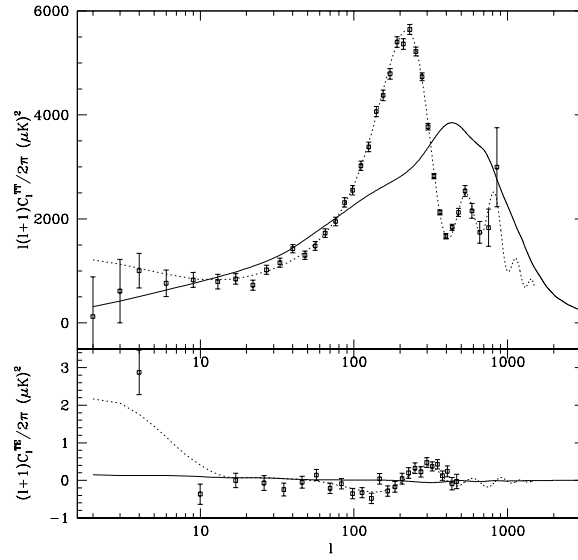


Figure 3.1: The CMB TT and TE spectra (solid lines) sourced by cosmic strings with wiggleness parameter  $\alpha_r = 1.9$ , as well as the adiabatic spectra for the same cosmological parameters (dashed lines) and WMAP's first year data. The string spectra are normalized so that the *total* TT power is the same for the two lines, which corresponds to  $B = 1$ .

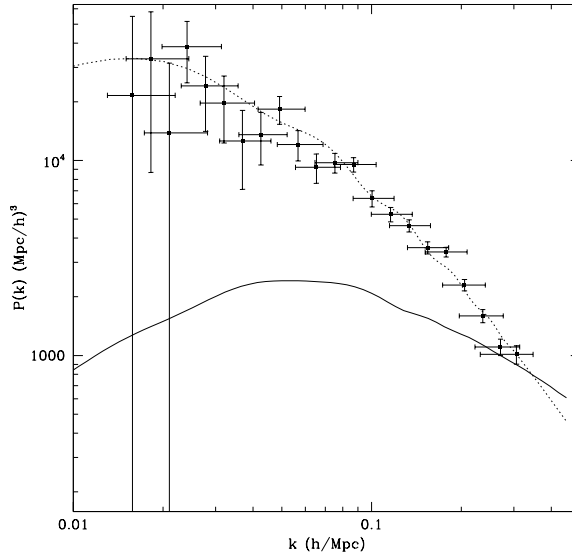


Figure 3.2: The string-generated matter power spectrum (solid line) for the same parameters as in Fig. 3.1, i.e., for  $B = 1$ . The dashed line represents the linear spectrum from adiabatic perturbations at  $z = 0$ .

where strings account for all the large-scale microwave anisotropy. Thus, since only a small portion of the relevant values of  $k$  are affected by the halo-fitting procedure, and since the effect is small on the scales we consider, we expect any inaccuracy introduced by our approximate treatment of nonlinearity to be unimportant. Next, we assumed that the galaxy bias factor and the correction due to peculiar velocities on the scales of our interest ( $k < 0.2$  h/Mpc) are approximately redshift- and scale-independent and can be combined into a single constant factor,  $F_b$ , multiplying the matter spectrum:

$$P(k) = F_b P^{\text{NL}}(k). \quad (3.2)$$

We then fit  $P(k)$  to the SDSS power spectrum data (for  $k < 0.2$  h/Mpc) with  $F_b$  as a free parameter.

The likelihood of the spectra for a given set of parameters was obtained using

the publicly-available likelihood codes produced by the WMAP [3] and SDSS [57] teams.

### 3.2.1 The Cosmic String Model

Unlike the adiabatic inflationary perturbations, which are set as initial conditions in the equations of motion of linear perturbations, cosmic strings act as a continual source of fluctuations as the universe evolves. The density and temperature fluctuations created in the immediate locality of a cosmic string are highly non-linear, e.g. the density contrast  $\delta\rho/\rho$  is significantly larger than unity in the wake formed behind a moving string. However, the effect of strings on cosmological scales is that of a small perturbation to the evolution of the average cosmic energy-momentum tensor. Hence, for the purpose of computing the CMB and LSS spectra, the metric and density perturbations caused by strings are described by the system of linearized Einstein-Boltzmann equations with strings acting as active sources.

Evaluation of the CMB and LSS spectra sourced by strings requires knowing their energy-momentum tensor (or its unequal time correlation functions [58]) for the entire dynamical range of the calculation, which is approximately four orders of magnitude in scale factor. Realistic simulations of cosmic string networks have so far been limited either in their dynamical range [59] or their resolution [60]. Hence, until full scale simulations become available, one is forced to resort to approximate methods to model the string sources.

Numerical simulations [61, 62, 63] show that during the radiation and matter dominated eras the string network evolves according to a scaling solution, which on sufficiently large scales can be described by two length scales. The first scale,  $\xi(t)$ , is the coherence length of strings, i. e. the distance beyond which directions

along the string are uncorrelated. The second scale,  $L(t)$ , is the average inter-string separation. Scaling implies that both length scales grow in proportion to the horizon. Simulations indicate that  $\xi(t) \sim t$ , while  $L(t) = \gamma t$ , with  $\gamma \approx 0.8$  in the matter era [61, 62]. The one-scale model [64, 65], in which the two length scales are assumed to be equal, has been quite successful in describing the general properties of cosmic string networks inferred from numerical simulations. These simulations assume that cosmic strings reconnect on every intersection. It is of interest to us, however, to also consider the case when the reconnection probability is less than one. If strings can move and interact in extra dimensions then, while appearing to intersect in our three dimensions, they may actually miss each other. Hence, the effective intercommutation rate of these strings will generally be less than unity. As a consequence, one would expect more strings per horizon in these theories [22, 23]. Because of the straightening of wiggles on sub-horizon scales due to the expansion of the universe, one would still expect  $\xi(t) \sim t$ . However, the string density would increase, therefore reducing the inter-string distance. Hence, smaller inter-commutation probabilities imply smaller  $\gamma$ .

In addition, numerical simulations show that long strings possess a great deal of small-scale structure in the form of kinks and wiggles on scales much smaller than the horizon. To an observer who cannot resolve this structure, the string will appear to be smooth, but with a larger effective mass per unit length  $\tilde{\mu}$  and a smaller effective tension  $\tilde{T}$ . An unperturbed string (with  $\mu = T$ ) exerts no gravitational force on nearby particles. In contrast, a wiggly string with  $\tilde{\mu} > \tilde{T}$  attracts particles like a massive rod. The effective equation of state of a wiggly strings is  $\tilde{\mu}\tilde{T} = \mu^2$  [66, 67]. Depending on the brane inflation model, the presence of extra dimensions could mean that even more small scale structure would be

present on the strings [22].

To calculate the sources of perturbations we use an updated version of the cosmic string model first introduced by Albrecht et al. [16] and further developed in refs. [53, 68], where the wiggly nature of strings was taken into account. In this model, the string network is represented by a collection of uncorrelated straight string segments produced at some early epoch, moving with uncorrelated, random velocities. At every subsequent epoch, a certain fraction of the number of segments decays in a way that maintains network scaling. The length of each segment at any time is taken to be equal to the correlation length of the network. This length and the root-mean-square (r.m.s.) velocity of segments are computed from the velocity-dependent one-scale model of Martins and Shellard [69]. The positions of segments are drawn from a uniform distribution in space, and their orientations are chosen from a uniform distribution on a two-sphere. This model is a rather crude approximation of a realistic string network. However, there are good reasons to believe that its predictions for the CMB and LSS spectra are close to what one would obtain by using full-scale simulations. Its parameters have been calibrated to produce source correlation functions in agreement with those in [70], where comparison to a full simulation was possible. Also, the *shape* of the spectra obtained using this model are in good agreement with results of other groups [71, 72, 73], who used different methods that are also approximate. Finally, on the cosmological scales probed by the CMB measurements, the fine details of the string evolution do not play a major role. It is the large-scale properties – such as the scaling distance, the equation of state (wiggleness), the r.m.s. velocity, and how all these characteristics evolve through the radiation-matter equality – that determine the shape of the string-induced spectra. All of these effects are

accounted for in our model and can, in principle, be adjusted to match any specific cosmic string model. We choose to work with this model because one can easily calculate the sources for different cosmological parameters and because it allows us to include the effect of the wiggleness [53], which could be one of the distinguishing features of strings produced in theories with extra dimensions [22]. Unfortunately, though, some errors in the implementation of our code [49] that were found after this analysis had been completed means that the present analysis is unable to say anything about cosmic string wiggleness. The other main effect of the presence of extra dimensions, the increased string density, can be approximately factored in by multiplying the spectra by  $N_s \sim \gamma^{-2}$ .

For technical details of the model, the reader is referred to [53] and references therein. In principle, the wiggly nature of strings is accounted for by modifying the string energy-momentum tensor so that it corresponds to the wiggly string equation of state:

$$\tilde{\mu} = \alpha\mu, \quad \tilde{T} = \alpha^{-1}\mu, \quad (3.3)$$

where  $\alpha$  is a parameter describing the wiggleness,  $\tilde{\mu}$  and  $\tilde{T}$  are the mass per unit length and the string tension of the wiggly string, and  $\mu$  is the tension (or, equivalently, the mass per unit length) of the smooth string. In addition to modifying the equation of state, the presence of small-scale structure slows strings down on large scales. We account for this by dividing the root mean squared string velocity by the parameter  $\alpha$ . The wiggleness of the strings remains approximately constant during the radiation and matter eras, but changes its value during the transition between the two. We take the radiation era value,  $\alpha_r$ , to be a free parameter that we vary, and set the matter era value to be  $\alpha_m = (1 + \alpha_r)/2$ , with a smooth interpolation between the two values (as prescribed in [53]). For conventional strings,

this roughly agrees with results of numerical simulations [61, 62] which show a decrease from  $\alpha_r \sim 1.8 - 1.9$  in the radiation era to  $\alpha_m \sim 1.4 - 1.6$  in the matter era.

The qualitative features of the cosmic string spectra are quite independent of the details of the model. Hence, the observational constraint that we report here are based only on the *shape* of the spectrum (such as the constraint on the parameter  $f$  defined below) can be viewed as less model-dependent than our other results.

It is well known that properties and possible observational signatures of global and local strings can be very different. Global strings predict almost no power on small angular scales for CMB temperature anisotropy [58], while local strings – as we have argued above – produce a quite significant broad peak at  $l \sim 450$  in a spatially flat universe [16, 53, 71, 72, 73, 74]; this can be seen in Fig. 3.1. We will only concern ourselves with local strings. For the most recent constraints on global strings the reader is referred to refs. [75] and [76].

Rather than working directly with the string parameter  $G\mu$ , we introduce a parameter  $B$ , defined as

$$B \equiv \left( \frac{\mu}{\mu_0} \right)^2, \quad (3.4)$$

where  $\mu_0$  is the tension that one obtains by setting the total power in string induced CMB anisotropy to be equal to the total power observed by WMAP. That is, we set

$$I^{cs} \equiv \sum_l \frac{(2l+1)}{4\pi} C_l^{cs}(\mu_0, \alpha_r^{(0)}, \vec{p}_0) = I^{\text{WMAP}}, \quad (3.5)$$

where we take  $\alpha_r^{(0)} = 1.9$  and  $\vec{p}_0$  is a fixed set of the remaining cosmological parameters that have taken to correspond to the the best fit  $\Lambda$ CDM model of Tegmark et al [5]. The value of  $G\mu_0$  that we obtain with this prescription is

$1.1 \times 10^{-6}$ . Speaking very loosely,  $B$  can be said to measure the fraction of the anisotropy due to strings. Note, however, that this meaning is modified if, for instance, the strings have a different amount of small-scale structure ( $\alpha_r \neq 1.9$ ) or if they have reduced intercommutation probabilities.  $B$  is only really useful as an intermediate parameter. Our main results are the constraints on  $G\mu$  that we obtain from  $B$  and the fraction  $f$  of the total CMB anisotropy due to strings (Eq. (3.6)).

### 3.2.2 Markov Chain Monte Carlo

Because of the large size of our parameter space (nine parameters in total), we have used the Markov Chain Monte Carlo (MCMC) method for exploring the likelihood surface and for generating marginalized posterior distribution functions for the model parameters. We employed the MCMC algorithm described in the Appendix of [5].

We ran eight separate chains initialized at randomly generated initial positions within our prior range. The priors, given in Table 3.1, were chosen with the expectation of the string contribution being subdominant and the best fit parameters being close to their WMAP best fit values [2]<sup>1</sup>. Since we expected values of  $B$  near zero to be preferred, we also allowed  $B$  to range slightly below zero so as not to restrict artificially the ability of the chain's random steps to explore near  $B = 0$ ; values below zero were discarded when the data were analyzed. One advantage to our use of multiple chains rather than a single, long chain was that we were able to verify directly that there was adequate mixing in each chain, since each

---

<sup>1</sup>The restriction on wiggleness,  $\alpha_r < 4$ , was to save computing time. In the end we only integrate over this parameter anyway, due to errors in our code [49].

Table 3.1: Prior constraints on the parameters

$0 \leq B$
$1 \leq \alpha_r \leq 4$
$0 \leq A_s$
$0.92 \leq n_s \leq 1.07$
$0.019 \leq \Omega_B h^2 \leq 0.028$
$0.1 \leq \Omega_M h^2 \leq 0.2$
$0.5 \leq h \leq 0.8$
$0 \leq \tau \leq 0.23$
$0 \leq F_b$

successfully forgot its starting location and located the same maximum likelihood region of the parameter space.

### 3.3 Results

#### 3.3.1 The fraction in strings and $G\mu$

To test our MCMC code we first ran a chain with the string contribution set to zero ( $B = 0$ ). The results are shown in Table 3.2. Our results are consistent with those found in a similar analysis of the same data by members of the SDSS team [5].

Each of our eight chains allowed variation in all nine parameters. The results are summarized in Fig. 3.3 and Table 3.2. In Fig. 3.3 we plot the marginalized 1-D posterior distribution functions for eight of the nine parameters we allowed to

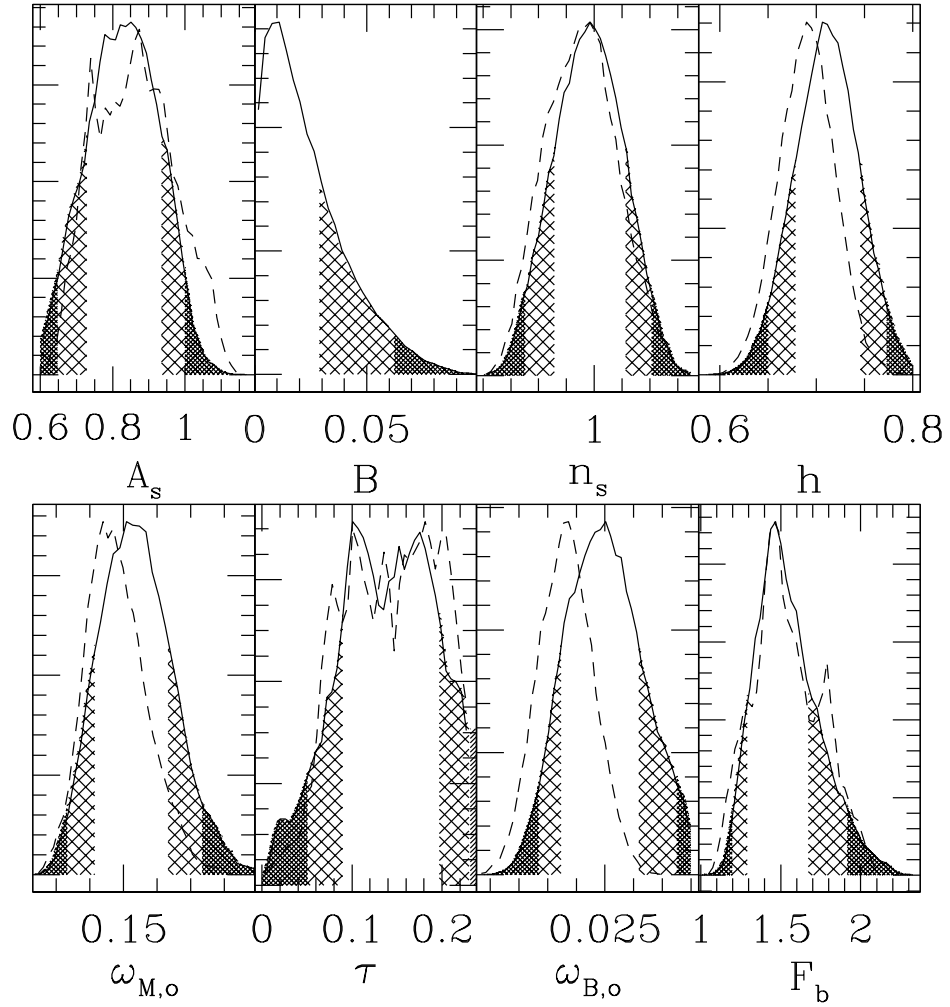


Figure 3.3: The one-dimensional projected PDFs for the 8 parameters varied by our Markov Chain Monte Carlo code; note that  $\omega_B = \Omega_B h^2$ ,  $\omega_M = \Omega_M h^2$ . The solid line represents the PDFs for models where cosmic strings are included; the dashed line represents the PDFs for models with  $B = 0$ , i.e. without cosmic strings. Each curve has been rescaled such that its area is unity. For each PDF the lightly shaded regions are excluded at the 68% confidence region; the dark regions are excluded at the 95% confidence region.

Table 3.2: The best fit results

Parameter	$B = 0$	$B > 0$
$f$	—	$< 0.068$ (68%), $< 0.14$ (95%)
$B$	—	$< 0.029$ (68%), $< 0.062$ (95%)
$A_s$	$0.87^{+0.08}_{-0.16}$	$0.85^{+0.09}_{-0.13}$
$n_s$	$1.0^{+0.02}_{-0.04}$	$1.0 \pm 0.026$
$\Omega_B h^2$	$0.024 \pm 0.001$	$0.025^{+0.0012}_{-0.0016}$
$\Omega_M h^2$	$0.15 \pm 0.01$	$0.15^{+0.013}_{-0.01}$
$h$	$0.69 \pm 0.03$	$0.71 \pm 0.034$
$\tau$	$0.155 \pm 0.057$	$0.143 \pm 0.054$
$F_b$	$1.46^{+0.24}_{-0.22}$	$1.47^{+0.2}_{-0.18}$

vary in our analysis; the cosmic string wiggleness is simply integrated over, since errors in our code washed out our ability to disentangle the contribution from wiggleness. The solid lines represent the PDFs for these parameters with cosmic strings included; the dashed lines show the results without cosmic strings ( $B = 0$ ). We have shaded the regions excluded at 68% (light) and 95 % (dark) confidence. The peaks of each of these PDFs and the one-sigma error bars are given in Table 3.2; for the parameter  $\tau$ , where the results lack a clear peak, we have taken the midpoint of the 68 % confidence region as our “peak” value.

The resulting cosmology with cosmic strings included is very close to the cosmology without cosmic strings. This verifies our hypothesis: a subdominant admixture of cosmic strings into the cosmological perturbation spectra gives a minor modification to the resulting cosmological parameters as determined in such a

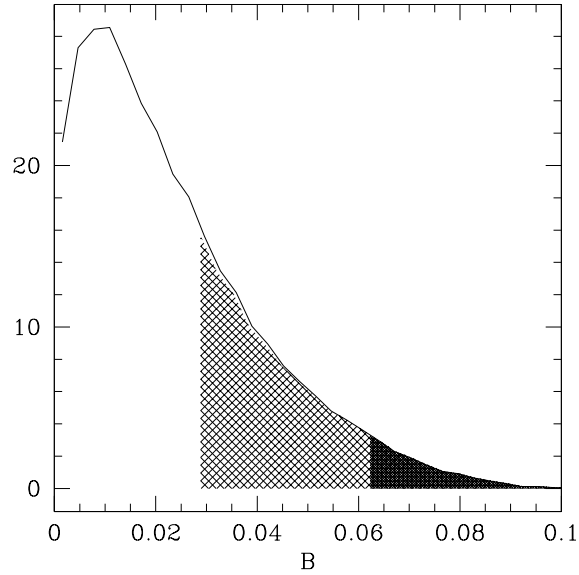


Figure 3.4: The PDF for the cosmic string weighting parameter,  $B \equiv (G\mu/1.1 \times 10^{-6})^2$ .

model. The only noticeable shift caused by including cosmic strings comes in the peak likelihood in the PDF for  $\Omega_B h^2$ , and even this shift is small. The only potentially worrisome aspect of these PDFs is the fact that the PDF for  $\tau$  appears to be running into the upper value of our prior range.

Let us examine the PDF for the cosmic string weighting parameter,  $B$ , given in Fig. 3.4. The light and dark shaded regions again represent the 68 and 95% confidence intervals.

To quantify the total string contribution to the CMB anisotropy for a given set of parameters  $\vec{s}$  we define the fraction  $f$  as

$$f(\vec{s}) = \frac{I^{cs}}{I^{cs} + I^{ad}} \quad (3.6)$$

where

$$I^{cs} = \sum_l \frac{(2l+1)}{4\pi} C_l^{cs}(\vec{s}) ,$$

and

$$I^{ad} = \sum_l \frac{(2l+1)}{4\pi} C_l^{\text{ad}}(\vec{s}) ,$$

where  $C_l^{\text{ad,cs}}$  are the temperature (TT) correlation spectra. We then compute the PDF for this new parameter, which we show in Fig. 3.5 along with the 68 and 95% probability regions. We find that about 7%(14%) of the CMB power can be sourced by strings at 68%(95%) confidence. Note that the dashed line, corresponding to the three parameter analysis of [21], shows a smaller allowed string contribution.

Figs. 3.4 and 3.5 are the principal results of this paper. Limits on  $B$  alone give limits on the string tension itself. Using the results in Fig. 3.4, we find a cosmic string weight of  $B \lesssim 0.029(0.06)$  allowed at the 68 (95)% confidence level. This corresponds to  $G\mu \lesssim 1.8(2.7) \times 10^{-7}$ . The peak of the PDF for  $B$  lies at  $B = 0.01$ , or  $G\mu \sim 1.1 \times 10^{-7}$ . These limits are relevant to searches for direct detections of cosmic strings, as the magnitudes of gravity wave and lensing events caused by cosmic strings depend directly on their tension.

The above bounds on  $G\mu$  are model-dependent. In order to match the total observed CMB power, our string model requires  $G\mu_0 \sim 1.1 \times 10^{-6}$ . Our  $G\mu_0$  is somewhat lower than the COBE normalized values in [77] ( $G\mu \approx 1.7 \times 10^{-6}$ ), in [12] ( $G\mu = (1.5 \pm 0.5) \times 10^{-6}$ ), in [78] ( $G\mu = (1.7 \pm 0.7) \times 10^{-6}$ ), and in [79] ( $G\mu \approx 2 \times 10^{-6}$ ). It is also lower than [16] (for similar model parameters). It is possible that these papers share a factor of  $\sqrt{2}$  error in overall spectrum amplitude with the original version of these results. An estimate of  $G\mu_0$  more in line with our value was found in [72], where the COBE normalized value of  $G\mu$  was  $\sim 1.0 \times 10^{-6}$  (for their parameter  $w^X = 1/3$ ), and similarly in [73]. The latest estimates of Landriau and Shellard [60] using realistic simulations of cosmic strings (reliable up to  $\ell \sim 20$ ) give the COBE normalized value of  $G\mu = (0.74 \pm 0.2) \times 10^{-6}$  for

a  $\Lambda$ CDM cosmology, which is consistent with results of a similar study in [80] where the value obtained was  $G\mu = (1.05 \pm 0.3) \times 10^{-6}$ . Note that most of the results obtained prior to 1999 assumed a CDM dominated cosmology – switching to  $\Lambda$ CDM leads to a  $\sim 10\%$  increase in COBE normalized value of  $G\mu$  [60].

Our bound on  $G\mu$  would also be altered if the strings intercommute at a rate less than unity, as is expected in many string theory models of cosmic strings. The effect of reduced intercommutation would be to reduce the upper limit on  $G\mu$ .

Our bound on the fraction of CMB power in strings,  $f$ , depends only on the *shapes* of the string-sourced CMB and LSS spectra. These shapes, as discussed in §3.2.1, are largely independent of the details of the string model. The bound on  $f$  can be used to derive an approximate bound on  $G\mu$ , given one’s favorite value of  $\mu_0$ . Indeed, the results reported here, given as they are in light of a corrected string spectrum [49], have been determined through use of this less-model-dependent shape-amplitude parameter.

It is also worth recognizing that  $f$  can serve as a measure of the goodness-of-fit of the paradigmatic inflationary scenario in comparison with a physically motivated model; isocurvature is another example of a model used in such a manner (e.g. [81]). Our results from cosmic strings, serving from this viewpoint merely as a self-consistent foil to the standard model, show that as much as 14 % of the CMB TT-correlation power could be sourced by a radically different spectrum without destroying the close agreement of the resulting spectrum with the anisotropy data. Loosely speaking, we can conclude from this bound that there is a cumulative ambiguity in the uniqueness of the adiabatic  $C_\ell$  spectrum shape, as determined from the WMAP data, of around 10%. As more CMB data become available in the future, repetition of this analysis might be worthwhile, if only to discover whether

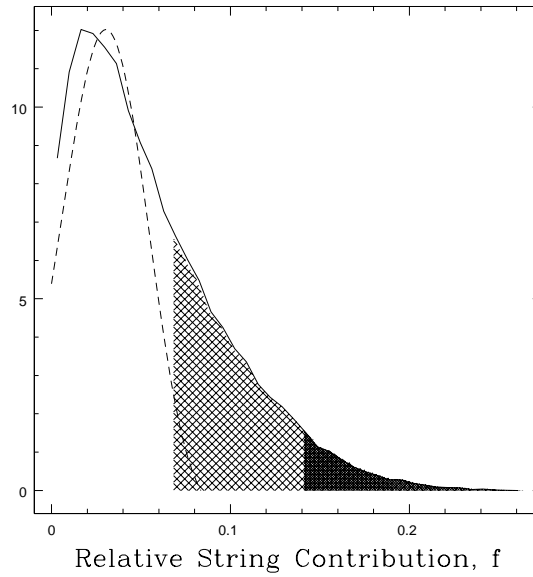


Figure 3.5: The PDF for the combination parameter  $f$ , which quantifies the fractional contribution of cosmic strings to the total  $C_l^{TT}$  spectrum. The solid line shows  $f$  from our full analysis, with the 68 % (light) and 95 % (dark) confidence regions shaded. The dotted line is the result for  $f$  from our previous three parameter analysis.

the intrinsic shape of the adiabatic spectrum is more uniquely picked out by the more-exact future data sets.

### 3.3.2 The B-polarization spectrum

In Fig. 3.6 we plot the B-mode polarization spectra in the case of smooth strings ( $\alpha_r = 1$ ) and wiggly strings  $\alpha_r = 1.9$  predicted by our string model for the case when the total contribution of strings to the CMB anisotropy is 10%. That is, for each of the curves, the value of  $G\mu$  was adjusted separately to correspond to  $f = 0.1$ . For comparison, we also plot the B-mode spectra from a purely adiabatic cosmology. The light dotted line represents the B-mode polarization arising from

gravitational lensing of E-mode polarization. The light dash-dotted line represents the B-mode arising from gravitational waves. This prediction is exciting because it shows that a cosmologically-viable network of cosmic strings can produce a CMB BB-mode polarization at an amplitude even higher than that expected for E to B-mode lensing. With gravity-wave generated B-modes peaking at a much lower  $\ell$ , any excess power in observed B-mode spectra at  $\ell \sim 1000$  could thus be a telling sign of cosmic string activity. Two planned experiments, QUIET and QUaD [82], expect to be able to measure such high- $\ell$  polarization with great precision. It is also worth noting that the amplitude of gravity-wave generated B-mode polarization is intimately tied to the as-yet undetermined scalar-to-tensor ratio,  $r$ . We have used  $r = 0.1$  in Fig. 3.6, which is usually regarded as an optimistically high value. Inflationary models frequently produce orders-of-magnitude lower estimates for  $r$  (in [45], for instance, investigations predict  $10^{-8} \lesssim r \lesssim 10^{-3}$  for KKLMMT-motivated brane inflation). For  $r \ll 0.1$ , cosmic strings could be the dominant source of B-mode polarization for low values of  $\ell$  ( $10 < \ell < 1000$ ), but with a spectrum that is recognizably distinct from the polarization generated by gravity waves. The proposed CLOVER experiment [83] and its space-based successors plan to focus their measurements on this region of  $\ell$ -space.

### 3.4 Summary

We found two types of constraints on cosmic string networks through our analysis of the WMAP and SDSS data. One is on the value of  $G\mu$ , which is sensitive to our normalization convention and to the string intercommutation rate, which we take to be unity in setting our bound. The other is on the fraction of total CMB power due to cosmic strings,  $f$ . The constraint on  $f$  depends chiefly on the general shape

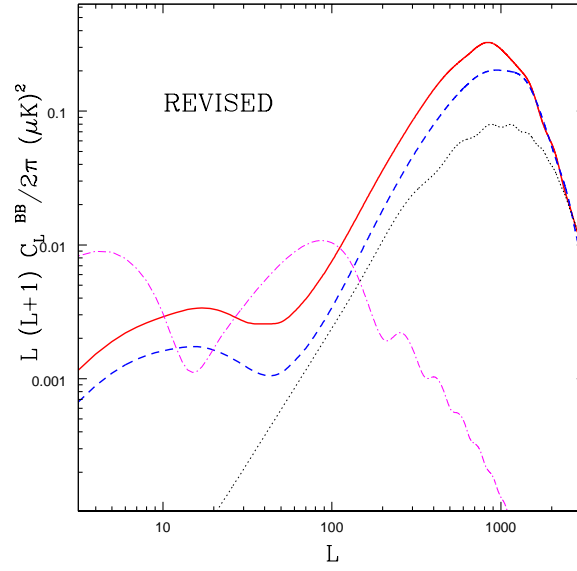


Figure 3.6: The B-type polarization spectra for  $\alpha_r = 1.9$  (dashed lined) and  $\alpha_r = 1$  (solid line) both corresponding  $f = 0.1$ . The light dotted line is the B-mode expected from gravitational lensing of adiabatic E-mode polarization; the light dash-dotted line is the B-mode expected from gravity wave-sourced polarization, for tensor-to-scalar ratio  $r = 0.1$ .

of the string induced spectrum. The shape of the spectrum is quite generic – a plateau on large scales due to superposition of the Kaiser-Stebbins effect of many strings (from a scaling network), followed by a broad peak on small scales. The peak is caused by the Doppler and Sachs-Wolfe effects produced by velocity and density perturbations caused by strings during the epoch of recombination. The rough position of the peak is set by the size of a typical wake at last scattering, while the wake size is set by the coherence (or curvature) length  $\xi(t)$  at that time. We can call these features generic because they are agreed upon by all groups that have studied string-induced CMB spectra. The fine details of the shape, e.g. the sharpness of the peak, depend on many factors.

In addition to quantifying the allowed fraction of the cosmic string contribution, our parameter  $f$  can also be interpreted as a measure of the goodness-of-fit of the fiducial adiabatic CMB spectrum model. The fact that the data permit approximately 10% of the TT-correlation power to arise from a very different competitor model gives a useful measure of how uniquely the data pick out the shape of the adiabatic spectrum.

Other recent constraints on local strings that also used WMAP data include ref. [84], where the narrowness of the first peak was used to constraint the size of the incoherent string contribution, and refs. [85, 86], where the constraint was based on the expected non-Gaussian signatures induced by strings. Ref. [84] suggests an interesting way to obtain a rough bound the string contribution to the CMB spectrum at  $\ell \sim 220$  from constraints on the width of the main peak. Our method has the advantage of including the information on all scales (not just the main peak) and the ability to account for changes in in cosmological parameters and the shape of the string spectra (by varying the wiggleness).

Our limit on the string tension,  $G\mu < 2.7 \times 10^{-7}$ , does not contradict a variety of recent claims of observational evidence for the existence of cosmic strings. The most prominent have been possible examples of cosmic string lensing. One possible cosmic string lensing observation [87] is the appearance of short time-scale variations in the brightness of the well-known gravitational lens system, Q0957 + 561, which could be explained by a passing cosmic string loop with a tension in the range  $10^{-8} \leq G\mu \leq 6 \times 10^{-7}$ . The inferred time scale of these variations is so short,  $\sim 100$  days, that very small scale string structure would be required, making the claim somewhat problematic (for more on these events, see [88]). In the arena of gravitational wave observation, current pulsar timing bounds are quite consistent with  $G\mu \sim 10^{-7}$  [89], while analysis of gravitational wave bursts from string loops suggests that  $G\mu \sim 10^{-7}$  cosmic strings will be readily observable by both LIGO and LISA [90].

It is often thought that a key observational test for cosmic strings would be whether non-Gaussianity is found in the primordial perturbations seen by such experiments as WMAP. This is a natural assumption, since each string acting alone would perturb the CMB in a highly non-Gaussian manner. However, the central limit theorem tells us that the superposition of perturbations produced by many strings must be Gaussian. Therefore, one expects to see string-related non-Gaussian features only on scales that are sufficiently small not to have been crossed by more than a few strings during the entire period of time during which strings have produced their effects. It is not difficult to get a conservative estimate of this scale. The dominant contribution to the anisotropy on small (sub-degree) scales comes from the Doppler and Sachs-Wolfe effects produced at the last scattering [91]. A natural length scale to start with is the angular size of the horizon at

recombination, which corresponds to  $\ell \sim 220/\sqrt{3}$ . Numerical simulations [61, 62] show that the typical distance between strings during matter domination is  $L \sim 0.8t$ . It is somewhat smaller in the radiation era, and can be much smaller if the intercommutation probability was less than unity, as may be the case in string theory models. A conservative estimate of the number of strings per horizon at any time in the matter era is  $\sim (4\pi t^3/3)/L^3 \sim 10$ . When projected onto the last scattering surface, about half of this number of strings would contribute. Hence, the CMB anisotropy in a patch corresponding to  $\ell \sim 220/\sqrt{3}$  would be a superposition of the effects of about 5 strings, and to isolate the effect of one string, one would have to go to scales of order:  $\ell \sim 220 \times 5/\sqrt{3} \sim 600$ . In doing this rough estimate we have ignored the density perturbations created by wakes between the radiation-matter equality and last scattering, which contribute a non-negligible fraction of the power near the main peak [91]. This contribution would tend to make the scale at which non-Gaussianity appears even smaller, since the wakes started to form from the onset of matter domination. Thus one will likely need a resolution of at least  $\ell \sim 1000$  to have any hope of seeing non-Gaussianity from strings. Furthermore, in the above argument we did not account for the fact that strings can produce only 10% of the total anisotropy. This makes the detection of their non-Gaussian signatures even more difficult. The possibility of low string intercommutation rates (high string density), in addition to making strings more Gaussian (via the central limit theorem), also strengthens the bound on their tension, hence further complicating the detection of their non-Gaussian properties. The analysis in refs. [85, 86] assumed  $\ell \sim 200$  as the scale for the onset of non-Gaussianity in the CMB caused by strings. A more realistic scale, as we have argued above, is likely to be an order of magnitude smaller, so the

detection of string sourced non-Gaussianity appears to be beyond the reach of WMAP, and quite possibly even Planck. The existing constraints on string-sourced CMB non-Gaussianity, such as those obtained in refs. [85, 86], appear to reflect the limitation that, given the variance of a CMB map on a certain scale,  $\sigma_\ell$ , one naturally has difficulty resolving any detailed features on those scales that have amplitudes comparable to  $\sigma_\ell$ . In light of this, it is not surprising that the upper bound on  $G\mu$  obtained in [85, 86] ( $G\mu \lesssim 10^{-5}$ ) roughly corresponds to the variance of the WMAP CMB map on sub-degree scales.

We find that cosmic strings with tensions of  $G\mu = 2.7 \times 10^{-7}$  are still allowed by the data from the WMAP and SDSS experiments, and that strings can account for as much as 14% of the the temperature fluctuations in a cosmic microwave background radiation dominated by adiabatic fluctuations without any significant changes in the underlying cosmology. Strings with allowed tensions are produced in brane inflation models, implying that such models are still viable and that the strings produced by them may be observable, giving us hope of an observational window on string theory. One promising signature of cosmic strings with these tensions in the early universe would be their creation of observable B-mode polarization in the CMB with spectra distinct both from those created by E-mode lensing and by gravity waves from primordial tensor modes. As we have seen, a cosmologically-viable cosmic string network could produce the most prominent B-mode polarization signal, with an amplitude even greater than the expected E-to-B lensing signal. Successful observation of such B-modes would in turn be our first direct observational probe into the physics of string theory, while continued non-detection of this B-mode could even more strictly bound the parameters of any cosmic string network.

## CHAPTER 4

### NETWORKS OF COSMIC SUPERSTRINGS

First appeared as *Scaling of Multi-Tension Cosmic Superstring Networks* in Phys. Rev. **D71** (2005) 103508; Erratum-ibid. **D71** (2005) 129906.

The cosmic superstrings produced in a D3-brane-antibrane inflationary scenario have a spectrum:  $(p, q)$  bound states of  $p$  fundamental (F) strings and  $q$  D-strings, where  $p$  and  $q$  are coprime. By extending the velocity-dependent one-scale network evolution equations for abelian Higgs cosmic strings to allow a spectrum of string tensions, we construct a coupled (infinite) set of equations for strings that interact through binding and self-interactions. We apply this model to a network of  $(p, q)$  superstrings. Our numerical solutions show that  $(p, q)$  networks rapidly approach a stable scaling solution. We also extract the relative densities of each string type from our solutions. Typically, only a small number of the lowest tension states are populated substantially once scaling is reached. The model we study also has an interesting new feature: the energy released in  $(p, q)$  string binding is by itself adequate to allow the network to reach scaling. This result suggests that the scaling solution is robust. To demonstrate that this result is not trivial, we show that choosing a different form for string interactions can lead to network frustration.

#### 4.1 Introduction

Consider a generic brane world scenario that closely describes our universe today (i.e., a KKLT-like vacuum [8]). If we take an extra brane-anti-brane pair in the early universe their brane tensions provide the cosmological constant that drives

inflation. There is an attractive force between a brane and an anti-brane so they tend to move towards each other while inflation is taking place. Thus, brane inflation is a natural feature of the brane world [6, 9, 39, 41]; in brane inflation, the inflaton is an open string mode identified with the interbrane separation. Inflation ends when the D3- $\bar{D}3$ -brane pair collides and annihilates, releasing energy that starts the hot big bang. Note that the inflaton field no longer exists after the annihilation of the D3- $\bar{D}3$ -brane pair. Towards the end of inflation, the D3- $\bar{D}3$ -brane collision produces D1-branes – or cosmic superstrings – but neither monopoles nor domain walls [10].

We can estimate the cosmic string tension  $\mu$  using the density perturbation magnitude in the CMBR data from COBE [14]. In the simplest realistic scenario, namely, the KKLMNT D3- $\bar{D}3$ -brane inflationary scenario [9], one finds that [45]

$$5 \times 10^{-7} \geq G\mu \geq 4 \times 10^{-10}$$

where  $G$  is the Newton's constant. The upper bound comes from WMAP data and other data [20, 21, 60, 84], while the lower values require some fine-tuning in the model. These predictions are not sensitive to different warping schemes because the normalization to COBE is always performed after the warp effect is taken into account. In this scenario, the density perturbation responsible for structure formation is dominated by the inflaton, with cosmic strings playing a secondary role.

The evolution of networks of cosmic strings is a well studied problem [18, 62, 92]. After the initial production of cosmic strings, the strings interact among themselves. When two cosmic strings intersect, they reconnect or intercommute. When a cosmic string intersects itself, a closed string loop is broken off. Such a loop will oscillate quasi-periodically and gradually lose energy via gravitational

radiation. Its eventual decay transfers the cosmic string energy to gravitational waves. A higher (lower) string density leads to a higher (lower) interaction rate so, not surprisingly, cosmic string networks evolve towards scaling solutions. A consequence of scaling is that the physics of simple, abelian Higgs networks is essentially dictated by a single parameter, the dimensionless string tension  $G\mu$ . This scaling feature can be seen by considering the evolution of the number density in a one-scale model, where the scaling solution emerges as an attractive fixed point.

There are many different hybrid inflationary models in which one can construct a variety of cosmic string-producing scenarios. What is different in brane inflation is that the string network that is produced has a large spectrum of possible string tensions [10, 22, 23]. For the D3- $\bar{D}3$ -brane inflationary scenario, one expects a spectrum of  $(p, q)$  string bound states [22, 23], where the tension of a particular bound state  $(p, q)$  is given by

$$G\mu_{(p,q)} = G\mu\sqrt{p^2g_s^2 + q^2}. \quad (4.1)$$

where  $g_s$  is the superstring coupling. For the string to be stable,  $p$  and  $q$  must be coprime, i.e.,  $p$  and  $q$  have no common factors greater than 1. Written this way,  $(1, 0)$  corresponds to the fundamental F-string while  $(0, 1)$  corresponds to the  $D1$ -brane, or D-string, so  $\mu$  is the tension of the  $(0, 1)$  superstring. We can see the emergence of such a spectrum in several ways. Consider the following simple picture: the gauge group at the end of inflation just before brane-antibrane annihilation is

$$U(1)_D \times U(1)_{\bar{D}} = U(1)_+ \times U(1)_-,$$

where the open string (complex) tachyon field stretching between the branes couples only to  $U(1)_-$ . The usual operation of the Higgs mechanism generates abelian

vortices following the spontaneous symmetry breaking of  $U(1)_-$ . These are the D-strings. Since no free  $U(1)$  gauge symmetry remains after the annihilation, it is believed that the  $U(1)_+$  symmetry becomes confining, yielding confining fluxes that may be identified as fundamental closed strings, or F-strings [93]. The production of D-strings may be estimated via the Kibble mechanism. Most of the decay products are expected to be very massive non-relativistic closed strings, which are expected to decay to gravitons, standard model particles and other light modes. We expect some of the massive closed strings to be extended. These are the F-strings. In a cosmological setting, their production is likely, again, to be dictated by the Kibble mechanism. The production of D- and F-strings are not independent, so we expect some initial spectrum of  $(p, q)$  strings to be produced.

Since the interactions between  $(p, q)$  strings is not simple [23], one expects that  $(p, q)$  network evolution might be quite involved. It is not obvious, *a priori*, that the network can even approach scaling. For example, it could oscillate (i.e., the density of any specific  $(p, q)$ -type could oscillate indefinitely), approach scaling only asymptotically, or simply frustrate. One way to address this problem would be to do a full numerical simulation of a  $(p, q)$  string network. However, this is a highly non-trivial problem. String network evolution is a complex physical process; accurately modeling the build-up of small-scale string structure is computationally demanding, even in the context of abelian Higgs models, which have only one type of vortex. A radically simpler alternative would be simply to generalize the one-scale string network model due to Kibble [94] to the case of  $(p, q)$  string evolution. Recall that the scaling of the cosmic string network appears as a stable fixed point in this one-scale model. However, previous researchers have found it useful to include more of the network physics than the original one-scale model allowed. In

particular, the velocity-dependent one-scale (VOS) model developed by Martins and Shellard for the abelian Higgs case [69] provides a very convenient and reliable method for calculating the large-scale quantitative properties of string networks in many contexts, including a cosmological setting. This model performs exceptionally well when tested against high resolution numerical simulations of string networks [62, 92]. It allows one to see analytically how scaling emerges, and to calculate reliably a small number of macroscopic quantities useful for cosmological applications. We take this model as the starting point for our own model building. We recognize that there are a number of other analytic approaches to the string evolution [95]. Some may characterize the details of small-scale stringy structures more accurately, but they also require more phenomenological input parameters which can only be obtained from simulations. Since there is, as yet, no simulation of a cosmic superstring network, and since we are chiefly interested in the overall properties of such a string network, we choose the simplest possible “analytic” model that highlights the most important physical effects.

In this paper we adapt the velocity-dependent one-scale model to describe a multi-tension cosmic string network that includes both string self-intersection and string-string binding interactions. For a multi-tension network, the string density evolution equation generalizes to a set of (infinitely many) coupled equations. We then specify the string interaction terms in our particular multi-tension,  $(p, q)$  string model and solve this set of equations numerically. Fortunately, we find that the  $(p, q)$  string network, with stringy interactions turned on, rapidly approaches scaling. This fast convergence and rapid decrease of string densities with increasing tension allows us to truncate the set of equations at low, computationally tractable values of  $(p, q)$ . To show that this scaling result is not somehow built into the model

we have constructed, we demonstrate that the same set of evolution equations with a different interaction term can lead to a frustrated network.

Because of the various approximations we use, our results are limited to overall macroscopic network features, which are nonetheless those features that are needed for cosmological applications. For instance, we find for the  $(p, q)$  superstring network :

- The  $(p, q)$  string network approaches a scaling network rapidly. The final scaling solution is independent of the initial densities of the various types of strings. The fractional density in strings, for  $F \neq 0$ , is given by

$$\Omega_{cs} = 8\pi G\mu_{(0,1)}\Gamma \quad \Gamma \simeq \begin{cases} 20/(0.55P + F) & g_s = 1.0 \\ 15/(0.53P + F) & g_s = 0.5 \end{cases} \quad (4.2)$$

where  $P$  measures the probability of self-interaction and  $F$  measures the overall probability of interaction among different types of strings. For the  $(p, q)$  cosmic superstring network, we do not know the value of  $F$ , though we expect  $P \lesssim F \lesssim 1$ . It is interesting to note that scaling is achieved even if we turn off the string self-interaction, i.e., when  $P = 0$ . For the abelian Higgs model we have  $\Gamma_{U(1)} \simeq 20$  and  $P \simeq 0.28$ . Using this value for  $P$  and taking  $F = P$ , we find that, for  $g_s = 1$ ,  $\Gamma \simeq 46$ ; for  $F = 1$ ,  $P = 0.28$ , we have  $\Gamma \simeq 17$ . Thus, the total density of the  $(p, q)$  cosmic superstring network is comparable to standard cosmic strings. Differentiating between the two kinds of networks based on their string densities will require more detailed modeling.

- The relative number density of each type of string is roughly given by

$$N_{(p,q)} \sim \mu_{(p,q)}^{-n} \quad 6 < n \lesssim 10. \quad (4.3)$$

The fall-off is power-like, not exponential. The rapid convergence of the coupled set of equations is brought about by this rapid fall-off. The power law is most accurate for high values of  $p$  and  $q$ ; the spectrum tends to be somewhat flatter for the first few string types. Indeed, we find that when scaling is reached, the relative numbers of  $(0, 1)$ ,  $(1, 0)$ , and  $(1, \pm 1)$  strings are comparable and far larger than the population of the remaining  $(p, q)$  states with  $p, |q| > 1$ . In the case of  $F = P = 0.28$ ,  $g_s = 1.0$ , we find  $N_{(p,q)} \propto \mu_{(p,q)}^{-7.5}$ .

- The adapted multi-tension velocity-dependent one-scale model (MTVOS) that we describe in §4.2 can be used for many different kinds of multi-tension networks by a simple change of the inter-string interactions term.

Clearly, this analysis can be improved in a variety of ways. We shall comment on some of them. However, we are confident that the rapid approach to scaling and the fast power drop-off in the densities are generic features of cosmic superstring networks.

In the past, the evolution of cosmic strings in models more complicated than the abelian Higgs model have been considered. For example, Pen and Spergel studied the evolution of  $S_N$  strings by simulating a network of  $S_3$  and  $S_8$  strings [96]. The  $S_N$  symmetry enforces identical tension and number densities among the  $N$  string types. In terms of the model we construct, the set of  $N$  coupled evolution equations collapses to a single equation. McGraw also modeled non-abelian  $S_3$  strings with two different tensions [97]. The evolution of networks of  $Z_N$  strings connected to monopoles, which have some qualitative similarities to the networks we consider, has been studied in ref. [98]. We believe that a network of  $(p, q)$  strings is the first network type that truly requires a set of coupled equations. The

formalism may be adapted for other non-trivial string network.

In Section 4.2, we adapt the velocity-dependent one-scale model to a model for the evolution of comic strings that have a spectrum of tensions. In Section 4.3, we specialize the model to the  $(p, q)$  superstring network by defining our string interaction term. In Section 4.4 we present our numerical results and in Section 4.5 we briefly discuss some observational implications of these networks.

## 4.2 A Multi-Tension Velocity-Dependent One Scale Model

Consider a set of different types of cosmic strings  $\{\alpha\}$  with tensions  $\{\mu_\alpha\}$ . Let the number of cosmic strings of type  $\alpha$  per unit area be  $n_\alpha$ . Suppose that all of the cosmic strings may be characterized by a single length scale  $L$  and a single average velocity  $v$ , and that cosmic strings of type  $\alpha$  can evolve either by interaction mediated loop formation or by binding to cosmic strings of other types  $\beta \neq \alpha$ . The following model is motivated by the model of Martins and Shellard [69], but has been altered somewhat to accommodate the new string physics we introduce.

We assume that the length scale evolves via the equation

$$\dot{L} = HL + c_1 v , \quad (4.4)$$

where the loop parameter  $c_1 \leq 1$  is a dimensionless factor and  $H$  is the Hubble parameter. We take the equation of motion for the velocity to have the Martins-Shellard form

$$\dot{v} = (1 - v^2) \left( -2Hv + \frac{c_2}{L} \right) ; \quad (4.5)$$

where the ‘‘momentum parameter’’  $c_2$  is a second constant. This term is the acceleration due to the curvature of the strings. In the absence of expansion, these two equations imply  $\gamma = (1 - v^2)^{-1/2} = (L/L_0)^{c_2/c_1}$ , and with  $c_1 = c_2 = 0$ ,

but with expansion retained, they imply  $\gamma v a^2 = \text{constant}$ ,  $L/a = \text{constant}$ , and so,  $\gamma v L^2 = \text{constant}$ . Thus, the “self-acceleration” due to string curvature and expansion have opposite effects: self-acceleration increases string velocity, whereas expansion dilutes it. This suggests that the two effects can cancel one another.

We can see how this comes about by rewriting Eq. (4.4) as

$$\frac{d(HL)}{dt} = H(HL + c_1 v) + \frac{\dot{H}}{H} HL = H(HL) \left[ \frac{c_1 v}{HL} - \left( \frac{1 + 3w}{2} \right) \right] \quad (4.6)$$

and combining it with the velocity equation; we then find that there is a quasi-steady solution

$$v = HL \left( \frac{1 + 3w}{2c_1} \right) = \frac{c_2}{2HL}, \quad (4.7)$$

which implies

$$HL = \sqrt{\frac{c_2 c_1}{1 + 3w}}, \quad v = \frac{1}{2} \sqrt{\frac{c_2(1 + 3w)}{c_1}}. \quad (4.8)$$

In this solution, both  $HL$  and  $v$  are constants that differ in the radiation ( $w = 1/3$ ) and matter ( $w = 0$ ) eras. Clearly, there is no quasi-steady solution for  $w \leq -1/3$ ; thus, quasi-steady solutions only exist in the radiation and matter eras. We require that in both eras,  $v \leq 1$ , a condition that is more restrictive in the radiation era, where it demands that  $c_2/2c_1 \leq 1$ . In practice, we choose  $c_1$  and  $c_2$  such that the scaling values of  $HL$  and  $v$  match the values given in [69], where similar constants  $\tilde{c}$  and  $k$  are chosen to line up with full network simulations. The translation between our constants and theirs is simple: The translation between our constants and theirs is simple: in the radiation era, our  $c_2 = k$ , while our  $c_1 = (k + \tilde{c})/2$ ; in the matter era,  $c_2 = (3/4)k$  and  $c_1 = (3/8)(k + \tilde{c})$ . For example, in the radiation era they find  $HL = 0.1375$  and  $v = 0.655$ , which for us fixes  $c_1 = 0.21$  and  $c_2 = 0.18$ .

Next, add to these equations an equation of energy conservation, at first in the absence of interactions between strings of different types. Let the cosmic string

energy density be

$$\rho = \frac{n\mu}{\sqrt{1-v^2}} \quad (4.9)$$

where  $\mu$  is the mass per unit length of a string, and  $n$  is the mean string number density. In the absence of interactions, assume that

$$\dot{\rho} = -2H\rho(1+v^2) \quad (4.10)$$

Differentiating the expression, Eq. (4.9) for the string energy density and using Eq. (4.10) and Eq. (4.5), the equation for  $\dot{v}$ , implies

$$\dot{n} = -\left(2H + \frac{c_2 v}{L}\right) n . \quad (4.11)$$

where we see that the first term comes from cosmological expansion. The second term can be interpreted in two different ways. For straight strings, it would reflect a net expansion in the velocity field orthogonal to the strings. For kinky strings, we should interpret  $n$  as the characteristic number of intersections per unit area on average for a two dimensional surface intersecting the network. As the strings straighten out (the source term in  $\dot{v}$ ) the number of intersections will fall, at a rate that is  $\sim nv/L$  characteristically. We may interpret this to mean that as string kinks straighten out, the number of intersections of strings with any two dimensional cut through three dimensional space will decrease; it is also the straightening of kinks that raises  $v$ . Note that when the string velocity approaches its asymptotic value  $v = c_2/2HL$ , the energy equation becomes

$$\dot{\rho} = -\left(2H + \frac{c_2 v}{L}\right) \rho = -H \left[2 + \frac{c_2(1+3w)}{2c_1}\right] \rho , \quad (4.12)$$

i.e. it assumes exactly the same form as the equation for the number density of strings. This is sensible because the energy per unit length per string  $\mu\gamma \rightarrow$  constant asymptotically.

Next, let us consider what happens when we allow interactions between strings. Recall that we assume a single characteristic length scale,  $L$ , for all types of strings; however, unlike the single- $\mu$  case, this length need not be related directly to string density. We further assume that the different types of cosmic strings interact by binding, first at a point and then zipping up to form a new cosmic string with the same length as the original two, which enforces equal lengths for all different kinds of strings. The zipping up takes a time  $L$ , but let us suppose that  $L$  is small enough compared to the Hubble length that we can regard the zipping up as instantaneous;  $HL \sim 0.1$  is good enough for our purposes. Let the equation for  $n_\alpha$  be

$$\dot{n}_\alpha + 2Hn_\alpha = -\frac{c_2 n_\alpha v}{L} - Pn_\alpha^2 vL + FvL \left[ \frac{1}{2} \sum_{\beta,\gamma} P_{\alpha\beta\gamma} n_\beta n_\gamma (1 + \delta_{\beta\gamma}) - \sum_{\beta,\gamma} P_{\beta\gamma\alpha} n_\beta n_\gamma (1 + \delta_{\beta\gamma}) \right], \quad (4.13)$$

where the first term on the RHS arises from the breaking off of loops from individual undulating strings of type  $\alpha$ , the second term arises from breaking off of loops after the collision of two strings of type  $\alpha$ , and the third term arises from the zipping up of two strings of different types that collide and bind.

As an aside, we note that the term proportional to  $P$  could equally well be written as a term under the summation, proportional to  $P_{0\alpha\alpha}$ . We have pulled this term out of the sum to make the contrast between self interaction and interaction between strings of different types clear. But a few comments on this term are in order:

- The term proportional to  $P$  or  $P_{0\alpha\alpha}$  is the usual term that drives networks without multiple string types to scaling.

- By writing  $P$  instead of  $P_{0\alpha\alpha}$ , we are assuming that the self-interaction rate does not depend upon  $\alpha$ .
- If we take  $P_{\alpha\beta\gamma} = 0$  for  $\beta \neq \gamma$ , then a self-interaction term of this form drives all string species which have a sufficient initial density to the same final scaling number density.
- After we have taken  $P$  out of the sum, we either restrict the sum to  $\beta \neq \gamma$  or assume  $P_{0\alpha\alpha} = 0$ .

We assume that our constants  $c_2$ ,  $P$ , and  $F$  are identical for cosmic strings of all types. We define  $F$  as a measure of the overall probability that two strings of different types interact at all. We have assumed that the interaction of strings of two different types can only result in zipping up, if anything – there are no reconstructions and no breaking off of loops directly associated with such interactions.

In the third term,  $P_{\alpha\beta\gamma}$  is the probability of forming a string of type  $\alpha$  when strings of types  $\beta$  and  $\gamma$  collide, whenever the strings interact at all. The factor

$$\frac{1}{2}(1 + \delta_{\beta\gamma})$$

is introduced so that we do not double count the production of strings of type  $\alpha$  when strings of *different* types  $\beta$  and  $\gamma$  collide; i.e. since we do not restrict the sum, symmetry on  $\beta \leftrightarrow \gamma$  implies we have two identical source terms from  $\beta + \gamma \rightarrow \alpha$ ; the factor

$$1 + \delta_{\gamma\alpha}$$

in the loss rate arises because in each  $\alpha - \alpha$  collision we lose *two* long strings. By

defining  $N_\alpha = a^2 n_\alpha$ , we can rewrite Eq. (4.13) as

$$\dot{N}_\alpha = -\frac{c_2 N_\alpha v}{L} - \frac{P N_\alpha^2 v L}{a^2} + \frac{F v L}{a^2} \left[ \frac{1}{2} \sum_{\beta, \gamma} P_{\alpha\beta\gamma} N_\beta N_\gamma (1 + \delta_{\beta\gamma}) - \sum_{\beta, \gamma} P_{\beta\gamma\alpha} N_\gamma N_\alpha (1 + \delta_{\gamma\alpha}) \right], \quad (4.14)$$

and if we define conformal time by  $d\eta = v dt/a$  and introduce the comoving string length,  $L = a\ell$ , then we find

$$N'_\alpha = -\frac{c_2 N_\alpha}{\ell} - P N_\alpha^2 \ell + F \ell \left[ \frac{1}{2} \sum_{\beta, \gamma} P_{\alpha\beta\gamma} N_\beta N_\gamma (1 + \delta_{\beta\gamma}) - \sum_{\beta, \gamma} P_{\beta\gamma\alpha} N_\gamma N_\alpha (1 + \delta_{\gamma\alpha}) \right], \quad (4.15)$$

with a prime denoting differentiation with respect to conformal time. In terms of  $N_\alpha$ , we find that  $\rho_\alpha = \mu_\alpha N_\alpha / a^2 \sqrt{1 - v^2}$ .

The remaining two equations are those for  $\ell$  and  $v$ . Substituting  $L = \ell a$  into Eq. (4.4) gives

$$\dot{\ell} = \frac{c_1 v}{a} \Rightarrow \ell = \ell(0) + c_1 \eta. \quad (4.16)$$

When we change the independent variable from  $t \rightarrow \eta$ , Eq. (4.5) becomes

$$v' = \frac{(1 - v^2)}{v} \left( -2Hav + \frac{c_2}{\ell} \right). \quad (4.17)$$

To complete the set of equations, we need to find  $a(\eta)$ ; we use

$$H = \frac{d(\ln a)}{dt} = \frac{d(\ln a)}{d\eta} \frac{d\eta}{dt} = \frac{v}{a} \frac{d(\ln a)}{d\eta} \quad (4.18)$$

to get

$$\frac{da}{d\eta} = \frac{Ha^2}{v}. \quad (4.19)$$

In the radiation dominated era, which is of greatest interest to us practically,  $Ha^2$  is approximately constant. Thus, in the quasi-steady state, the scale factor grows linearly with  $\eta$ .

Eq. (4.13) may yield a steady state solution of the form  $N_\alpha = f_\alpha/\ell^2 = f_\alpha/[\ell(0) + c_1\eta]^2$  provided that

$$-2c_1 f_\alpha = -(c_2 f_\alpha + P f_\alpha^2) + F \left[ \frac{1}{2} \sum_{\beta,\gamma} P_{\alpha\beta\gamma} f_\beta f_\gamma (1 + \delta_{\beta\gamma}) - \sum_{\beta,\gamma} P_{\beta\gamma\alpha} f_\beta f_\gamma (1 + \delta_{\gamma\alpha}) \right] \quad (4.20)$$

has a nontrivial solution.

It is instructive to consider what we get when  $F = 0$ . In that case, Eq. (4.20) has two solutions,  $f_\alpha = 0$ , which is not relevant, and

$$f_\alpha = \frac{2c_1 - c_2}{P}, \quad (4.21)$$

which is physically realizable only if  $2c_1 > c_2$ . Let us assume that this is so. At sufficiently late times, we will therefore find that

$$\rho_\alpha = \frac{\mu_\alpha(2c_1 - c_2)}{P c_1^2 (a\eta)^2 \sqrt{1 - v^2}}, \quad (4.22)$$

where we have assumed that  $c_1\eta \gg \ell(0)$ , and that  $v$  relaxes to its asymptotic value. In this limit, we find that  $a \approx Ha^2\eta/v$  in the radiation era, and therefore  $\eta \approx va/Ha^2 = v/Ha$ ; use this in Eq. (4.22) to find

$$\rho_\alpha \approx \frac{\mu_\alpha H^2 (2c_1 - c_2)}{P c_1^2 v^2 \sqrt{1 - v^2}} \Rightarrow \Omega_\alpha = \frac{8\pi G \rho_\alpha}{3H^2} \approx \frac{8\pi G \mu_\alpha (2c_1 - c_2)}{3P c_1^2 v^2 \sqrt{1 - v^2}}. \quad (4.23)$$

Because this version of the network equations assumes common  $L$  and  $v$  for all string types, when  $F = 0$  we expect to find  $\Omega_\alpha/\mu_\alpha$  independent of  $\alpha$ , assuming nonzero initial populations. (Remember that  $\Omega_\alpha \propto f_\alpha = 0$  is also a solution.) Notice that Eq. (4.23) implies  $\Omega_\alpha \propto (2c_1 - c_2)/P$ , and for small self-interaction probability, this is the expected  $P^{-1}$  scaling. Moreover, nonzero  $P$  is essential for time-independent  $\Omega_\alpha$  to arise in networks with only interactions among strings of

the same type. Also, since this is the limit in which our model reduces to the abelian Higgs case, we can use prior simulation results to fix the value of our parameter  $P$ . Numerical studies of the radiation dominated era have  $\Gamma = \Omega_{cs}/(8\pi G\mu) \approx 20$ , which for us implies  $P = 0.28$ , taking  $c_1 = 0.21$ ,  $c_2 = 0.18$ , and  $v = 0.655$ . Because of this we take  $P = 0.28$  as the fiducial value for  $P$  in our numerical solutions.

It is also instructive to consider what happens if  $P = F = 0$ . In this case, Eq. (4.13) has an exact solution

$$N_\alpha = \frac{N_\alpha(0)\ell(0)^{c_2/c_1}}{[\ell(0) + c_1\eta]^{c_2/c_1}} \rightarrow N_\alpha(0) \left[ \frac{\ell(0)}{c_1\eta} \right]^{c_2/c_1} \quad (4.24)$$

(Eq. (4.24) is a special case of the general solution

$$\frac{1}{N_\alpha} = \left[ \frac{1}{N_\alpha(0)} - \frac{P\ell^2(0)}{2c_1 - c_2} \right] \left[ \frac{\ell}{\ell(0)} \right]^{c_2/c_1} + \frac{P\ell^2}{2c_1 - c_2}$$

that can be found for  $F = 0$ , and the results of this and the previous paragraph follow from appropriate limiting cases of this solution.). From this result, we find that

$$\Omega_\alpha \approx \frac{8\pi G\mu_\alpha N_\alpha(0)[\ell(0)]^{c_2/c_1}}{3(Ha)^{2-c_2/c_1} v^{c_2/c_1} \sqrt{1-v^2}}. \quad (4.25)$$

In the radiation dominated era, when  $Ha \propto a^{-1}$ , we find that  $\Omega_\alpha \propto a^{2-c_2/c_1}$ , which either rises or falls depending on the sign of  $2 - c_2/c_1$ .

Note that the network equation, Eq. (4.13), may also be used to describe entanglement. In that case, instead of setting  $\alpha = (p_\alpha, q_\alpha)$ , as we shall do to describe  $(p, q)$  networks, we simply let  $\alpha = p_\alpha$ . Moreover, we set  $P_{\alpha\beta\gamma} = \delta_{\alpha-(\beta+\gamma)}$ ; taking  $c_2 = P = 0$ , the network equations are

$$N'_\alpha = F\ell \left[ \frac{1}{2} \sum_{\beta,\gamma} \delta_{\alpha-(\beta+\gamma)} N_\beta N_\gamma (1 + \delta_{\beta\gamma}) - N_\alpha \sum_\gamma N_\gamma (1 + \delta_{\gamma\alpha}) \right]. \quad (4.26)$$

These equations cannot lead to a scaling solution because there is a conservation law, basically conservation of energy, that restricts the evolution of the system.

Multiply Eq. (4.26) by  $\alpha$  and sum over  $\alpha$ ; the result is

$$\begin{aligned}
\left(\sum_{\alpha} \alpha N_{\alpha}\right)' &= F\ell \left[ \frac{1}{2} \sum_{\alpha, \beta \neq \gamma} \alpha \delta_{\alpha - (\beta + \gamma)} N_{\beta} N_{\gamma} - \sum_{\alpha \neq \gamma} \alpha N_{\alpha} N_{\gamma} \right. \\
&\quad \left. + \sum_{\alpha, \beta} \alpha \delta_{\alpha - 2\beta} N_{\beta}^2 - 2 \sum_{\alpha} \alpha N_{\alpha}^2 \right] \\
&= F\ell \left[ \frac{1}{2} \sum_{\beta \neq \gamma} (\beta + \gamma) N_{\beta} N_{\gamma} - \sum_{\alpha \neq \gamma} \alpha N_{\alpha} N_{\gamma} + 2 \sum_{\beta} \beta N_{\beta}^2 - 2 \sum_{\alpha} \alpha N_{\alpha}^2 \right] \\
&= F\ell \left[ \sum_{\beta \neq \gamma} \beta N_{\beta} N_{\gamma} - \sum_{\alpha \neq \gamma} \alpha N_{\alpha} N_{\gamma} + 2 \sum_{\beta} \beta N_{\beta}^2 - 2 \sum_{\alpha} \alpha N_{\alpha}^2 \right] \\
&= 0, \tag{4.27}
\end{aligned}$$

where the next to last line was obtained by relabelling  $\gamma \rightarrow \beta$  in one of the two sums over  $\beta \neq \gamma$ . Thus, here we have an example where scaling is *not* achieved. The network evolves toward ever larger values of  $\mu$ , but its overall comoving energy density does not decline.

Thus, neither the existence nor the nature of a scaling solution for a particular multi-tension network is obvious. If each type of string evolves independent of all other types, scaling will be achieved eventually for all types present originally, with  $\Omega_{\alpha} \propto \mu_{\alpha}/P$ . Turning on the interactions between string types will populate the different tensions, and, once produced, their self-interactions and energy-losing binding interactions will propel them toward scaling solutions. The final spectrum of string tensions may be broad or narrow, depending on the efficiency with which the reaction terms operate. The reaction terms themselves may promote scaling even if there are no self-interactions, but the fact that entanglement can be described by a reaction network with particular choices of interaction probabilities shows that there are certainly circumstances in which scaling cannot arise solely from the reactions among strings of different types. Note, finally, that we have assumed very little about the nature of the multi-tension network that is described

by these equations beyond the assumption that string interactions lead either to loop formation or the formation of other kinds of strings through some sort of binding. Thus these equations may easily be adapted for any particular multi-tension string network model simply by determining the form of  $P_{\alpha\beta\gamma}$  for that model; the particular  $(p, q)$  network that we consider below is only one example of the sort of network these equations can describe.

### 4.3 F- and D-String Network

To specialize the preceding network to the  $(p, q)$  strings of [23], we define  $P_{\alpha\beta\gamma}$  – taking  $\alpha = (p, q)$ ,  $\beta = (k, l)$ , and  $\gamma = (m, n)$  – and motivate the overall interaction probability,  $F$ . For this investigation, we make a first and very crude approximation: we assume that the probability of two strings of different types interacting is a single, universal constant, rather than a function of  $\alpha, \beta, \gamma$  or the relative velocity of the strings. By discarding all these complexities, we retain only a kinematically determined branching ratio (see both Fig. 4.1 and the discussion in the text below); in future work, we may attempt to retain more of the physics contained in  $F$  to obtain more realistic results. Before we can write down this branching ratio, we shall state the relevant properties of  $(p, q)$  strings, since these determine the form of  $P_{\alpha\beta\gamma}$ :

- Strings with positive and negative values of  $p$  and  $q$  are generically allowed; the sign of  $p$  or  $q$  indicates the direction of the string's charge. Because of a reflection symmetry, we can always choose the orientation of the string such that  $p \geq 0$ . For  $p = 0$ ,  $q > 0$ ; for  $p > 0$ ,  $q \in \mathbb{Z}$ .
- Strings with  $q = 0$  are only stable for  $p = 1$ . It is probable that  $(0, q)$

strings are marginally bound; operationally, we assume that the non-zero momentum transfers in the string collisions that accompany binding unbind these states. An interaction that formally would create an  $(N, 0)$  or  $(0, N)$  string thus, in fact, creates  $N$   $(1, 0)$  or  $(0, 1)$  strings.

- We assume that two strings of different types interact with probability  $F$ . If two strings of different types do interact, there are two possible products, or bound states, that they can form: a  $(p, q)$  string interacting with a  $(p', q')$  string can form either a  $(p + p', q + q')$  string or a  $(p - p', q - q')$  string, where we always take  $p > p'$ . As stated above, if either of these product bound states has a resulting  $p''$  and  $q''$  that are not coprime, then what is actually formed is a set of strings with stable, lower  $p, q$  values.
- In agreement with our comments above, we assume  $P_{0\alpha\alpha} = 0$  or, equivalently, restrict our summations to  $\beta \neq \gamma$ .
- For bound states of strings to be stable,  $p$  and  $q$  must be coprime. If a bound state of a string is formed with  $p$  and  $q$  not coprime, then the new state is, in reality, a collection of lower-tension  $p$  and  $q$  strings that are coprime: i.e., a string which nominally has  $p = Nk, q = Nl$  is actually a set of  $N$   $(k, l)$  strings. We may view this as the “decay” of a  $(Nk, Nl)$  string:
  - comes about because the  $N$   $(k, l)$  strings that compose this “state” are BPS with respect to each other; that is to say, they have no mutual binding interactions. Any possible marginal binding may be ignored since the strings are moving with relativistic speeds.
  - has no energy cost – the resulting collection of strings always has lower energy than the strings that bound to form them; there is no actual

$(Nk, Nl)$  bound state – a collection of stable  $(k, l)$  strings is formed immediately following the interaction.

- can untie itself through reconnection events if the collection of  $(k, l)$  strings that are created in the interaction are tangled or tied up immediately after their creation.

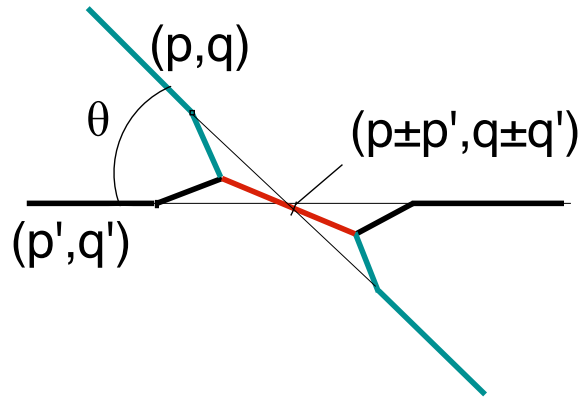


Figure 4.1: A schematic view of a string intersection. The intersection angle,  $\theta$ , determines whether the additive –  $(p + p', q + q')$  – or subtractive –  $(p - p', q - q')$  – binding occurs.

Whether the interaction of two strings forms a  $(p + p', q + q')$  bound state or a  $(p - p', q - q')$  bound state is determined by a simple consideration of force balance: if the angle between the interacting strings is small enough, then the heavier, additive bound state is formed because the two interacting strings' tensions can balance the tension of the heavier bound state; if the angle is greater than some critical angle of force balance, then the lighter, subtractive bound state is formed. The critical angle which determines which binding occurs is given by [23]

$$\cos \theta_{klmn}^{crit} = \frac{e_{kl} \cdot e_{mn}}{|e_{kl}| |e_{mn}|} \quad e_{mn} = ([m - Cn]g_s, n)$$

where  $C$  is the RR scalar. If we assume a stochastic distribution of string orientations, then the strings' interaction angle should have a flat distribution in  $\cos \theta$ , that is, that each value of the cosine between -1 and 1 should be equally likely. If we assume this, and remember that the directionality of the  $F$  and  $D$  charge must be taken into account – i.e.,  $\theta = \pi/4$  is not equivalent to  $\theta = 3\pi/4$  – then the probability of forming the additive bound state is simply the fraction of cosine-space with  $\theta$  less than the angle of force balance; the subtractive bound state is formed otherwise. We can write this as:

$$P_{\alpha\beta\gamma}^{\pm} = \frac{1}{2} \left( 1 \mp \left( \frac{(k + Cl)(m + Cn)g_s^2 + ln}{[(k + Cl)^2 g_s^2 + l^2]^{1/2} [(m + Cn)^2 g_s^2 + n^2]^{1/2}} \right) \right), \quad (4.28)$$

where  $P^+$  indicates  $\alpha = (p, q) = (k + m, l + n)$  and  $P^-$  indicates  $\alpha = (p, q) = (k - m, l - n)$ . This form captures the kinematic branching ratio, but as stated leaves out an important process: the creation of non-coprime  $(p, q)$  strings, which are in reality collections of two or more coprime strings. To take this into account, we must slightly modify the way in which we insert  $P_{\alpha\beta\gamma}$  into our equations: we take

$$P_{(Nk, Nl)(p, q)(p', q')} = NP_{(k, l)(p, q)(p', q')}.$$

The inclusion of this process is extremely important. This break-up of non-coprime strings is a nonreversible process that is fundamentally dissipative – it helps to keep the average tension of the network low both by limiting the pathways by which high-tension bound states can be reached and by providing a mechanism through which a single interaction can destroy a high-tension bound state and replace it with a collection of low-tension strings. Thus, in summary,

- Two strings of different types  $\alpha$  and  $\beta$  interact with probability  $F$ .
- When these strings interact, either a subtractive or additive bound state

is formed, with probabilities  $P^-$  and  $P^+$  given by Eq. (4.28). The two interacting strings are annihilated in the production of the new bound string state.

- When the bound state  $\gamma$  is stable, one such string is produced.
- When the nominal bound state  $\gamma$  is unstable, it immediately forms  $N$  lower-tension stable strings, which helps keep the tension dependence of string density spectrum steep.

In all our numerical runs we have assumed  $C = 0$ .

Some possible physical effects that our model neglects include:

- Velocity dependence of the interaction probabilities due to variation in the binding energy of the resulting bound states: the increase binding energy that holds very high tension states together is small – the energy gained by binding decreases greatly for high- $\mu$  states. Thus we expect that the momentum transferred in even moderate-velocity interactions that involve these lightly-bound states may lead them to unbind spontaneously.
- This velocity dependence may lead to an effective cut-off in  $\mu$ , irrespective of the interaction dynamics.
- We might not expect strings of widely varying tensions all to have the same velocities and characteristic length scale in reality, contrary to what our model assumes.
- We have decoupled the evolution of the r.m.s. velocity and length scale of our network from the network's  $P$  and  $F$  dependent interactions, though one

would generally expect these interactions to be relevant to determining the network parameters.

#### 4.4 Network Results

The equations given in §4.2 require numerical solution. For all numerical results, we work in the radiation-dominated era, assume (for convenience) that the RR scalar,  $C = 0$ , and fix our constants  $c_1 = 0.21$  and  $c_2 = 0.18$  to match [69] (these choices are made so that, at scaling, we have  $HL = 0.1375$  and  $v = 0.655$ ). Furthermore we have done each run twice, with two different values of the superstring coupling,  $g_s = 0.5$  and  $1.0$ . We were less certain about how to initialize the cosmic string network; cosmic string creation immediately after brane inflation is not understood completely. Fortunately, scaling has proven to be quite robust to a wide variety initial conditions; for an illustration of this, see Fig. 4.2. On energetic grounds, we believe that, in general, networks will be formed with primarily the lowest-lying states populated; thus, for our calculations we chose initially to populate only the  $(1, 0)$  and  $(0, 1)$  states, and those with equal number densities. Final scaling results are always insensitive to these choices; at worst, very different initial conditions can alter the rate at which the network approaches the scaling regime. We similarly find that any initial choices for network velocity,  $v$ , and length scale,  $L$ , quickly approach their analytically-predicted scaling values. To integrate our equations numerically, another choice we had to make was how many  $(p, q)$  states to allow. After testing networks of many different sizes, we found that our results showed a steep, power law dependence of number density on tension in all cases. The relative densities of the low-lying tension states, furthermore, were not changed when more high-tension states were included. Thus we were able to obtain accurate

results from a relatively small network: for the runs we show here, we have taken  $p \in [0, 5]$ ,  $q \in [-5, 5]$ , though the way in which we solve the equations allows nominally higher-valued, temporary  $(p, q)$  states to “form” if the values of  $p$  and  $q$  are non-coprime, but only if the decay products of the unstable  $(p, q)$  state are a collection of stable  $(k, l)$  strings with  $k, |l| \leq 5$ . Finally, we take the scale factor of the universe  $a = 1$  at network initialization.

An interesting new result from this network model is that string networks with no loop creation – those with  $P = P_{0\alpha\alpha} = 0$  – still exhibit cosmologically acceptable scaling; enough energy is lost through string binding and binding-mediated annihilation to keep the comoving network number densities  $N_\alpha \eta^2$  constant, regardless of initial conditions, after an initial relaxation period following network formation. Because of this, these networks are very robust: though there are regions of parameter space where the network never truly reaches scaling, in all reasonable cases (where we keep  $F \neq 0$ ,  $P \lesssim F$ ) we never find cosmologically-disastrous solutions where cosmic strings come to dominate the energy density of the Universe.

There are three regimes of interest for these solutions:

1. For  $F \gg P$  : The network will be dominated by  $F$ ,  $D$ , and  $(1, \pm 1)$  strings. Higher tension states are present, but maximally suppressed (these networks have the steepest spectra).
2. For  $F \rightarrow 0$ : All string tensions that are present initially eventually reach the same scaling density. If there are a great many string states, this can cause a catastrophe, since the formation of loops tends to drive all types of strings to the same value of  $\Omega_{cs}/\mu_\alpha$ .
3. For  $P \sim F$ : The interactions terms will populate the higher  $(p, q)$ 's, and

the  $P$  terms will flatten the spectrum somewhat because of its tendency to equally populate all levels. The larger  $P$  is, the more quickly this happens. In Figs. 4.3, 4.4, 4.5, & 4.6 a variety of combinations are shown. For larger values of  $P$ , the “final” scaling state is not an exact scaling solution, but one that continues to evolve slowly to late times. Some features that appear to be generic in this regime include

- $\Omega_{cs}/((8/3)\pi G\mu_{(0,1)}) = 60/(F + 0.55P)$  for  $g_s = 1.0$ ,  $46/(F + 0.53P)$  for  $g_s = 0.5$ . This formula is only valid for  $F \neq 0$ .
- $a_{\text{scaling}} \sim 1000$ , so scaling is achieved at  $T_{\text{scaling}} \sim 10^{-3}T_{\text{reheat}}$ , where  $T_{\text{reheat}}$  is the temperature to which the universe reheats at the end of inflation. Since  $T_{\text{reheat}} \sim M_s$ , the string scale,  $T_{\text{scaling}} \sim 10^{-3}M_s \gg \text{TeV}$ , so scaling is reached long before the electroweak phase transition.
- Scaling results are insensitive to initial conditions unless  $F = 0$
- Steep final spectra:  $N_\alpha^{\text{final}} \propto \mu_\alpha^{-n}$ ,  $6 < n \lesssim 10$

There are several aspects of these results that require further discussion.

#### 4.4.1 Scaling

- The overall properties of the networks are fairly insensitive both to initial conditions [51] and to particular parameter choices; i.e.,  $\Omega_{cs}$  never grows fast enough ever to come to dominate the universe.
- However, the final state of the string network depends upon the relationship between  $F$  and  $P$ . When  $P \sim F$ , the network does not quickly reach a true scaling solution. Instead, it continues to evolve to late times (see

Figs. 4.3 and 4.5). Because of the efficient energy loss from both binding and loop formation, the network's overall density grows very slowly – e.g.,  $(d \log \Omega / d \log a) \sim 0.07$  for  $a \sim 10^4$ ;  $\sim 0.01$  for  $a \sim 10^5$ , for the case of  $P = F = 0.28$ ; note that  $(d \log \Omega / d \log a) = 0$  defines entry into the scaling regime. This late growth comes about because of the continuing competition between loop formation, which wants equally to populate all string states, and binding interactions, which tend to destroy high-tension bound states. This late evolution is not dangerous cosmologically.

- In agreement with our understanding of the late evolution of  $P \sim F$  networks, such networks tend to develop somewhat flatter final spectra, as their high-tension bound states tend to be more populated than those in  $F \gg P$  networks. Their spectra still exhibit very steep power law behavior, however (see Figs. 4.4 and 4.6).
- The scale factor at which the network enters the scaling regime is somewhat dependent upon initial conditions: networks with more states initially populated tend to take slightly longer to reach scaling, though the greater frequency of interactions caused by such initial conditions means that these networks tend to be less dense throughout their evolution than networks that are formed with only low-lying string states (see Fig. 4.2); networks that begin with much smaller initial  $L$ , on the other hand, can take a good bit longer to reach scaling. Recall also that the binding interactions of high-tension states will very often lead to non-coprime combinations, which leads such networks quickly to develop the same kinds of steep spectra that are seen when less democratic initial conditions are used.

### 4.4.2 Low-F Catastrophe

- An aspect of superstring networks that has been as-yet unappreciated is that their ability to populate arbitrarily high tensions through the formation of bound states can lead to a cosmological catastrophe if such states cannot be made to decay. In traditional network evolution, which is what our equations reduce to when  $F \rightarrow 0$ , even very small initial populations of each possible string state will each eventually reach the same final scaling density. When this happens,  $\Omega_{cs} = \sum_{\alpha} \Omega_{\alpha}^{cs} \propto \sum_{\alpha} N_{\alpha} \mu_{\alpha}$  can become huge, and thus disastrous, even if the energy density in each individual state is small.

### 4.4.3 Final Spectra

- The fact that our numerical solutions have found a very strong dependence of string number density on tension – with  $N_{\alpha} \propto \mu_{\alpha}^{-n}$ , and  $6 < n \lesssim 10$  – is another important aspect of these networks. If the spectrum were flat, or nearly so, a scenario very much like the low-F catastrophe outlined above would ensue: since the effect of many string states is additive, and since there are many more possible states at higher tensions, such a flat-spectrum network would be ruled out immediately by cosmological considerations.
- Computationally, the steepness of the spectra greatly eases our task. Numerical tests showed that the addition of many high-tension states with low number densities scarcely affected any of the results. We were thus able to limit ourselves to small networks, with  $p_{\max} = |q_{\max}| = 5$ .
- Careful study of Figs. 4.4 and 4.6 shows that the spectra plotted there are not strict power laws. The spectra are, in fact, somewhat flatter for very

low tensions, where the number of possible states is small. Thus, in all cases there are proportionally more  $F$ ,  $D$ , and  $(1, 1)$  strings than anything else; particularly when  $F \gg P$ , these states will dominate the cosmic string network. The relative populations of these low-lying states are tabulated in Tab. 4.1.

- The effect of varying the superstring coupling,  $g_s$ , is to vary the tension of the F strings relative to the D strings, with this variation propagating up the ladder of bound states. Here, we have taken only two representative values of  $g_s$ : 0.5 and 1.0. Reducing  $g_s$  affected the network as our  $N \propto \mu$  results suggest: those states which were previously degenerate (equally populated) –  $(1, 0)$  or  $[(2, 1) + (2, -1)]$  relative to  $(0, 1)$  or  $[(1, 2) + (1, -2)]$ , for instance – had their degeneracy lifted, with the lighter state’s number density increasing. The precise amount of increase was dependent upon the values of  $F$  and  $P$ . Again, see Tab. 4.1.
- We note in passing that (unphysical) networks with  $P = 0$  and with the loop term  $\propto c_2$  removed from Eq. (4.13) also go to scaling.
- In all our networks, the lowest tension states dominate the network energy density. We expect this to be a feature of any multi-tension networks that interact via binding, even if the spectrum of possible bound states is much more complicated than the one we have considered.

## 4.5 Observational Consequences

Several aspects of  $(p, q)$  networks are potentially observationally distinct from regular cosmic string networks. The most obvious difference is that these networks

Table 4.1: The relative populations of the three lowest-lying tension states, which in all cases dominate the networks' energy density.

		$g_s = 1.0$		$g_s = 0.5$	
		$\frac{\mu_{(1,0)}}{\mu_{(0,1)}} = 1 \quad \frac{\mu_{(1,\pm 1)}}{\mu_{(0,1)}} = \sqrt{2}$		$\frac{\mu_{(1,0)}}{\mu_{(0,1)}} = \frac{1}{2} \quad \frac{\mu_{(1,\pm 1)}}{\mu_{(0,1)}} = 1.12$	
F	P	$N_{(1,0)}/N_{(0,1)}$	$N_{(1,\pm 1)}/N_{(0,1)}$	$N_{(1,0)}/N_{(0,1)}$	$N_{(1,\pm 1)}/N_{(0,1)}$
1	0	1	0.769	3.24	1.21
1	0.14	1	0.803	2.50	1.19
1	0.28	1	0.836	2.19	1.19
0.56	0.14	1	0.829	2.24	1.19
0.56	0.28	1	0.887	1.96	1.21

feature a spectrum of string tensions. We suggest a few possible observational signatures that could allow one to distinguish a  $(p, q)$  network from a standard, abelian Higgs network:

- Previous studies of cosmic string lensing probability [99] have been based on results from standard, abelian Higgs network models. In such networks,  $\Gamma = \Omega_{cs}/(8\pi G\mu) \approx 20$ . In principle, our model allows values for  $\Gamma$  both less than and greater than the abelian Higgs value. However, we expect the extra-dimensional nature of superstrings to reduce their interaction rates, which leads to higher values of  $\Gamma$  and  $\Omega_{cs}$ . If future lensing surveys find a rate of cosmic string lensing substantially higher than that predicted by a abelian Higgs network, that rate could both be a signature of a cosmic superstring network as well as an observational constraint on the parameters of such a network.

- If the overall densities in cosmic superstring networks are generally higher than those in abelian Higgs models, then observational bounds on cosmic string tension (e.g. [21]) that depend on overall network properties will need to be reinterpreted. We expect that the net effect will be to tighten such bounds, though how much the bounds will change is difficult to predict since observational bounds depend on many aspects of string networks (e.g., string substructure, or “wiggleness”), while the detailed properties of multi-tension networks have not yet been fully fleshed out.
- The  $Y$ -shaped junction of two strings in the act of binding is a good signature of the non-trivial properties of cosmic superstrings. Such a junction, if present, could be detected by cosmic string lensing, or by observation of the Kaiser-Stebbins effect, where a temperature difference is seen in the cosmic microwave background radiation due to a string-induced Doppler shift [100]. In the latter case, we would expect to see a different temperature in each of the 3 patches of sky. The relativistic motion of the binding strings could also be an indicator of a binding event: the cosmic string lensing angle is enhanced by a factor of  $\gamma$  for moving strings [101] (depending on string orientation), which is moderate for usual network motions ( $\sim 1.3$ , in the radiation-dominated era). The strings motions near a binding site, however, are very relativistic, though over a very small spatial region, and thus would exhibit exaggerated lensing near the binding site. Random variation among string velocities within the network should also lead to the existence of some individual fast-moving strings whose lensing will also be enhanced.
- A recent analysis [86] of the direct detectability of cosmic string-generated

temperature anisotropies in the data from the upcoming Planck satellite suggests that relatively high tension or fast moving strings within cosmic superstring networks would be marginally within the Planck range of detectability (they estimate that strings with  $G\mu \approx 6 \times 10^{-6}$ ,  $v = 1/\sqrt{2}$  would be directly detectable by Planck; for a multi-tension network with a fiducial tension  $G\mu \sim 3 \times 10^{-7}$ , only strings with a combined  $\beta\gamma$  and high- $(p, q)$  tension enhancement of  $\sim 10$  would be seen).

- Direct observation of more than one cosmic string tension from observational techniques, such as gravity wave bursts [90] or gravitational lensing, that are sensitive to a particular string's tension would be a definite prediction of this kind of network. In the case of lensing, however, the velocity, orientation, and string substructure dependences of the lensing angle may overwhelm this effect for the most probable lensing strings (since over 90% of the strings in our network are  $F$ ,  $D$ , and  $(1, \pm 1)$  strings, whose tensions are all of the same approximate magnitude). For random string orientations, the string lensing angle can vary by as much as a factor of six because of velocity dependent effects, though we expect typical velocity dependent variation of only a factor of two or so (these variations arise because the string lensing angle is proportional both to the sine of the orientation angle of the cosmic string relative to the line of sight as well as  $\gamma(1 + \hat{n} \cdot v)$ , where  $v$  is the string velocity and  $\hat{n}$  is a unit vector in the direction between the observer and the string [101]). Thus, there are two ways that lensing measurements could indicate the existence of a multi-tension network. The most dramatic would be a single very large ( $\gtrsim 10$ ) variation between two observed lensing angles. Just as compelling, however, would be if a large number of lensing measurements were made with

a typical variation among events that is greater than one would expect to arise, statistically, from random string orientations and string velocity directions. In any event, accurate follow-up observations of the Kaiser-Stebbins effect, where the string's relative velocity enters the equations differently (in a cross product rather than a dot product) could perhaps allow us to disentangle to some degree the string's velocity and intrinsic tension. Another possible avenue for discriminating between variation due to string orientation and velocity and intrinsic string tension would be if a series of lensing events were observed along a single long string within a small patch of the sky. Since we expect strings to be curved, it could be possible to observe the same cosmic string at several different orientations. This could allow us to extract the string's actual tension through a statistical analysis of the events' lensing angles.

- Another signature would be a mismatch between a particular string tension measured directly – from lensing, perhaps – and a  $G\mu$  measurement coming from a technique like CMB fluctuations or pulsar timing analysis that is only sensitive to the averaged network as a whole; however, the effects of string substructure (i.e., string wiggleness), which alter string-generated CMB spectra, could mask more subtle expressions of this effect. If limits on string substructure (see [21]) improve, then a direct detection via lensing of a string with a tension that is several times larger than what CMB limits would lead us to expect for a single-tension network would be a strong indication of the existence of a multi-tension network.

By combining different observations and gathering sufficient data, one should be able to measure a set of properties of the cosmic strings and so distinguish

between different scenarios. This goal will be easier to reach if the true cosmic string tension is closer to today's observational bound.

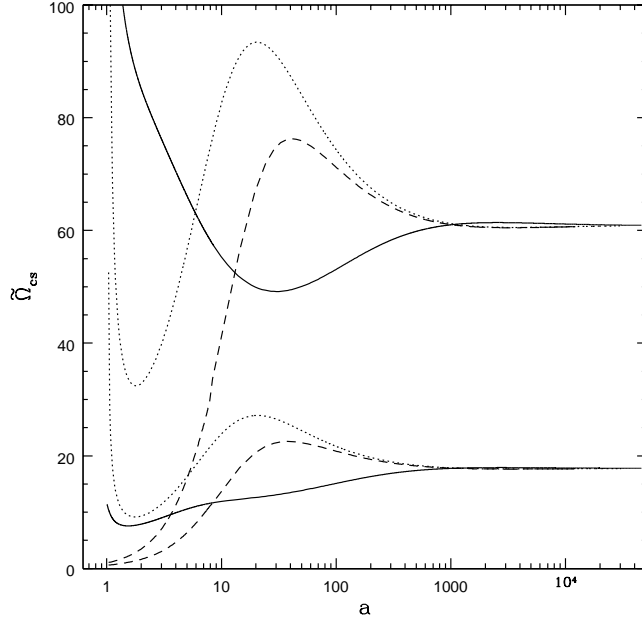


Figure 4.2: Comparison among three different sets of network initial conditions, all taking  $F = 1$ ,  $P = 0$ . The higher three lines represent the evolution of the overall density in cosmic strings (summed over all string states),  $\tilde{\Omega}_{cs} \equiv \Omega_{cs}/((8/3)\pi G\mu_{(0,1)})$ , with scale factor,  $a$ . The lower three lines represent the evolution of the density in  $(0, 1)$ , or  $D$ -, strings,  $\tilde{\Omega}_{cs}^{(0,1)} \equiv \Omega_{cs}^{(0,1)}/((8/3)\pi G\mu_{(0,1)})$ , with  $a$ . Our standard initial conditions, equal initial populations of  $(1, 0)$  and  $(0, 1)$  strings and  $HL = 1$ , are shown by the dashed lines. The solid line represents the results from a network run with a short initial length scale ( $10^{-2}$  of our usual choice) and with over half of the initial string  $(p, q)$  states in our network equally populated. Finally, the dotted line shows the results for a very large initial population of strings –  $\tilde{\Omega}_{cs} \sim 1000$  – equally spread over half of the tension states included in our network, with our usual choice for the initial network length scale. For all the runs shown here we have set the superstring coupling,  $g_s = 1.0$ .

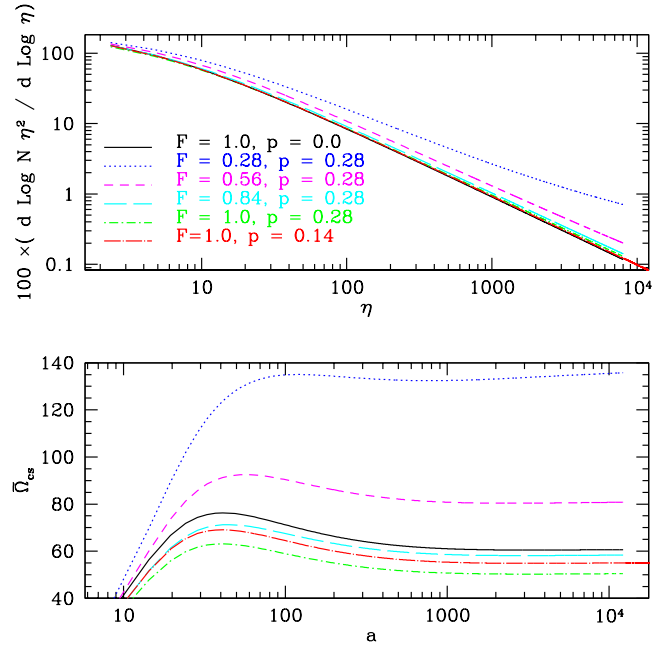


Figure 4.3: The bottom panel shows the evolution of  $\tilde{\Omega}_{cs} = \Omega_{cs}/((8/3)\pi G\mu_{(0,1)})$  for various parameter values, taking the string coupling  $g_s = 1.0$ . The top panel shows the rate of change in the comoving number density  $N\eta^2$ ; in the scaling regime,  $d \log N\eta^2/d \log \eta = 0$ .

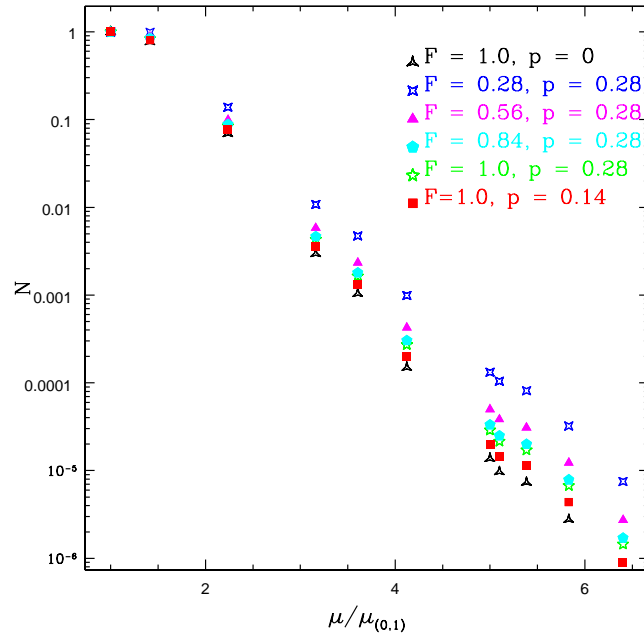


Figure 4.4: The final scaling-era spectra for a variety of parameter combinations, taking the string coupling  $g_s = 1.0$ , with  $N_{(0,1)}$  normalized to unity and the other number densities altered accordingly.

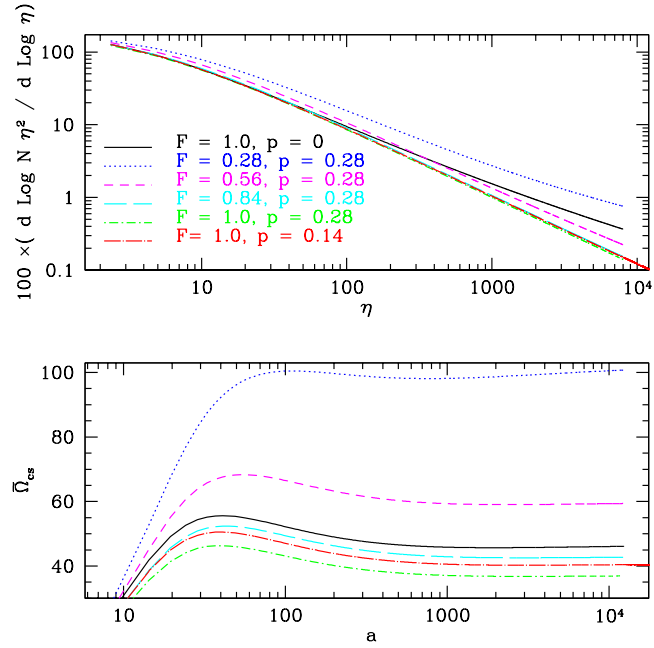


Figure 4.5: The bottom panel shows the evolution of  $\tilde{\Omega}_{cs} = \Omega_{cs}/((8/3)\pi G\mu_{(0,1)})$  for various parameter values, taking the string coupling  $g_s = 0.5$ . The top panel shows the rate of change in the comoving number density  $N\eta^2$ ; in the scaling regime,  $d \log N\eta^2 / d \log \eta = 0$ .

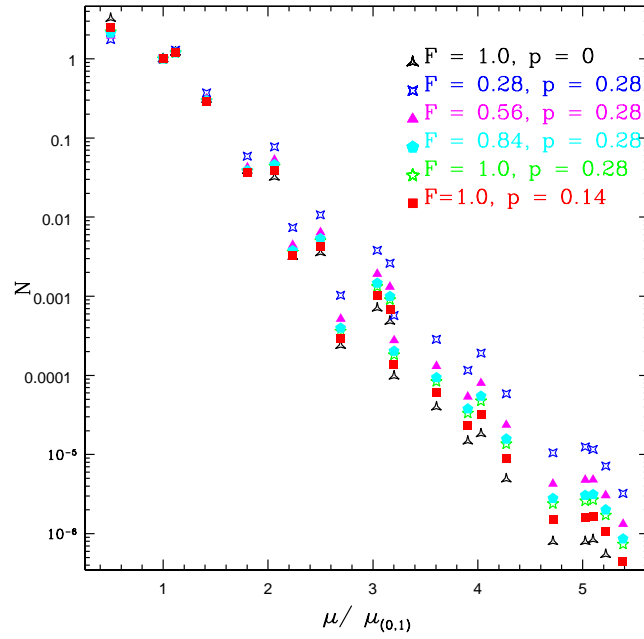


Figure 4.6: The final scaling-era spectra for a variety of parameter combinations, taking the string coupling  $g_s = 0.5$ , with  $N_{(0,1)}$  normalized to unity and the other number densities altered accordingly.

## CHAPTER 5

### COSMIC SUPERSTRING LENSING

First appeared as *Cosmic Superstring Gravitational Lensing Phenomena: Predictions for Networks of  $(p,q)$  Strings* in Phys. Rev. **D72** (2005) 123504.

The unique, conical spacetime created by cosmic strings brings about distinctive gravitational lensing phenomena. The variety of these distinctive phenomena is increased when the strings have non-trivial mutual interactions. In particular, when strings bind and create junctions, rather than intercommute, the resulting configurations can lead to novel gravitational lensing patterns. In this brief note, we use exact solutions to characterize these phenomena, the detection of which would be strong evidence for the existence of complex cosmic string networks of the kind predicted by string theory-motivated cosmic string models. We also correct some common errors in the lensing phenomenology of straight cosmic strings.

#### 5.1 Introduction

Some time after the existence of cosmic strings was proposed [102], several researchers recognized that the conical spacetime generated by cosmic strings leads to a unique gravitational lensing signature: undistorted double images [103]; the discovery of even a single such gravitational lensing event would be seen as irrefutable evidence for the existence of cosmic strings. Previous detailed studies of string lensing phenomena have focused on infinite strings and string loops, whether straight or wiggly [104]. For standard, abelian Higgs strings, these are the only lensing effects that one would expect to find.

As we have discussed, there has been a renaissance of interest in cosmic strings. This renewal was begun by the recognition that cosmic strings are copiously produced in the aftermath of the brane collision that generates reheating in brane-world models of inflation in string theory [10]. In addition to reviving interest in cosmic strings, these new studies have enriched cosmic string phenomenology by proposing the existence of two basic cosmic string types: Fundamental, or F-strings, and one-dimensional Dirichlet-brane strings, or D-strings. These two kinds of strings are able mutually to interact to form bound states. These bound states are known as  $(p, q)$  strings, as they are composed of  $p$  F-strings and  $q$  D-strings [23]. String binding allows for a variety of new observational phenomena, yet does not cause any cosmological catastrophes [26]. In particular, the existence of string binding interactions generically implies that there will be  $Y$ -shaped junctions of three strings that form each time there is a string binding event. These  $Y$ -shaped junctions, though possibly quite rare, give rise to lensing phenomena that are qualitatively distinct from anything standard abelian Higgs models can produce.

Since cosmic strings are perhaps the only directly observable remnant of brane inflation, it is vital that we identify any distinctive effects that are peculiar to the cosmic “superstrings” that are produced in brane-collision reheating. Cosmic superstrings may be our best hope for directly observing some aspects of string theory. The observation of even a single distinctive lensing event – one that could not be explained in an abelian Higgs model – would be a “smoking gun” for the existence of a non-trivial cosmic string network that is the hallmark of cosmic superstring models. We note, however, that similar junctions are found in non-abelian string networks as well (e.g., the  $S_3$  networks studied in ref. [96, 97]).

In this brief note, we describe the principal novel phenomena arising from the

binding junctions that characterize non-trivial networks of cosmic superstrings. In §5.2, we review lensing by a straight cosmic string, writing down some general formulae that have not previously appeared in the literature. In Fig.5.1 we illustrate the quintessential signature of a  $(p, q)$  network junction. This is an imaginative construction of what the galaxy NGC 2997 <sup>1</sup> might look like if it were lensed by a Y-shaped string junction. In §5.3, we derive the simple procedure used to generate this image.

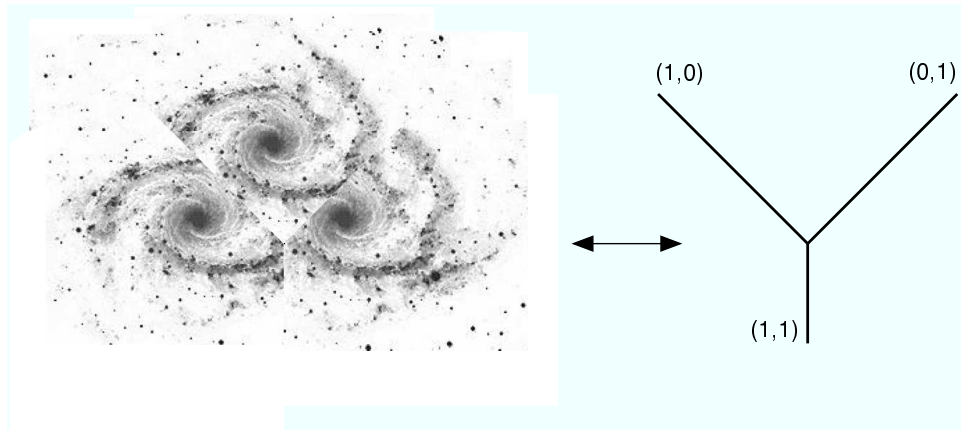


Figure 5.1: Illustration of lensing of a single galaxy by a  $(p, q)$  network junction. Note that each image is partially obscured, which is a generic feature of cosmic string lensing events [105]. This image is an imaginative construction, not an actual observation.

## 5.2 Review of straight string lensing

The lensing due to a straight string is surprisingly simple; this comes about because the surrounding space-time is locally flat. Many details of this lensing can nevertheless be quite subtle, and so here we correct two errors found in the liter-

<sup>1</sup>Anglo-Australian Observatory/David Malin Images

ature, namely the angular separation formula and the orthogonality of the image pairs with respect to the observed cosmic string. A string oriented in a direction  $\hat{\mathbf{s}}$  produces two images on opposite sides of the string separated by an “angular separation vector”  $\vec{\delta\varphi}$  of magnitude

$$|\vec{\delta\varphi}| = 8\pi G\mu\sqrt{\gamma^2(1 + \hat{\mathbf{n}} \cdot \mathbf{v})^2 - \cos^2\theta} \frac{D_{s,cs}}{D_{s,o}}. \quad (5.1)$$

In our notation, bold face variables represent 3-vectors, bold hatted variables are unit 3-vectors, and over-arrows signify 2-vectors which live in the plane orthogonal to the direction of sight. Here  $G\mu$  is the dimensionless string tension,  $\gamma = 1/\sqrt{1 - \mathbf{v}^2}$ ,  $\mathbf{v}$  is the string velocity,  $\hat{\mathbf{n}}$  is the unit vector directed along the line of sight,  $\theta$  is the angle between the cosmic string and  $\hat{\mathbf{n}}$  (i.e., it is defined by  $\hat{\mathbf{n}} \cdot \hat{\mathbf{s}} = \cos\theta$ ),  $D_{s,cs}$  is the distance from the source to the cosmic string, and  $D_{s,o}$  is the distance from the source to the observer. Because cosmic strings are boost invariant along their axis, we will always work in the gauge where  $\mathbf{v}$  satisfies  $\mathbf{v} \cdot \hat{\mathbf{s}} = 0$ . Vilenkin [103] pointed out that a straight cosmic string in motion will appear curved, like a large hyperbola in the sky; we note that, as expected, the apparent vanishing point of the hyperbola corresponds to the point where the magnitude of the angular separation vector goes to zero ( $\vec{\delta\varphi} \rightarrow 0$ ). The reason for the apparent curvature is because what we see is the cosmic string world sheet intersected with our past light cone, which we mentally project onto the  $t = 0$  hyper-plane. The cosmic string equations of motion are solved by

$$\mathbf{x}(\sigma, t) = \hat{\mathbf{s}}\sigma/\gamma + \mathbf{v}t + \mathbf{b} \quad (5.2)$$

with impact parameter  $\mathbf{b}$  (with respect to the origin/observer) orthogonal to both  $\hat{\mathbf{s}}$  and  $\mathbf{v}$ . The *observed* cosmic string is described by the illusory embedding

$$\mathbf{y}(\sigma, t) = \mathbf{x}(\sigma, t - |\mathbf{y}(\sigma, t)|) \quad (5.3)$$

and so solving for  $\mathbf{y}$  yields

$$\mathbf{y}(\sigma, t) = \hat{\mathbf{s}}\sigma/\gamma + \mathbf{v}(\gamma^2 t - \sqrt{\mathbf{b}^2\gamma^2 + \sigma^2 + \mathbf{v}^2\gamma^4 t^2}) + \mathbf{b}. \quad (5.4)$$

The apparent string then has orientation given by  $\hat{\mathbf{s}}_{\text{apparent}} = \mathbf{y}'(\sigma, t)/|\mathbf{y}'|$ , which is in general not equal to  $\hat{\mathbf{s}}$ . These string orientation vectors may be pulled back onto the sky via

$$\vec{\mathbf{s}} = \hat{\mathbf{s}} - (\hat{\mathbf{n}} \cdot \hat{\mathbf{s}})\hat{\mathbf{n}} \quad (5.5)$$

$$\vec{\mathbf{s}}_{\text{apparent}} = \hat{\mathbf{s}}_{\text{apparent}} - (\hat{\mathbf{n}} \cdot \hat{\mathbf{s}}_{\text{apparent}})\hat{\mathbf{n}}. \quad (5.6)$$

The difference between apparent and actual string orientation can then be characterized by the angle between these two 2-vectors:

$$\cos \beta = \frac{\vec{\mathbf{s}} \cdot \vec{\mathbf{s}}_{\text{apparent}}}{|\vec{\mathbf{s}}||\vec{\mathbf{s}}_{\text{apparent}}|} = \frac{\cos \theta \mathbf{v} \cdot (\hat{\mathbf{n}} \times \hat{\mathbf{s}})\gamma}{\sin \theta \sqrt{\gamma^2(1 + \hat{\mathbf{n}} \cdot \mathbf{v})^2 - \cos^2 \theta}}. \quad (5.7)$$

Interestingly, the relative angle between  $\delta\vec{\varphi}$  and  $\vec{\mathbf{s}}$  can be shown to be  $\pi/2 + \beta$  which implies that the angular separation vector is always orthogonal to the *apparent* cosmic string as in Fig. 5.2.

$$\delta\vec{\varphi} \cdot \vec{\mathbf{s}}_{\text{apparent}} = 0 \quad (5.8)$$

One might wonder how it is possible for a cosmic string that appears to be bent in the shape of a hyperbola to produce an undistorted image. In fact, the two images are not completely identical: They are moving at slightly different velocities, which gives rise to both the Kaiser-Stebbins (blue-shift) effect [100], as well as a relative “hyperbolic distortion” due to the finite travel time of light. So the distortion induced by an extremely relativistic string is none other than the distortion that all moving bodies appear to have; c.f. Eqn. (5.3).

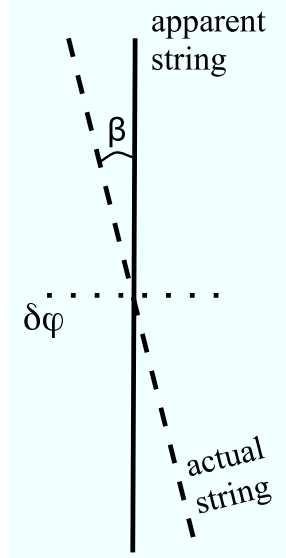


Figure 5.2: A schematic view of the lensing due to a single string in the most general case; when the string’s velocity is non-zero, the angular separation vector is perpendicular to the apparent string, rather than to the actual string.

### 5.3 Lensing by $Y$ -Junctions

A feature of superstring networks is that they are composed of at least two distinct string species: so-called fundamental or F-strings as well as D1-branes, or D-strings. These different types of strings can mutually interact via binding, creating  $(p, q)$  bound states composed of  $p$  F-strings and  $q$  D-strings [23]. The tension of such strings is given by

$$\mu_{p,q} = \sqrt{p^2 \mu_F^2 + q^2 \mu_D^2} \quad (5.9)$$

Networks of such strings are cosmologically safe, as they are expected readily to go to scaling [26]. However, uncertainties about the dynamics of such networks means that the number of visible  $Y$ -junctions is hard to estimate and could be quite small.

It is in the region near the  $Y$ -shaped junctions formed after collisions that

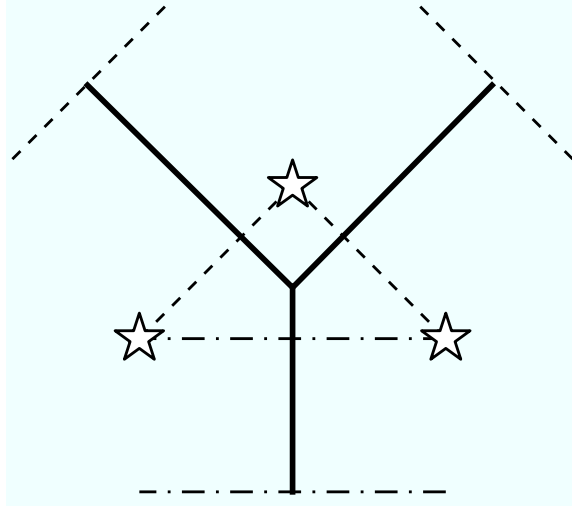


Figure 5.3: The imaging pattern of a three-way junction. The dark lines represent the force-balanced string junction; in reality, strings themselves are invisible. The dotted and dot-dashed lines represent, schematically, the angular separation vectors associated with the strings. We suppress the heads of the vectors, since their orientation is arbitrary. For string tensions in the upper range allowed by observations – that is,  $G\mu \sim 10^{-7}$  [21] – the size of the angular separation vectors would be of order 1 arc-second. The stars represent the lensed images, with the angular separation vectors drawn in for illustrative purposes.

the new string lensing effects are seen. In Fig. 5.1, we showed an image as it might actually appear, with the invisible strings and angular separation vectors suppressed. In Fig. 5.3, we show a mock-up of the triple image formed in the vicinity of a  $Y$ -junction together with the strings that produce the image. In brief, each leg of the  $Y$ -junction lenses exactly like an infinite straight string.

To motivate the above result, let us begin by considering a source simultaneously imaged by two long strings.

For two overlapping strings, it is straightforward to construct a set of rules

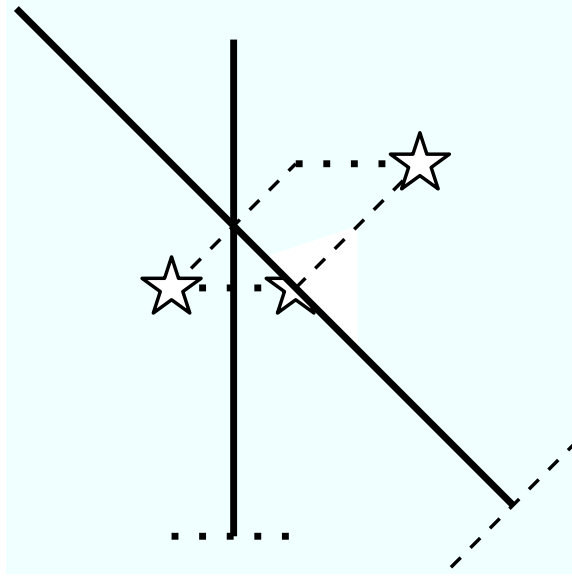


Figure 5.4: The imaging pattern for two overlapping cosmic strings. The dotted and dot-dashed lines represent, schematically, the angular separation vector associated with the strings. Notice that only the object and two of the three images are visible.

for the multiple imaging of a single source. Each straight cosmic string has an associated two dimensional “angular separation vector” the length of which is given by Eqn. (1). For string tensions in the upper range allowed by observations [21], the magnitudes of these angular separation vectors are of order 1 arc-second. The orientation of the angular separation vector is perpendicular to the associated cosmic string.

1. Begin with an original image (i.e. the object); the choice of which image to begin with is arbitrary.
2. Construct a parallelogram originating at the object and generated by the angular separation vectors associated with each cosmic string; each corner represents a new image.

- (a) Each image (except the object) will be associated with the set of cosmic strings whose angular separation vectors were used to create it.
  - (b) If exactly those strings that are associated with an image – and no others – lie between the object and that image, then that image will be visible; otherwise, that image will be invisible.
3. Thus, given the existence of one visible image (the object), the location and status – visible or invisible – of the other three images is known. An example of this is shown in Fig. 5.4.
  4. This procedure is consistent with the fact that a visible image is made invisible when and only when any cosmic string moves across it, and an invisible image is made visible only when a cosmic string moves across it.

For three overlapping strings, we follow the same procedure as before, with the same rules. The only difference is that rather than forming a parallelogram, three angular separation vectors lead to a parallelepiped. We show an example of this sort of diagram in Fig. 5.5.

Finally, let us stipulate that the three strings are coplanar and intersect at one point. If they are to be in force balance, then their orientation unit vectors must obey

$$\sum_{i=1}^3 \mu_i \gamma_i \hat{\mathbf{s}} = 0. \quad (5.10)$$

The  $\gamma$ -factors correct for the Lorentz contraction caused by boosting in a direction not perpendicular to all three strings.

If the three infinite strings satisfy Eqn. (5.10) then one may “cut-and-paste” them into two  $Y$ -junctions without changing the energy-momentum tensor. One of

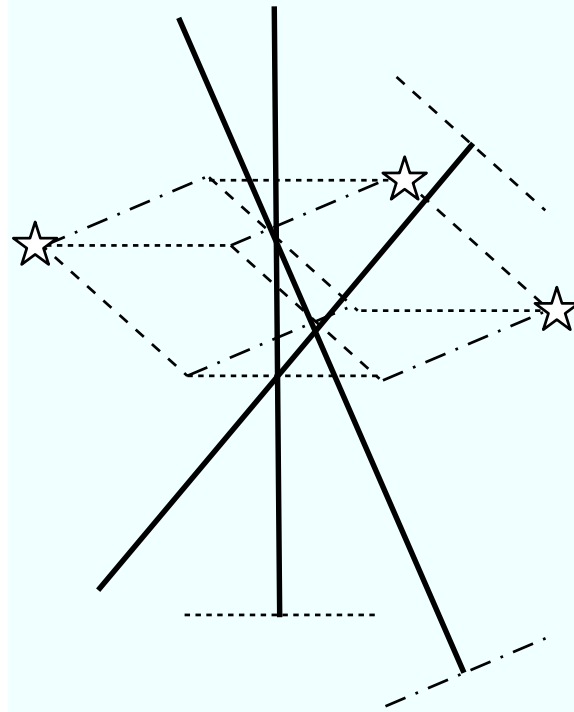


Figure 5.5: The imaging pattern for three overlapping cosmic strings. Only the object and two of the seven images are visible.

the  $Y$ -junctions can then be pulled away to reveal a single junction and its lensed images.

When cosmic strings intersect at a three-way junction, the background metric is solvable if and only if [106] the strings obey the force balance equation. Dynamically, however, the force balance equation is always satisfied since the neighborhood of the junction point can be taken to have an arbitrarily small mass, thus allowing it to respond instantaneously to any net force. This would not be the case if the vertex had a large mass (e.g., if it were a monopole). Thus there is a consistency check that must be performed for lensing by  $Y$ -junctions: each string lenses the two images surrounding it, and so the picture is over determined. In other words, each object has two images which must also satisfy the lensing equation of the

string separating them. This means we must check that the angular separation vector triangle closes:

$$\sum_{i=1}^3 \delta\vec{\varphi}_i = 0. \quad (5.11)$$

In fact, we find that the force balance Eqn. (5.10) is a sufficient condition for Eqn. (5.11) to be satisfied. This could be inferred from the first claim of this paragraph, but is also easy to verify directly using the equations found in §5.2.

## 5.4 Conclusion

We have presented an exact solution for both the lensing of three-string junctions and for multiple overlapping strings. We do not yet know how prevalent such junctions would be in realistic networks of (p,q) strings. There are many uncertainties about the dynamics of (p,q) string networks. These uncertainties mean that the density of Y-junctions is hard to predict. A great predominance of one string species over all others – many more (1,0) than (0,1) strings, say – could result in junctions being unobservably rare. In more general networks, dynamics that lead to generally low string number densities should also lead to a rarity of junctions. Thus, observable string junctions may be extremely uncommon, and so our chief hope for locating such a junction would be, first, to locate an actively lensing cosmic string. As yet, no astronomical observations have yielded unambiguous evidence for such a lensing event. Should such an event be found, we might hope to track it across the sky by interpolation between further lensing events or through the Kaiser-Stebbins effect [85, 86, 100] until a junction could be located along its length. Within any such search, the discovery of even one triple imaging event as described in this paper would be an unmistakable indicator of the existence of a cosmic string network with non-trivial interactions, the very kind predicted in

brane inflationary models. Finding this sort of smoking gun – so rare as to be invisible to serendipitous discovery – might be possible in such a scenario, giving us hope for an experimental examination of string theory unthinkable even a few years ago.

## 5.5 Appendix: Fly’s Eye Effect

A surprising secondary effect can be obtained if a large number of  $Y$ -junctions are arranged near one another: a single source can be identically imaged many, many times. We include this effect, though it is unlikely to arise in nature – where the junctions tend to speed apart relativistically – as an example of the extreme limit of the  $Y$ -lensing phenomenon. We further note that, while unlikely in present models, it has frequently been mentioned in the past [23, 96, 97] that networks of strings that become frozen could have a fly’s eye-style structure. We illustrate, on a small scale, what such a configuration could look like in Fig. 5.6; on a cosmic scale, the number of links and associated images could, of course, be multiplied almost indefinitely.

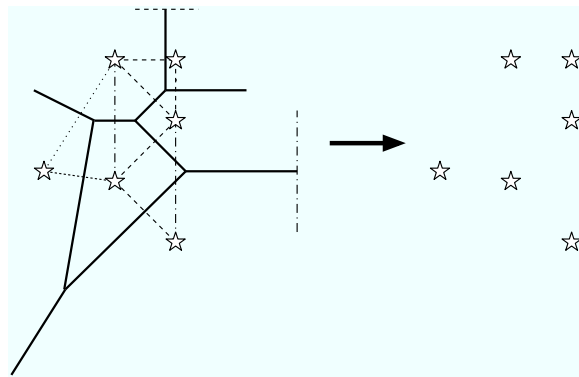


Figure 5.6: This set-up of strings and associated images is unlikely ever to occur in nature. It is included for illustrative purposes.

## A MODEL FOR COSMIC SUPERSTRING BINDING

**6.1 Introduction**

The success of the multi-tension one-scale model that was proposed in ref. [26] (see also Chapter 4) is based upon a radical simplification of the physics of cosmic superstring binding. The simplifying assumption is that when two cosmic superstrings interact through binding, we take their binding to be so fast compared with cosmological time scales as to be indistinguishable from instantaneous binding, which we call the “quick zip” approximation. Two lines of thought support this assumption. The first is the recognition that these binding interactions are energy-losing [23]; thus, we assume that the strings will quickly conform themselves to the energetically-favorable bound state. Secondly, we note the parallel between this problem and earlier computational work on non-intercommuting, low-velocity Abelian strings, where such zipping-up dynamics were observed [107].

Taking inspiration from ref. [107], we decided to tackle this problem numerically. To this end, we have adapted a lattice gauge theory code [29] for modeling cosmic string binding so that it can realize a  $U(1) \times U(1)$  gauge theory of the kind proposed in refs. [30, 31]. This gauge theory was first proposed in the context of superconducting string models, albeit in another parameter regime than we will utilize [108]. In this model, each of the Higgs fields separately acquires a vacuum expectation value, giving rise two two distinct gauge vortices. We hope to identify them with the F- and D-strings. To model string binding, an interaction term is added to the potential. We also hope to experiment with velocity-dependent

couplings that could also lead to binding. The Lagrangian for this theory is [30]:

$$\mathcal{L} = -D_\mu \bar{\phi} D^\mu \phi - \mathcal{D}_\mu \bar{\psi} \mathcal{D}^\mu \psi - \frac{1}{4} F_{\mu\nu} F^{\mu\nu} - \frac{1}{4} \mathcal{F}_{\mu\nu} \mathcal{F}^{\mu\nu} - V(|\phi|, |\psi|), \quad (6.1)$$

where we have the following gauge-covariant derivatives, field strengths and potential,

$$\begin{aligned} D_\mu &= \partial_\mu - ieA_\mu, & \mathcal{D}_\mu &= \partial_\mu - igB_\mu, \\ F_{\mu\nu} &= \partial_\mu A_\nu - \partial_\nu A_\mu, & \mathcal{F}_{\mu\nu} &= \partial_\mu B_\nu - \partial_\nu B_\mu, \\ V(|\phi|, |\psi|) &= \frac{\lambda_1}{4} (\bar{\phi}\phi - \eta^2)^2 + \frac{\lambda_2}{4} (\bar{\psi}\psi - \nu^2)^2 - \kappa (\bar{\phi}\phi - \eta^2) (\bar{\psi}\psi - \nu^2). \end{aligned}$$

There are, for general values of the coupling constants, four critical points for this theory. For each of the U(1) symmetries to be broken, we will need to make

$$(\bar{\phi}\phi, \bar{\psi}\psi)_0 = (\eta^2, \nu^2) \quad (6.2)$$

a minimum. Saffin [30] finds that, given this minimum, the parameter range for which binding occurs is

$$0 < \kappa < \frac{1}{2} \sqrt{\lambda_1 \lambda_2}. \quad (6.3)$$

To discretize this theory for computational solution, we generalize the methods described in ref. [29]. There, the techniques of lattice gauge theory have been used to set up a constrained Hamiltonian formalism. The advantage of this technique is that it is explicitly constructed to preserve the local gauge symmetries at the lattice points. The lattice gauge theory approach is reviewed in refs. [109]. In this approach, space is discretized to a cubic lattice with lattice spacing  $a$ . The field values  $\phi(\mathbf{x})$  ( $\psi(\mathbf{x})$ ) are represented by the variables  $\phi_{\mathbf{x}}$  ( $\psi_{\mathbf{x}}$ ), which live on the lattice sites  $\mathbf{x}$ . The gauge fields  $A^\mu(\mathbf{x})$  and  $B^\mu(\mathbf{x})$  are replaced by phase space rotation variables:

$$\theta_{\mathbf{x}}^\mu = aeA^\mu(\mathbf{x}) \quad \Theta_{\mathbf{x}}^\mu = agB^\mu(\mathbf{x}) \quad (6.4)$$

where  $e$  and  $g$  are the coupling constants for the two gauge fields. These variables  $\theta_{\mathbf{x}}^{\mu}$  and  $\Theta_{\mathbf{x}}^{\mu}$  live on links between lattice sites. Their purpose becomes clearer when we define the covariant derivative in this language:

$$\nabla_{\mu}^A \phi(\mathbf{x}) \equiv \frac{1}{a} [\exp\{-i\theta_{\mathbf{x}}^{\mu}\} \phi_{\mathbf{x}+a\hat{\mu}} - \phi_{\mathbf{x}}], \quad (6.5)$$

where  $\hat{\mu}$  is a unit vector in the  $\mu$  direction. We write  $\nabla_{\mu}^B$  to denote the covariant derivative for the other gauge field. Using this scheme, we can immediately write down a Hamiltonian for the discretized system, taking  $a^d \pi_{\mathbf{x}}^{\dagger}$  ( $a^d \Pi_{\mathbf{x}}^{\dagger}$ ) and  $a^{(d-1)} E_{\mathbf{x}}^{\mu}$  ( $a^{(d-1)} \mathcal{E}_{\mathbf{x}}^{\mu}$ ) as the momenta conjugate to the fields  $\phi_{\mathbf{x}}$  ( $\psi_{\mathbf{x}}$ ) and  $\theta_{\mathbf{x}}^{\mu}$  ( $\Theta_{\mathbf{x}}^{\mu}$ ). Since we will eventually want to work in the temporal gauge, we separate out the time component of the gauge field, writing  $A_{\mathbf{x}}^0$  for  $A_0(\mathbf{x})$  and  $B_{\mathbf{x}}^0$  for  $B_0(\mathbf{x})$ . This Hamiltonian should not be thought of as a discretized version of a Hamiltonian that is really given in continuous space. Instead, it should be thought of as an ansatz, lattice Hamiltonian describing a theory on a grid that can be shown to be equivalent to the continuum theory in the limit where the lattice spacing  $a \rightarrow 0$ .

$$\begin{aligned} H = & \sum_{\mathbf{x}} a^d \left\{ \pi_{\mathbf{x}} \left( \frac{1}{2} \pi_{\mathbf{x}}^{\dagger} - ie A_{\mathbf{x}}^0 \phi_{\mathbf{x}}^{\dagger} \right) + \pi_{\mathbf{x}}^{\dagger} \left( \frac{1}{2} \pi_{\mathbf{x}} + ie A_{\mathbf{x}}^0 \phi_{\mathbf{x}}^{\dagger} \right) + \Pi_{\mathbf{x}} \left( \frac{1}{2} \Pi_{\mathbf{x}}^{\dagger} - ig B_{\mathbf{x}}^0 \psi_{\mathbf{x}}^{\dagger} \right) + \right. \\ & \Pi_{\mathbf{x}}^{\dagger} \left( \frac{1}{2} \Pi_{\mathbf{x}} + ig B_{\mathbf{x}}^0 \psi_{\mathbf{x}}^{\dagger} \right) + \sum_i \left[ \frac{1}{2} (E_{\mathbf{x}}^i)^2 + \frac{1}{2} (\mathcal{E}_{\mathbf{x}}^i)^2 + (\nabla_i^A \phi_{\mathbf{x}})^{\dagger} (\nabla_i^A \phi_{\mathbf{x}}) + \right. \\ & \left. (\nabla_i^B \psi_{\mathbf{x}})^{\dagger} (\nabla_i^B \psi_{\mathbf{x}}) + \frac{1}{a} E_{\mathbf{x}}^i (A_{\mathbf{x}+i}^0 - A_{\mathbf{x}}^0) + \frac{1}{a} \mathcal{E}_{\mathbf{x}}^j (B_{\mathbf{x}+i}^0 - B_{\mathbf{x}}^0) \right] + \\ & \frac{1}{2a^4} \sum_{i \neq j} [(1 - \cos(\theta_{\mathbf{x}}^i + \theta_{\mathbf{x}+i}^j - \theta_{\mathbf{x}+j}^i - \theta_{\mathbf{x}}^j)) + \\ & (1 - \cos(\Theta_{\mathbf{x}}^i + \Theta_{\mathbf{x}+i}^j - \Theta_{\mathbf{x}+j}^i - \Theta_{\mathbf{x}}^j))] + \frac{\lambda_1}{4} (\phi_{\mathbf{x}}^{\dagger} \phi_{\mathbf{x}} - \eta^2)^2 \\ & \left. + \frac{\lambda_2}{4} (\psi_{\mathbf{x}}^{\dagger} \psi_{\mathbf{x}} - \nu^2)^2 - \kappa (\phi_{\mathbf{x}}^{\dagger} \phi_{\mathbf{x}} - \eta^2) (\psi_{\mathbf{x}}^{\dagger} \psi_{\mathbf{x}} - \nu^2) \right\} \quad (6.6) \end{aligned}$$

This Hamiltonian has been constructed to be invariant under the following transformations:

$$\phi_{\mathbf{x}} \rightarrow \exp\{i\chi_{\mathbf{x}}\} \phi_{\mathbf{x}}, \quad \psi_{\mathbf{x}} \rightarrow \exp\{i\chi_{\mathbf{x}}\} \psi_{\mathbf{x}},$$

$$\begin{aligned}\pi_{\mathbf{x}} &\rightarrow \exp\{i\chi_{\mathbf{x}}\}\pi_{\mathbf{x}}, & \Pi_{\mathbf{x}} &\rightarrow \exp\{i\chi_{\mathbf{x}}\}\Pi_{\mathbf{x}}, \\ \theta_{\mathbf{x}}^{\mu} &\rightarrow \theta_{\mathbf{x}}^{\mu} + \chi_{\mathbf{x}+a\hat{\mu}} - \chi_{\mathbf{x}}, & \Theta_{\mathbf{x}}^{\mu} &\rightarrow \Theta_{\mathbf{x}}^{\mu} + \chi_{\mathbf{x}+a\hat{\mu}} - \chi_{\mathbf{x}},\end{aligned}$$

where  $\chi_{\mathbf{x}}$  is an arbitrary function of position.

The initial data for our simulations is generated numerically, following a relaxation method similar to that of ref. [30] and described in greater detail by ref. [29]. Essentially, this method consists of taking vortex ansatzes for the scalar and gauge fields – i.e., that they are cylindrically symmetric – then writing down equations for those functions. We then solve them on a numeric grid using a successive over-relaxation technique. This one-dimensional configuration is then placed onto a three-dimensional computational grid. Finally, the resulting three-dimensional vortex configuration is rotated and Lorentz-boosted to its final, desired initial configuration.

Our code is able to realize two types of boundary conditions – periodic and free boundaries. Since we are dealing with a gauge theory, making periodic boundaries that, for instance, preserve winding number requires some care. Following ref. [29], we handle this by making a time-independent gauge transformation between periodically-identified lattice sites. This is done through the use of “patching” functions:

$$\begin{aligned}\phi(\mathbf{x}_T) &= \exp\{i\chi(\mathbf{x}_F)\}\phi(\mathbf{x}_F), & \pi(\mathbf{x}_T) &= \exp\{i\chi(\mathbf{x}_F)\}\pi(\mathbf{x}_F), \\ \theta^i(\mathbf{x}_T) &= \theta^i(\mathbf{x}_F) + \Delta\theta^i(\mathbf{x}_F), & E^i(\mathbf{x}_T) &= E^i(\mathbf{x}_F),\end{aligned}$$

where the data from the sites  $\mathbf{x}_F$  are carried to the  $\mathbf{x}_T$  sites. A similar set of transformations applies to the second set of  $U(1)$  fields. The value of the gauge transformation parameter is determined by the phase of the Higgs field in the

initial configuration:

$$\chi(\mathbf{x}_F) = \arg \phi(\mathbf{x}_T) - \arg \phi(\mathbf{x}_F), \quad \Delta\theta^i(\mathbf{x}_F) = \chi(\mathbf{x}_F + \hat{\mathbf{i}}) - \chi(\mathbf{x}_F).$$

These functions are computed once when the code is initialized then stored for subsequent use.

What we call “free” boundary conditions are conditions where the fields are gradient-free across the boundary – the fields retain their values, but are copied over to the boundary sites from the nearest-neighbor site to make the value of the derivative zero. The field values along the boundary evolve as if they were alone in space: they continue forward at their initial velocity without interacting with the field within the box proper.

For both boundary conditions, the vortex collisions are arranged to occur at the exact center of the box. We then stop the simulations before disturbances arising from these collisions reaches the box walls.

## 6.2 Current Status

We began our study by testing our code in the case where  $\kappa = 0$ ; that is, where the  $U(1)$  fields are not permitted mutually to interact. Under this set-up we are able to reproduce past results for two-dimensional vortex scattering [110] and to observe intercommutation between two vortices of the same type. Energy is conserved in these tests to within a few percent as long as simulations are not allowed to run so long that the boundary effects become important.

Computational study of full Hamiltonian, with  $\kappa \neq 0$ , is ongoing. We do not yet have reliable results to report. However, we can explain some of the questions we are hoping to answer. The first is, simply, does vortex binding continue indefi-

nately? Although there seems to be a naive energy argument in favor of binding, this is not universally accepted [111]. We also hope to determine whether, and how accurately, the solution to the Nambu-Goto equations for a constant-velocity growing “zipper” configuration given in ref. [112] is reproduced by the binding up of these gauge theory vortices. In this solution, the zipper growth velocity  $v$  is related to the ratio of the energy density in the two strings being bound to the energy density in the bound state:

$$v = \frac{\xi - \frac{1}{\epsilon}}{\epsilon - \xi}, \quad (6.7)$$

where  $\epsilon = (\mu_\alpha + \mu_\beta)/\mu_\gamma$  – for an  $\alpha$  and  $\beta$  string forming a  $\gamma$  bound state – and  $\xi$  is a constant related to the velocity and angle of the strings when they collide.

Phenomenologically, the first way in which we hope to use our results is more accurately to calibrate the parameter  $F$  defined in our multi-tension network model in Chapter 4.

## BIBLIOGRAPHY

- [1] C. L. Bennett et al., *Astrophys.J.Suppl.* **148**, 1 (2003), astro-ph/0302207.
- [2] D. N. Spergel et al., *Astrophys.J.Suppl.* **148**, 175 (2003), astro-ph/0302209.
- [3] L. Verde et al., *Astrophys.J.Suppl.* **148**, 195 (2003), astro-ph/0302218;  
<http://lambda.gsfc.nasa.gov/product/map/>
- [4] W. J. Percival et al., *MNRAS* **327**, 1297 (2001).
- [5] M. Tegmark et al., *Astrophys. J.* **606** (2004) 702, astro-ph/0310725; *Phys. Rev.* **D69** (2004) 103501.
- [6] G. Dvali and S.-H.H. Tye, *Phys. Lett.* **B450** (1999) 72, hep-ph/9812483.
- [7] C. Burgess J. M. Cline, H. Stoica, and F. Quevedo, *JHEP* **0409** (2004) 033, hep-th/0403119;  
N. Iizuka & S. Trivedi, *Phys.Rev.* **D70** (2004) 043519, hep-th/0403203;  
G. Dvali, Q. Shafi, and S. Solganik, hep-th/0105203;  
K. Dasgupta, C. Herdeiro, S. Hirano and R. Kallosh, *Phys.Rev.* **D65** (2002) 126002, hep-th/0203019.
- [8] S. Kachru, R. Kallosh, A. Linde and S. P. Trivedi, *Phys. Rev. D* **68**, 046005 (2003), hep-th/0301240.
- [9] S. Kachru, R. Kallosh, A. Linde, J. Maldacena, L. McAllister and S. P. Trivedi, *JCAP* **0310** (2003) 013, hep-th/0308055.
- [10] N. Jones, H. Stoica and S.-H.H. Tye, *JHEP* **07** (2002) 051, *Phys. Lett. B* **563** (2003) 6;  
S. Sarangi and S.-H. H. Tye, *Phys. Lett. B* **536** (2002) 185, hep-th/0204074.
- [11] F. R. Bouchet, D. P. Bennett, and A. Stebbins, *Nature* **335** (1988) 410.
- [12] D.P. Bennett, A. Stebbins, and F.R. Bouchet, *Astrophys. J. Lett.* **399**, L5 (1992).
- [13] Y. Zeldovich, *MNRAS* **192** (1980) 663.
- [14] G.F. Smoot et. al., *Astrophys. J.* **396** (1992) L1;  
C.L. Bennett et. al., *Astrophys. J.* **464** (1996) L1, astro-ph/9601067.
- [15] J. A. Peacock and S. J. Dodds, *MNRAS* **267** (1994) 1020;  
P. Ferreira, *Phys. Rev. Lett.* **74** (1995) 3522;  
C. van de Bruck, *Proceedings of the Second International Workshop on Dark Matter* (1998), H. V. Klapdor-Kleingrothaus & L. Baudis, eds.  
P. P. Avelino, E. P. S. Shellard, and J. H. P. Wu, *MNRAS* **318** (2000) 329, astro-ph/9906313.

- [16] A. Albrecht, R. A. Battye and J. Robinson, Phys. Rev. Lett. **79**, 4736 (1997); Phys. Rev. **D59**, 023508 (1999).
- [17] J. Polchinski, hep-th/0412244; hep-th/0410082.
- [18] A. Vilenkin and E.P.S. Shellard, Cosmic strings and other topological defects, Cambridge University Press, 2000.
- [19] F. R. Bouchet, P. Peter, A. Riazuelo, and M. Sakellariadou, Phys. Rev. **D65**, 21301(R) (2001).
- [20] L. Pogosian, S.-H. Henry Tye, I. Wasserman, M. Wyman, Phys. Rev. **D68**, 023506 (2003).  
L. Pogosian, I. Wasserman, and M. Wyman, JCAP **09** (2004) 008.
- [21] M. Wyman, L. Pogosian, and I. Wasserman, Phys. Rev. **D72** (2005) 023513, astro-ph/0503364; Erratum: astro-ph/0604141
- [22] G. Dvali and A. Vilenkin, JCAP 0403 (2004) 010, hep-th/0312007.
- [23] E. J. Copeland, R. C. Myers and J. Polchinski, JHEP **0406**, 013 (2004), hep-th/0312067,  
M. G. Jackson, N. T. Jones and J. Polchinski, hep-th/0405229.
- [24] A. Hanany and K. Hashimoto, JHEP 0506 (2005) 021, hep-th/0501031.
- [25] A. Avgoustidis and E. P. S. Shellard, Phys. Rev. **D73** (2006) 041301, astro-ph/0512582.
- [26] S.-H. H. Tye, I. Wasserman, M. Wyman, Phys. Rev. **D71** (2005) 103508; *ibid.* **D71** (2005) 129906(E), astro-ph/0503506.
- [27] M. Majumdar, hep-th/0512062.
- [28] B. Shlaer and M. Wyman, hep-th/0509177.
- [29] K. J. M. Moriarty, E. Myers, and C. Rebbi, Computer Physics Comm. 54 (1989) 273.
- [30] P. M. Saffin, hep-th/0506138.
- [31] S. M. Carroll and M. Trodden, Phys. Rev. **D57** (1998) 5198, hep-th/9711099.
- [32] R. A. Matzner, Computers in Physics, Sept./Oct. (1988) 51;  
E. P. S. Shellard, Nucl. Phys. **B283** (1987) 624.
- [33] A.T. Lee et. al. (MAXIMA-1), Ap. J. **561**, L1 (2001), astro-ph/0104459;  
C.B. Netterfield et. al. (BOOMERANG), Ap. J. **571**, 604 (2002) astro-ph/0104460;  
C. Pryke, et. al. (DASI), Ap. J. **568**, 46 (2002), astro-ph/0104490.

- [34] A.H. Guth, Phys. Rev. **D23**, 347 (1981);  
A.D. Linde, Phys. Lett. **B108**, 389 (1982);  
A. Albrecht and P.J. Steinhardt, Phys. Rev. Lett. **48**, 1220 (1982).
- [35] H. V. Peiris et al., astro-ph/0302225.
- [36] E. Komatsu et al., astro-ph/0302223.
- [37] L. Kofman, A. Linde and A. A. Starobinsky, Phys. Rev. Lett. **76**, 1011 (1996);  
I. Tkachev, S. Khlebnikov and L. Kofman, A. Linde, Phys. Lett. **B440**, 262 (1998);  
C. Contaldi, M. Hindmarsh and J. Magueijo, Phys. Rev. Lett. **82**, 2034 (1999);  
R. A. Battye and J. Weller, Phys. Rev. **D61**, 043501 (2000);  
J. Yokoyama, Phys. Lett. **B212**, 272 (1988);  
J. Yokoyama, Phys. Rev. Lett. **63**, 712 (1989).
- [38] R. Jeannerot, J. Rocher, and M. Sakellariadou, Phys. Rev. **D68**, 103514 (2003), hep-ph/0308134;  
J. Rocher and M. Sakellariaou, hep-ph/0412143, accepted to PRL.
- [39] C. P. Burgess, M. Majumdar, D. Nolte, F. Quevedo, G. Rajesh and R. J. Zhang, JHEP **0107**, 047 (2001), hep-th/0105204.
- [40] J. García-Bellido, R. Rabadán and F. Zamora, JHEP **0201** (2002) 036, hep-th/0112147;  
M. Gomez-Reino and I. Zavala, JHEP 0209 (2002) 020, hep-th/0207278,  
C. Herdeiro, S. Hirano, R. Kallosh, JHEP **0112**, 027 (2001), hep-th/0110271.
- [41] G. R. Dvali, Q. Shafi and S. Solganik, hep-th/0105203;  
S. Buchan, B. Shlaer, H. Stoica and S.-H. H. Tye, JCAP **0402**, 013 (2004), hep-th/0311207.
- [42] J. Polchinski, *String Theory*, Cambridge University Press, 1998.
- [43] G. Shiu, S.-H.H. Tye and I. Wasserman, hep-th/0207119;  
J.M. Cline, H. Firouzjahi and P. Martineau, hep-th/0207156;  
G. Felder, J. Garcia-Bellido, P.B. Greene, L. Kofman, A. Linde and I. Tkachev, Phys. Rev. Lett. **87** (2001) 011601;  
G. Felder, L. Kofman and A. Linde, hep-th/0106179.
- [44] S. E. Shandera and S.-H. H. Tye, hep-th/0601099.
- [45] H. Firouzjahi & S.-H. H. Tye, hep-th/0501099.
- [46] A. Sen, JHEP **9808**, 010 (1998), hep-th/9805019; JHEP **9809**,023 (1998), hep-th/9808141;  
E. Witten, JHEP **9812**, 019 (1998), hep-th/9810188;  
P. Horava, Adv. Theor. Math. Phys. **2**, 1373 (1999), hep-th/9812135.

- [47] A. Melchiorri and C. Odman, Phys. Rev. **D67**, 021501 (2003), astro-ph/0302361.
- [48] J. Kovac et al., Nature, **420**, 772 (2002) astro-ph/0209478.
- [49] L. Pogosian, I. Wasserman, and M. Wyman, astro-ph/060414.
- [50] R. Jeannerot, Phys. Rev. **D53**, 5426 (1996), hep-ph/9509365; R. Jeannerot, Phys. Rev. **D56**, 6205 (1997).
- [51] N. Barnaby, A. Berndsen, J. Cline, H. Stoica, hep-th/0412095.
- [52] X. Chen, hep-th/0501184.
- [53] L. Pogosian, and T. Vachaspati, Phys. Rev. **D60**, 83504 (1999).
- [54] U. Seljak and M. Zaldarriaga, Astrophys. J. **469**, 437 (1996); <http://www.cmbfast.org>
- [55] R. Jimenez, L. Verde, H. Peiris, A. Kosowsky, Phys. Rev. **D70** (2004) 023005, astro-ph/0404237.
- [56] R. E. Smith et al., MNRAS 341 (2003) 1311.
- [57] <http://www.hep.upenn.edu/~max/sdss.html>
- [58] N. Turok, U.-L. Pen and U. Seljak, Phys. Rev. Lett. **79**, 1611 (1997); Phys. Rev. **D58** (1998) 023506.
- [59] P. P. Avelino, E. P. S. Shellard, J.-H. P. Wu, B. Allen, Phys. Rev. Lett. **81**, 2008 (1998).
- [60] M. Landriau, E. P. S. Shellard, Phys. Rev. **D69**, 023003 (2004).
- [61] D. P. Bennett and F. R. Bouchet, Phys. Rev. **D41**, 2408 (1990).
- [62] B. Allen and E. P. S. Shellard, Phys. Rev. Lett. **64**, 119 (1990).
- [63] A. Albrecht and N. Turok, Phys. Rev. **D40**, 973 (1989).
- [64] A. Vilenkin, Phys. Rev. **D24**, 2082 (1981).
- [65] T. W. B. Kibble, Nucl. Phys. B261, 750 (1985).
- [66] B. Carter, Phys. Rev. **D41**, R3869 (1990).
- [67] A. Vilenkin, Phys. Rev. **D41**, 3038 (1990).
- [68] A. Gangui, L. Pogosian and S. Winitzki, Phys. Rev. **D64**, 43001 (2001).

- [69] C. J. A. P. Martins and E. P. S. Shellard, Phys. Rev. **D54** 2535 (1996), hep-ph/9602271;  
Phys. Rev. **D53** R575 (1996), hep-ph/9507335; Phys. Rev. **D65** 043514 (2002), hep-ph/0003298.
- [70] G. R. Vincent, M. Hindmarsh, M. Sakellariadou, Phys. Rev. **D55**, 573 (1997).
- [71] J. Magueijo, A. Albrecht, D. Coulson, P. Ferreira, Phys. Rev. Lett. **76**, 2617 (1996).
- [72] C. Contaldi, M. Hindmarsh and J. Magueijo, Phys. Rev. Lett. **82**, 679 (1999).
- [73] E. J. Copeland, J. Magueijo and D. A. Steer, Phys. Rev. **D61**, 063505 (2000).
- [74] L. Pogosian, Int. J. Mod. Phys. **A16S1C**, 1043 (2001).
- [75] N. Bevis, M. Hindmarsh, and M. Kunz, Phys. Rev. **D70**, 043508 (2004), astro-ph/0403029.
- [76] A. Fraisse, astro-ph/0503402.
- [77] B. Allen, R.R. Caldwell, E. P. S. Shellard, A. Stebbins, S. Veeraraghavan, Phys.Rev.Lett. **77** (1996) 3061.
- [78] L. Perivolaropoulos, Phys. Lett. **B298**, 305 (1993).
- [79] D. Coulson, P. Ferreira, P. Graham, and N. Turok, Nature **368**, 27 (1998).
- [80] B. Allen, R. R. Caldwell, S. Dodelson, L. Knox, E. P. S. Shellard, A. Stebbins, Phys. Rev. Lett. **79** (1997) 2624.
- [81] K. Moodley, M. Bucher, J. Dunkley, P. G. Ferreira, C. Skordis, Phys. Rev. **D70** (2004) 103520.
- [82] <http://quiet.uchicago.edu/>  
[http://www.stanford.edu/group/quest\\_telescope/](http://www.stanford.edu/group/quest_telescope/)  
M. Bowden et al., MNRAS **349** (2004) 321, astro-ph/0309610  
M. Tucci, E. Martinez-Gonzalez, P. Vielva, and J. Delabrouille, MNRAS **360** (2005) 926, astro-ph/0411567.
- [83] M. Piat, C. Rosset, et al., astro-ph/0412590.
- [84] J-H. P. Wu, astro-ph/0501239.
- [85] E. Jeong, G.F. Smoot, astro-ph/0406432.
- [86] A. S. Lo and E. L. Wright, astro-ph/0503120.
- [87] R. E. Schild, I. S. Masnyak, B. I. Hnatyk and V. I. Zhdanov, astro-ph/0406434.

- [88] T.W.B. Kibble, astro-ph/0410073.
- [89] V. M. Kaspi, J. H. Taylor and M. F. Ryba, Ap. J., **428**, 713, (1994);  
A. N. Lommen and D. C. Backer, Ap. J., **562**, 297 (2001), astro-ph/0107470;  
A. N. Lommen, astro-ph/0208572;  
A. H. Jaffe and D. C. Backer, Ap. J., **583**, 616 (2003), astro-ph/0210148.
- [90] T. Damour and A. Vilenkin, Phys. Rev. D64 (2001) 064008, gr-qc/0104026;  
hep-th/0410222.
- [91] L. Perivolaropoulos, Ap. J. **451** (1995).
- [92] A. Albrecht and N. Turok, Phys. Rev. Lett. **54** (1985) 1868;  
D. P. Bennett and F. R. Bouchet, Phys. Rev. Lett. **60** (1988) 257.
- [93] O. Bergman, K. Hori and P. Yi, Nucl. Phys. B **580**, 289 (2000), hep-th/0002223.
- [94] T. W. B. Kibble, Nucl. Phys. **B252**, 277 (1985);  
D. P. Bennett, Phys. Rev. **D33**, 872, Erratum **D34**, 3932 (1986).
- [95] B. Allen and R. R. Caldwell, Phys. Rev. **D43**, R2457 (1991);  
D. Austin, Phys. Rev. **D48**, R3422 (1993);  
F. Embacher, Phys. Rev. **D49**, 5030 (1994);  
D. Austin, E. J. Copeland and T. W. B. Kibble, Phys. Rev **D48**, 5594 (1993).
- [96] D. Spergel and U. Pen, Astrophys. J. Lett., **491** (1997) 67S, astro-ph/9611198.
- [97] P. McGraw, hep-th/9603153; Phys.Rev. **D57** (1998) 3317, astro-ph/9706182.
- [98] T. Vachaspati and A. Vilenkin, Phys. Rev. **D35** (1987) 1131.
- [99] C. Hogan and R. Narayan, MNRAS **211** (1984) 575.
- [100] N. Kaiser and A. Stebbins, Nature **310** (1984) 391;  
J.R. Gott, Ap. J. **288** (1985) 422.
- [101] B. Shlaer and S.-H. H. Tye, hep-th/0502242.
- [102] T. W. B. Kibble, J. Phys. **A9** (1967) 1387.
- [103] A. Vilenkin, Phys. Rev. **D23** (1981) 852.  
A. Vilenkin, Nature 322 (1986) 613.
- [104] C. Hogan and R. Narayan, MNRAS **211** (1984) 575,  
F. Bernardeau and J.-P. Uzan, Phys. Rev. **D63** (2001) 023004, astro-ph/0004105; **D63** (2001) 023005, astro-ph/0004102,  
B. Shlaer and S.-H. H. Tye, Phys. Rev. **D72** (2005) 043532, hep-th/0502242,

- A. A. de Laix and T. Vachaspati, Phys. Rev. D **54**, 4780 (1996), astro-ph/9605171.  
A. de Laix, L. M. Krauss, and T. Vachaspati, Phys. Rev. Lett. **79** (1997) 1968, astro-ph/9702033.  
M. Oguri and K. Takahashi, astro-ph/0509187.
- [105] B. Paczynski, Nature **319** (1986) 567.
- [106] C. Csaki and Y. Shirman, Phys. Rev. D **61**, 024008 (2000), hep-th/9908186.
- [107] L. M. A. Bettencourt, P. Laguna, and R. Matzner, Phys. Rev. Lett. **78** (1997) 2066.
- [108] E. Witten, Nucl. Phys. B **249** (1985) 557,  
R. L. Davis and E. P. S. Shellard, Phys. Lett. B **209** (1988) 485.
- [109] L. Kadanoff, Rev. Mod. Phys. **49** (1977) 267;  
J. Kogut, Rev. Mod. Phys. **51** (1979) 659; Rev. Mod. Phys. **55** (1983) 775;  
M. Creutz, L. Jacobs, and C. Rebbi, Phys. Rep. **95** (1983) 201.
- [110] K. J. M. Moriarty, E. Myers, and C. Rebbi, Phys. Lett. B **207** 1988 411.
- [111] A. Vilenkin, *private communication*
- [112] L. M. A. Bettencourt and T. W. B. Kibble, Phys. Lett. B **332** (1994) 297.